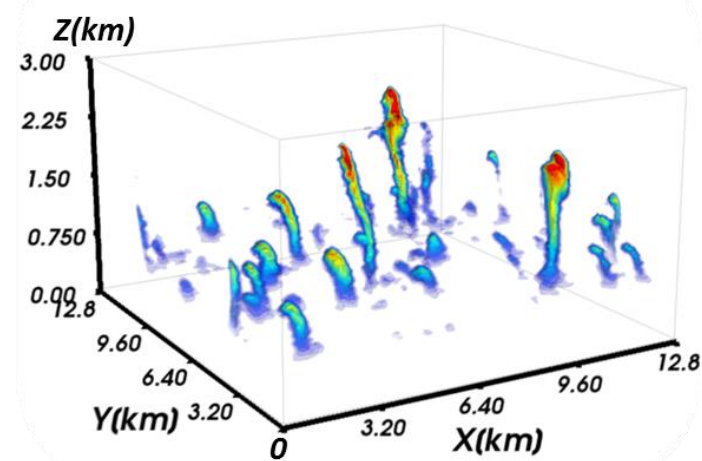




מכון ויצמן למדע
WEIZMANN INSTITUTE OF SCIENCE



The new COSMO parameterization of sub-grid-scale cloud microphysics using LES simulations

P. Khain¹, R. Heiblum², U. Blahak³, Y. Levi¹, H. Muskatel¹, E. Vadislavsky¹,
O. Altaratz², I. Koren², J. Shpund⁴ and A. Khain⁴

¹The Israel Meteorological Service, Israel

²Weizmann Institute of Science, Israel

³Deutscher Wetterdienst, Germany

⁴Hebrew University of Jerusalem, Israel

COSMO General Meeting, Jerusalem, September 2017

Outline

1. Motivation

2. COSMO new parametrization (**p1**) of SGS cloud properties (for radiation)

3. COSMO new parametrization (**p2**) based on LES simulations

A. Simulations design

B. Schematic explanation: How should LWC, NC and Reff behave with height?

C. Parametrization of mean Reff(z) and LWC(z)

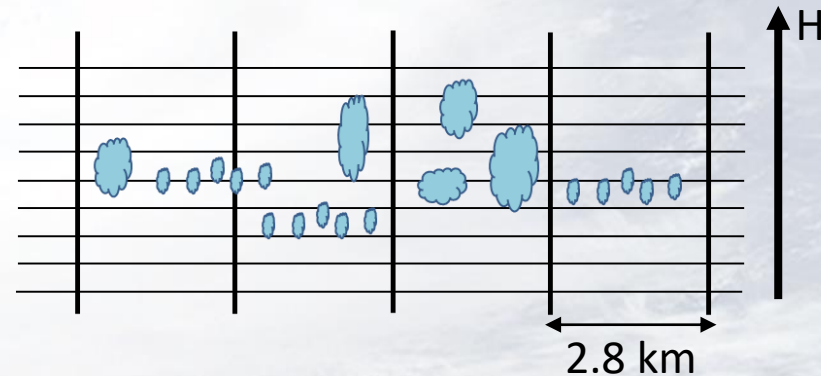
D. Towards the parametrization of the Optical Depth

4. Implementation in COSMO code: (really) first results

5. Summary

Motivation

- Shallow cumulus are extremely important to radiation budget
- In COSMO these clouds are subgrid, liquid water content in grid points is zero!
- To estimate radiation transfer, we need the optical properties of subgrid clouds
- To calculate them we need the profiles of
 1. Cloud cover (CLC)
 2. Liquid water content (LWC)
 3. Effective radius of droplets (R_{eff})
- **Question: How to estimate 1,2,3 ?**
- There are 2 options:



➤ **Already in the COSMO model (new scheme by U. Blahak):**

- CLC from the relative humidity at a grid point
- LWC from saturation mixing ratio at a grid point
- R_{eff} from droplets number concentration (NC) and LWC

➤ **LES simulation with detailed (Spectral-Bin) microphysics:**

- Simulate shallow cumulus explicitly for different stratifications and aerosols concentrations
- Average the profiles of CLC, LWC, R_{eff} over space and time to mimic COSMO resolution

Outline

1. Motivation

2. COSMO new parametrization (p1) of SGS cloud properties (for radiation)

3. COSMO new parametrization (p2) based on LES simulations

A. Simulations design

B. Schematic explanation: How should LWC, NC and Reff behave with height?

C. Parametrization of mean Reff(z) and LWC(z)

D. Towards the parametrization of the Optical Depth

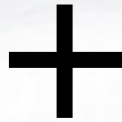
4. Implementation in COSMO code: (really) first results

5. Summary

COSMO new scheme (by U. Blahak)

Aerosol concentration climatic profile

(derived from Tegen et al. 1997)

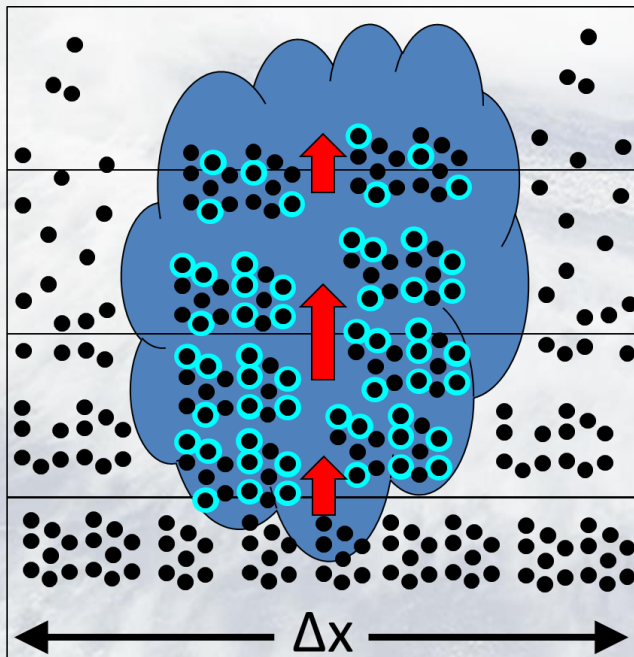


Effective updraft speed profile

(including turbulence, radiative cooling and parameterized convection)

Cloud droplets concentration profile

(from Segal & Khain 2006)



Subgrid clouds Liquid Water Content profile

(assuming proportionality to saturation mixing ratio)

Subgrid clouds effective radius profile

$$R_{eff}(z) = \alpha \left(\frac{LWC}{N_c} \right)^\beta$$

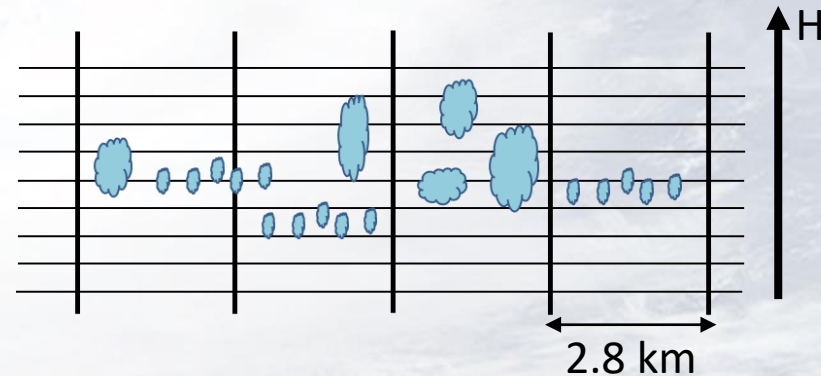
Much better than the operational

$$R_{eff} = 5\mu m$$

but problematic due to wrong LWC

Motivation

- Shallow cumulus are extremely important to radiation budget
- In COSMO these clouds are subgrid, liquid water content in grid points is zero!
- To estimate radiation transfer, we need the optical properties of subgrid clouds
- To calculate them we need the profiles of
 1. Cloud cover (CLC)
 2. Liquid water content (LWC)
 3. Effective radius of droplets (R_{eff})
- **Question: How to estimate 1,2,3 ?**
- There are 2 options:



➤ **Already in the COSMO model (new scheme by U. Blahak):**

- CLC from the relative humidity at a grid point
- LWC from saturation mixing ratio at a grid point
- R_{eff} from droplets number concentration (NC) and LWC

➤ **LES simulation with detailed (Spectral-Bin) microphysics:**

- Simulate shallow cumulus explicitly for different stratifications and aerosols concentrations
- Average the profiles of CLC, LWC, R_{eff} over space and time to mimic COSMO resolution

Outline

1. Motivation

2. COSMO new parametrization (**p1**) of SGS cloud properties (for radiation)

3. COSMO new parametrization (**p2**) based on LES simulations

A. Simulations design

B. Schematic explanation: How should LWC, NC and Reff behave with height?

C. Parametrization of mean Reff(z) and LWC(z)

D. Towards the parametrization of the Optical Depth

4. Implementation in COSMO code: (really) first results

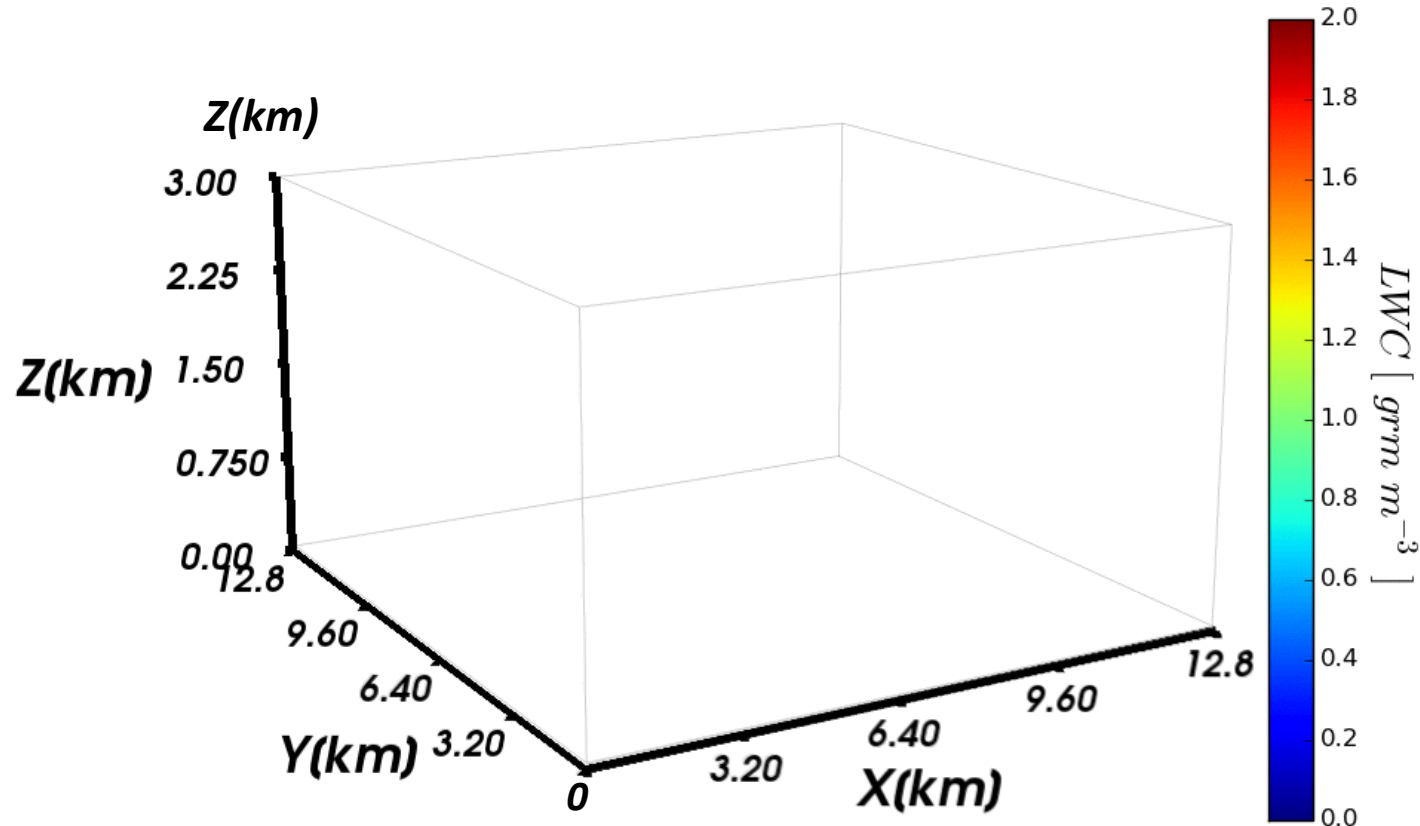
5. Summary

Simulations design

- **System for Atmospheric Modelling (SAM) (Khairoutdinov and Randall, 2003) is used to conduct LES simulations (<http://rossby.msrc.sunysb.edu/~marat/SAM.html>)**
- **Nonhydrostatic, anelastic, cyclic horiz. boundary conditions, maintaining temp. & moisture gradients at model top**
- **Microphysics: Spectral-Bin (Khain et al., 2013) with 33 mass bins for drops (radii from 2 μm to 3.2mm) to simulate warm processes: droplet nucleation, diffusional growth, collision coalescence, sedimentation, breakup (ice processes are also available but $T > 0$)**
- **Resolution: horiz. 100m, vertical 40m, time step: 1s, runtime: 8h. Domain: 12.8 X 12.8 X 5.1km**
- **Initial temp. perturbations near the surface at first time step**
- **Simulated case: Barbados Oceanographic and Meteorological Experiment (BOMEX) (Siebesma et al., 2003) – trade wind cumulus cloud field**
- **Aerosols: different size distributions (from 100 to 5000 cm^{-3}), where only the large size tails are activated in cumulus**

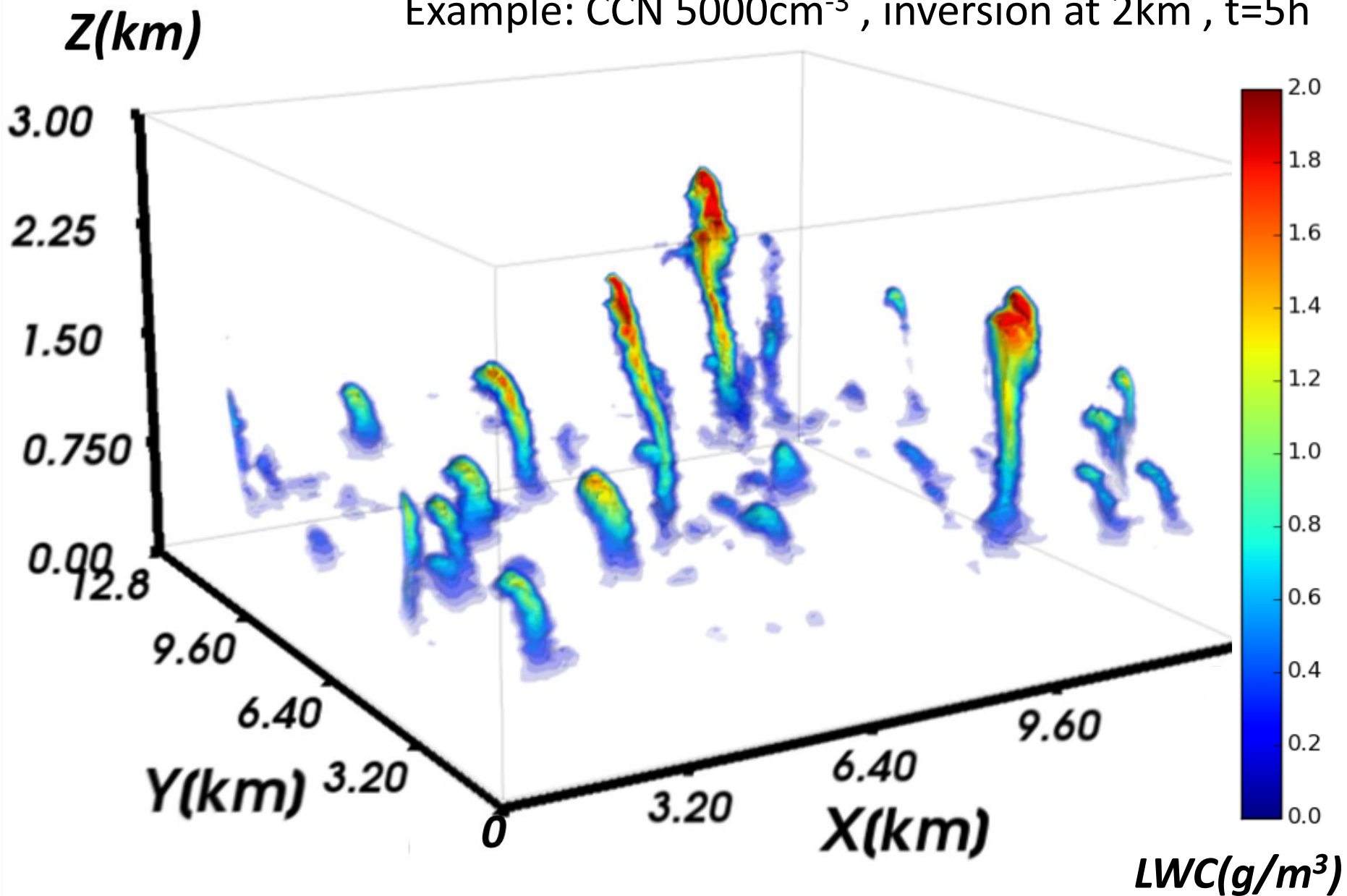
Shallow cumulus simulations

SAM-SBM: BOMEX case $\text{CCN}=5000\text{cm}^{-3}$ 4 (min)



Shallow cumulus simulations

Example: CCN 5000cm^{-3} , inversion at 2km, $t=5\text{h}$

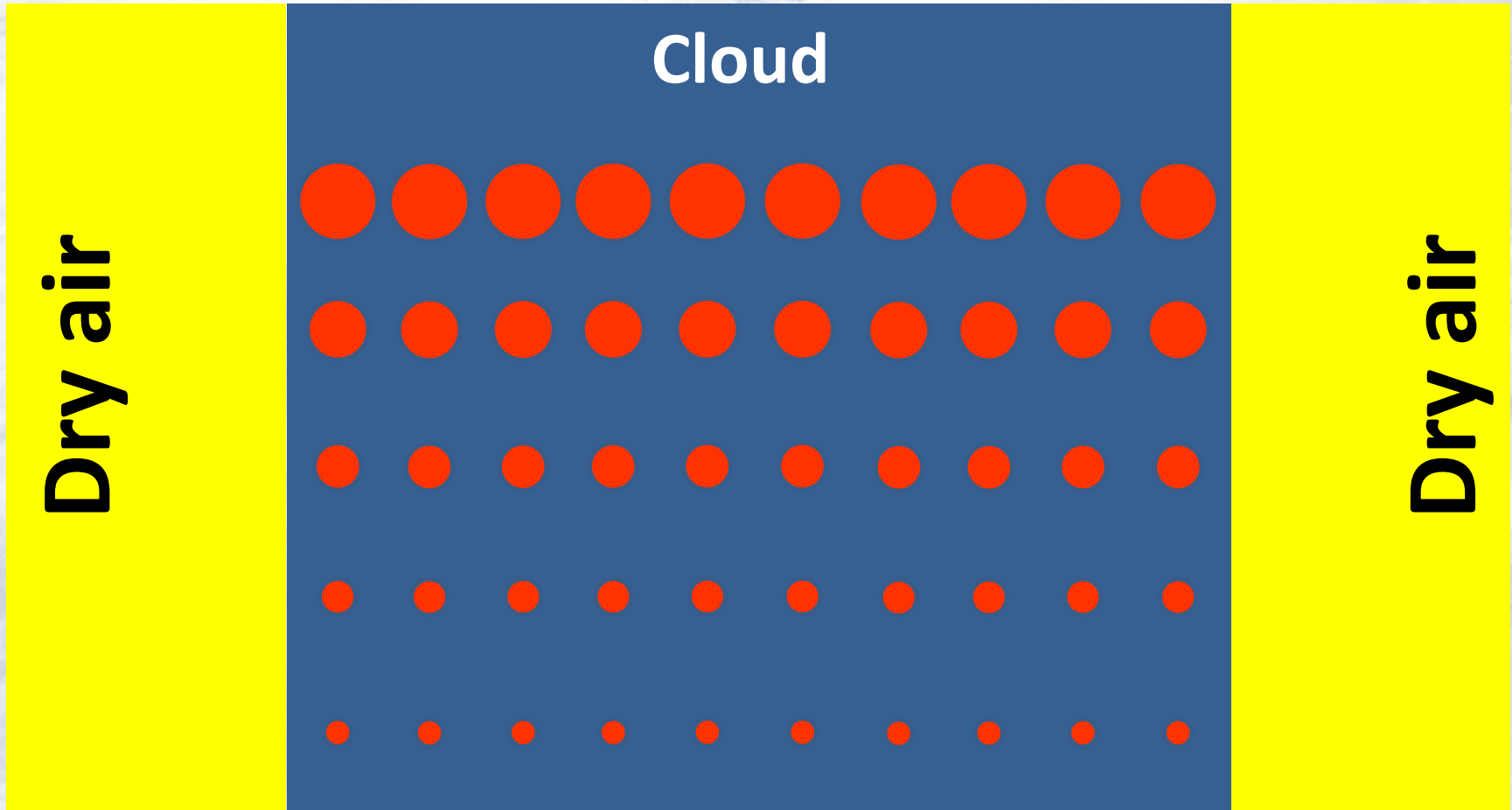


Outline

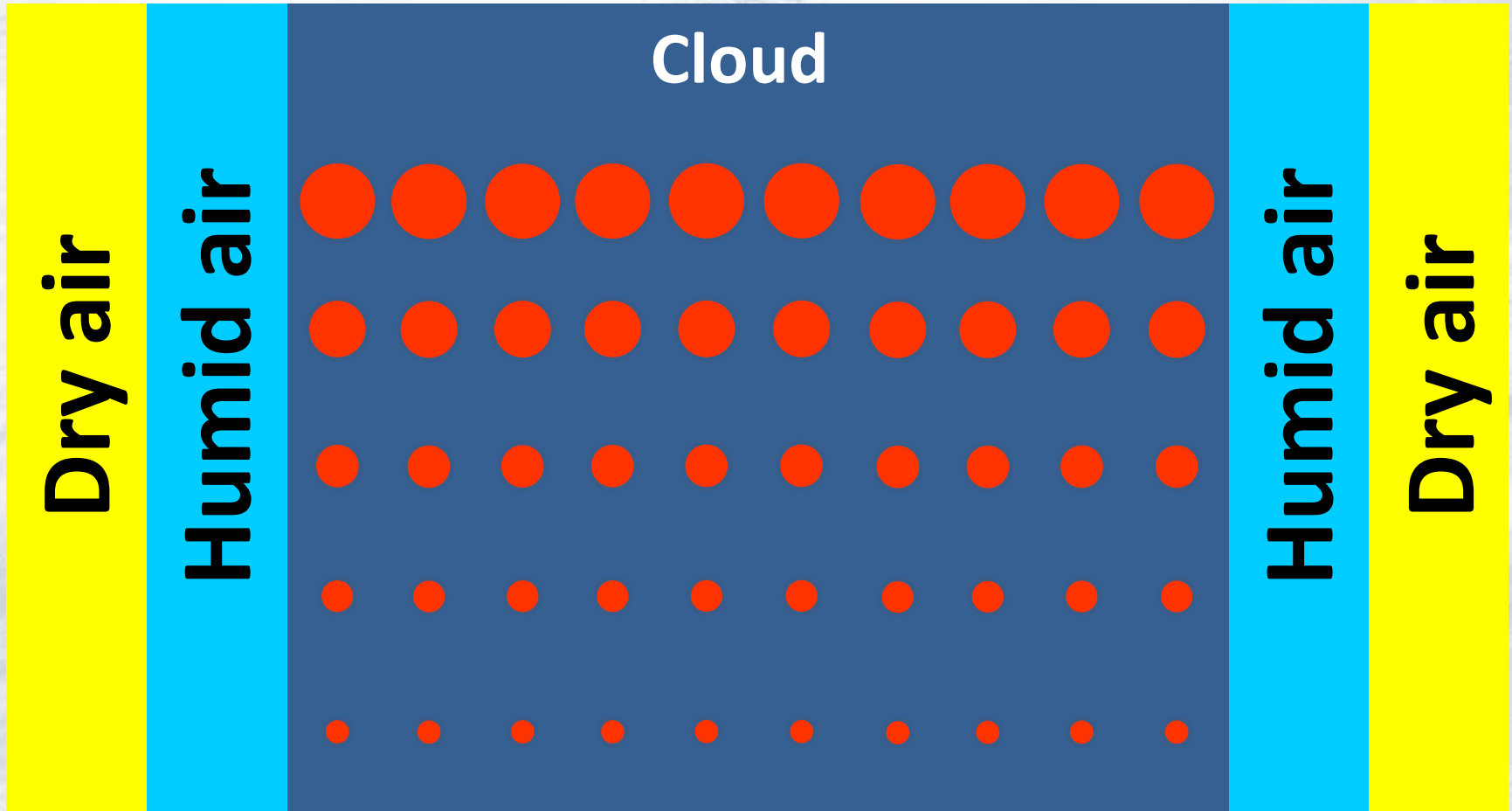
1. Motivation
2. COSMO new parametrization (**p1**) of SGS cloud properties (for radiation)
3. COSMO new parametrization (**p2**) based on LES simulations
 - A. Simulations design
 - B.** Schematic explanation: How should LWC, NC and Reff behave with height?
 - C. Parametrization of mean Reff(z) and LWC(z)
 - D. Towards the parametrization of the Optical Depth
4. Implementation in COSMO code: (really) first results
5. Summary

1. Assume no mixing with surrounding

- The droplets are growing with height (diffusional growth)
- The number concentration stays similar with height
- *Each “droplet”  represents size distribution



2. Air close to the cloud is very humid



How does the mixing at cloud edges occur?

2 important time scales:

- t_1 - Turbulent mixing in response to gradients
- t_2 - Condensation/evaporation towards thermodynamic equilibrium

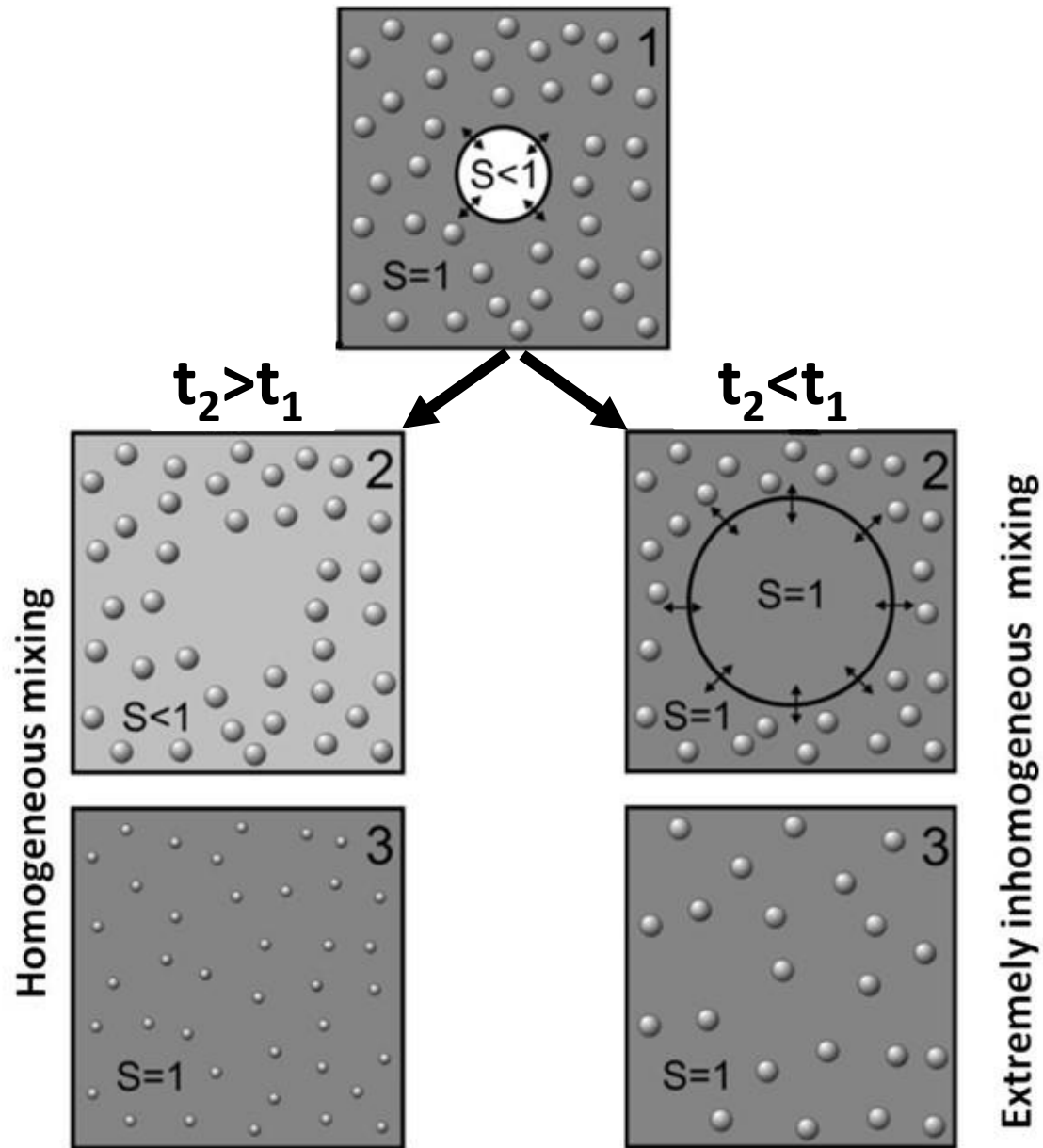
In reality:

$t_2 < t_1$ for scales above $> \sim 0.5\text{m}$

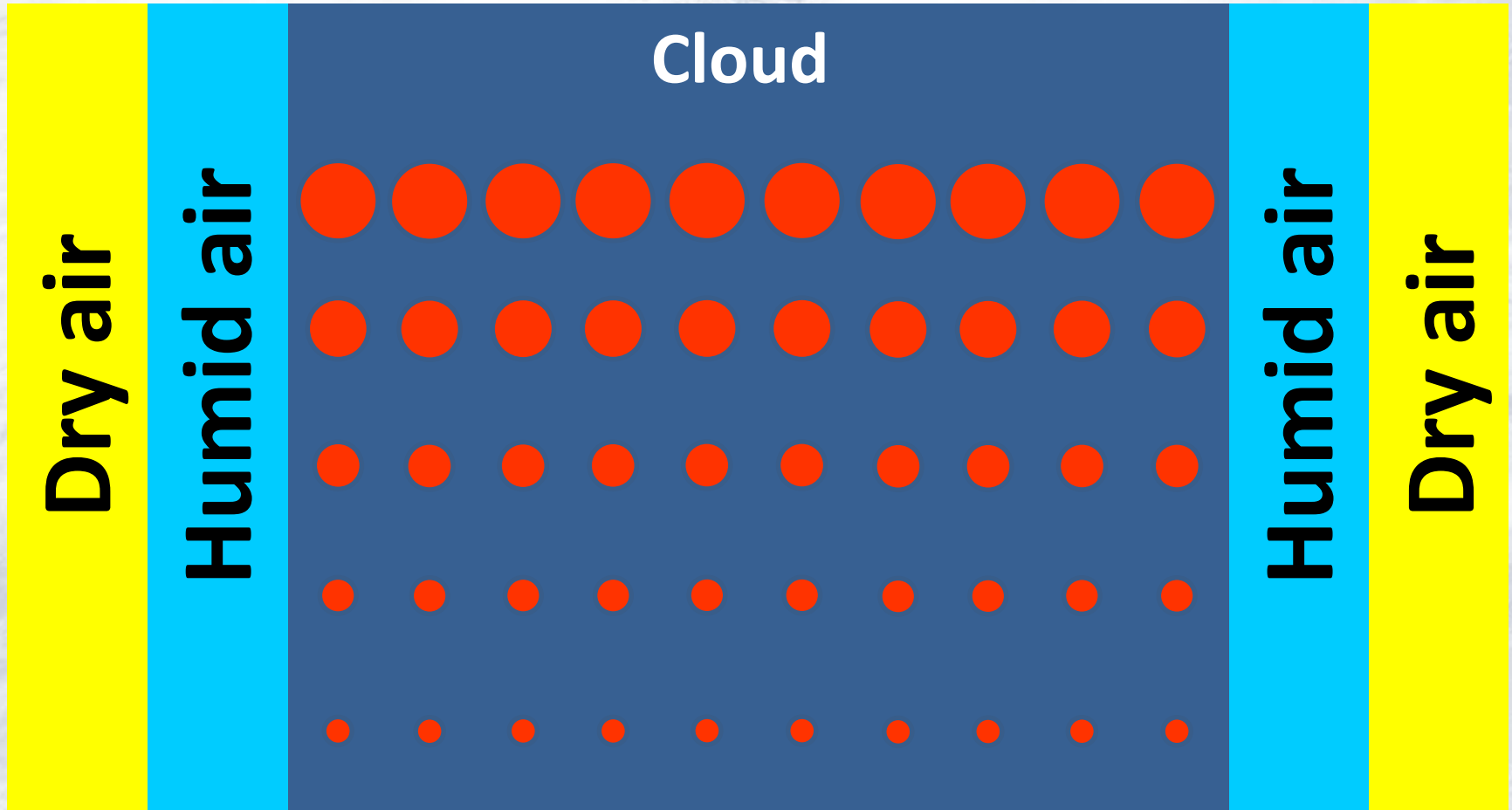
When subsaturated parcel enters the cloud, it evaporates the droplets, saturates, and then mixes with rest of the cloud without any effect!

Pinsky et al. (2016):

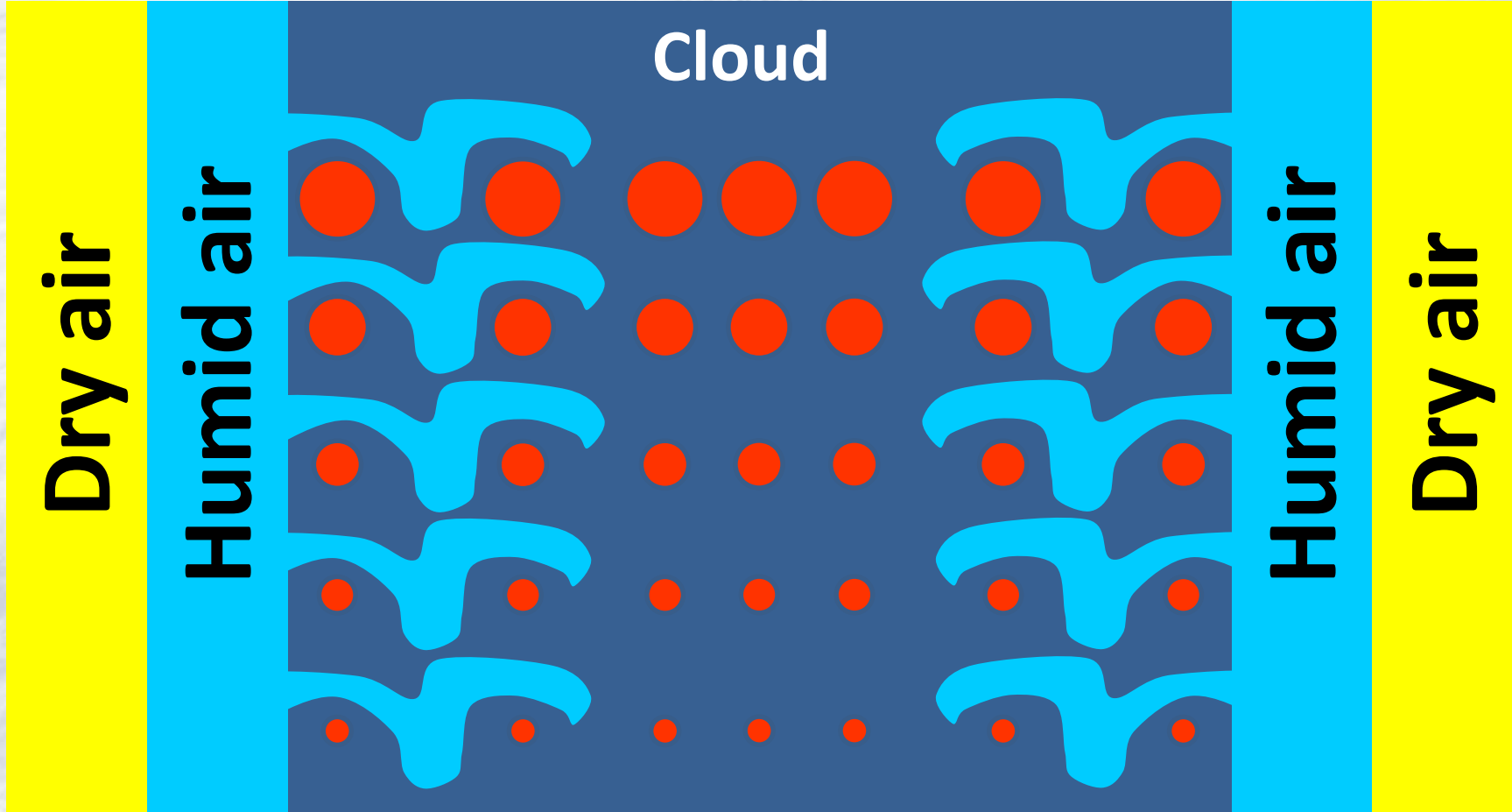
Models with resolution below $\sim 200\text{m}$ simulate the mixing at cloud edges correctly



2. Air close to the cloud is very humid



3. Entrainment leads to decreasing droplets concentration, keeping their size ~constant



4. Neglecting the dissipation at cloud top...

Height dependence?

NC – stay more or less constant

LWC – increase with height

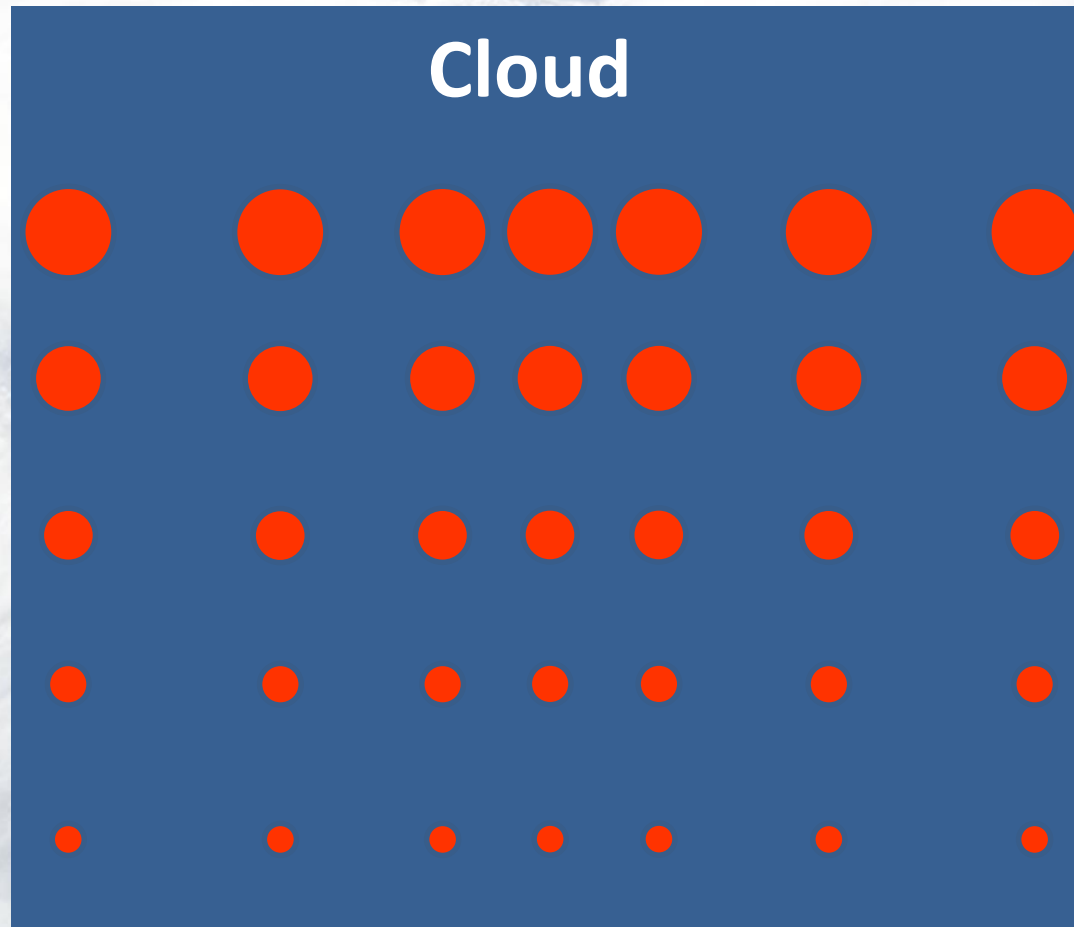
Reff – increase with height

Horizontal dependence?

NC – big variation

LWC – big variation

Reff – small variation



On average over many cloudy grid-points?

Height dependence?

NC – stay more or less constant

LWC – increase with height

Reff – increase with height

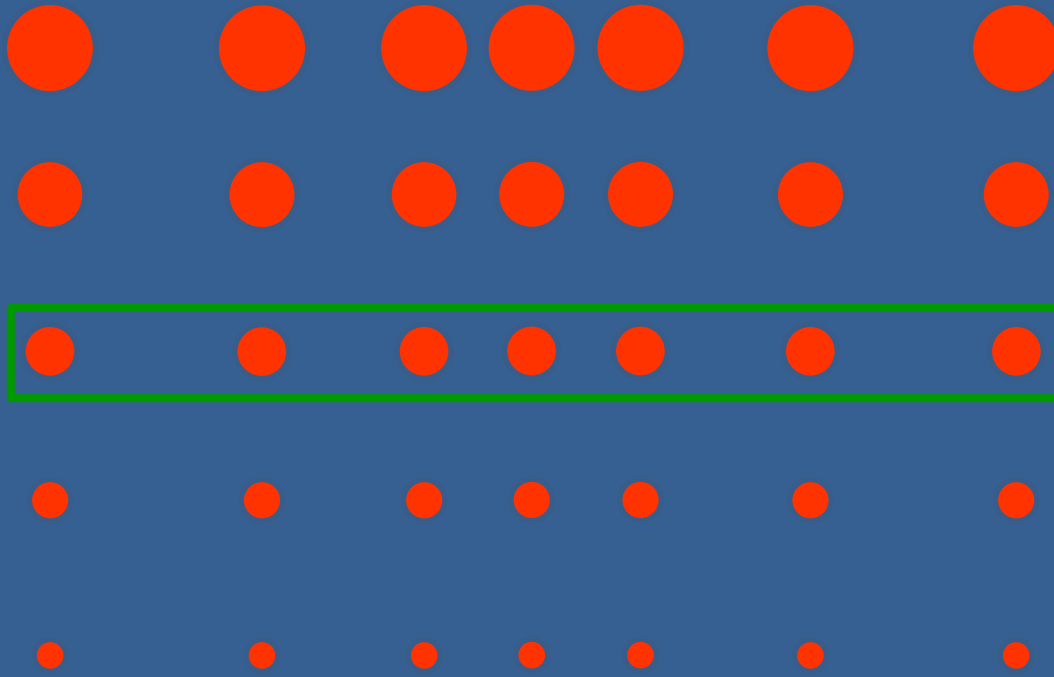
Horizontal dependence?

NC – big variation

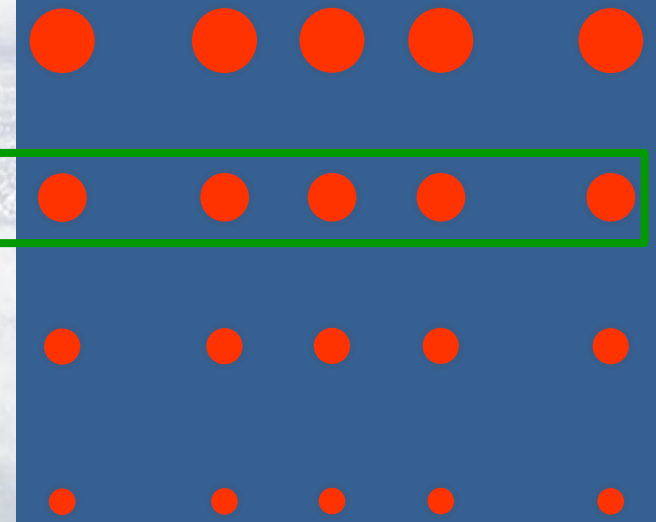
LWC – big variation

Reff – **small variation**

Cloud 1

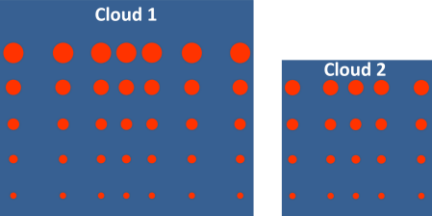


Cloud 2

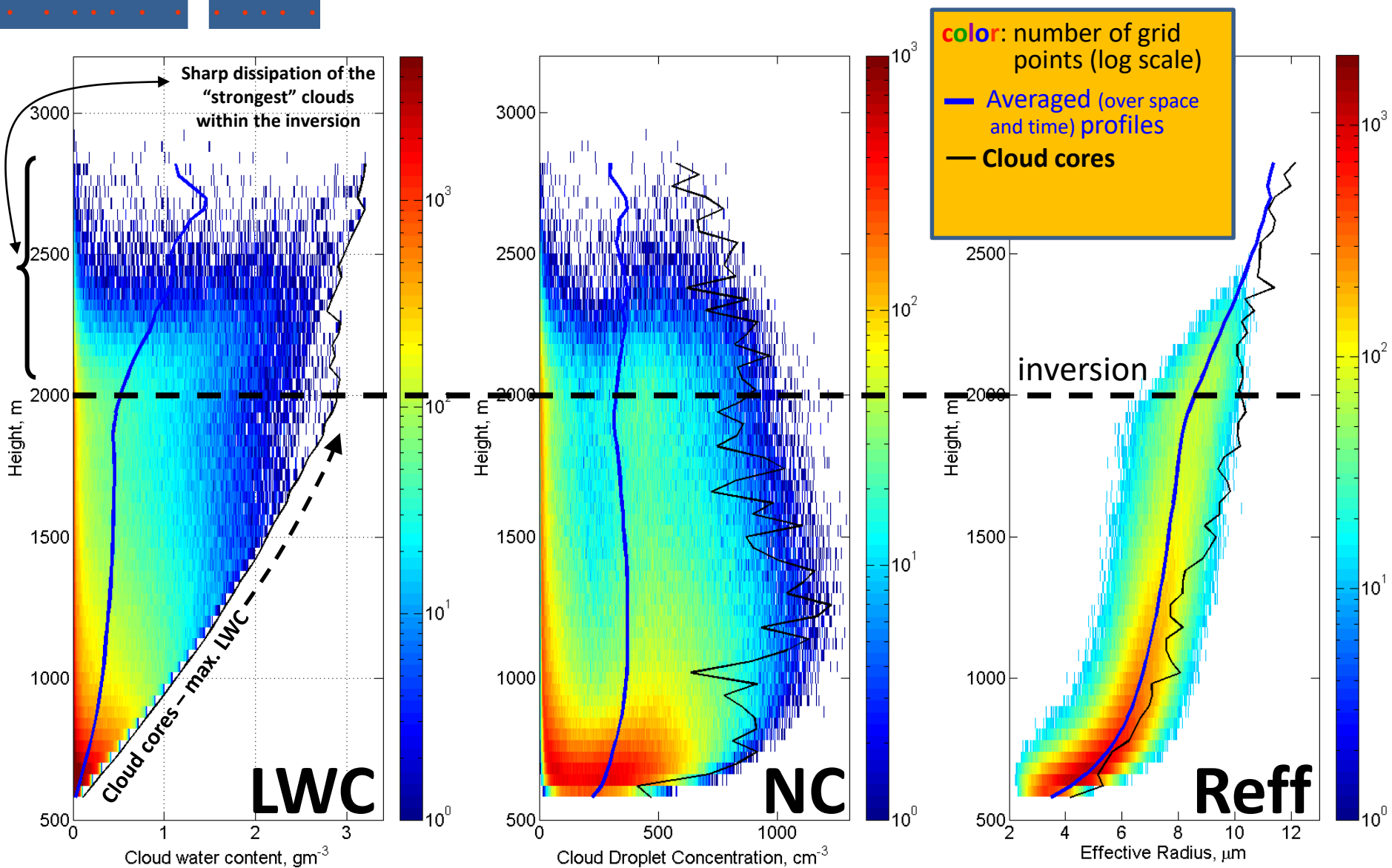


Outline

1. Motivation
2. COSMO new parametrization (**p1**) of SGS cloud properties (for radiation)
3. COSMO new parametrization (**p2**) based on LES simulations
 - A. Simulations design
 - B. Schematic explanation: How should LWC, NC and Reff behave with height?
 - C.** Parametrization of mean Reff(z) and LWC(z)
 - D. Towards the parametrization of the Optical Depth
4. Implementation in COSMO code: (really) first results
5. Summary



Example of simulation results for 5000 CCN cm^{-3} : scatter over all grid points and times



Horizontal dependence: **LWC, NC** – big variation, **Reff** – small variation

Effective Radius vs. Mean Volume Radius

$$LWC = \frac{4\pi\rho_w}{3} NC \cdot R_v^3$$

Liquid Water Content Number Concentration Mean Volume Radius

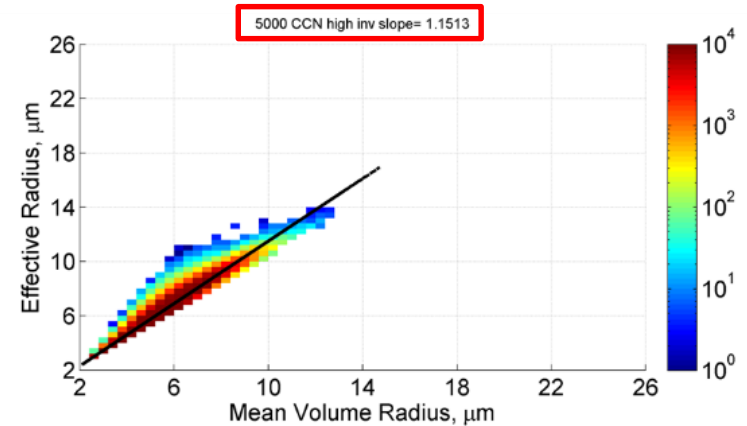
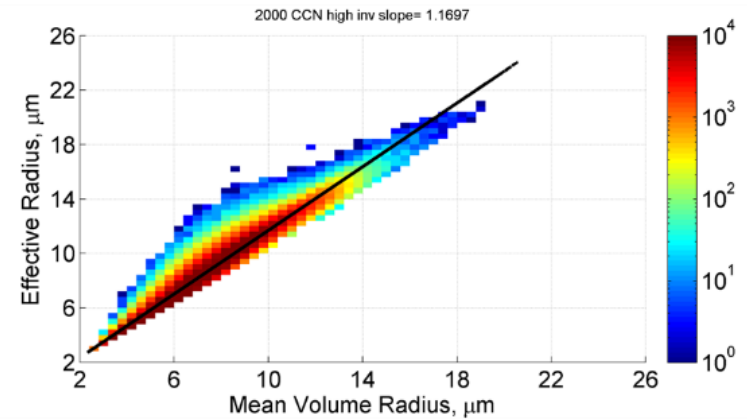
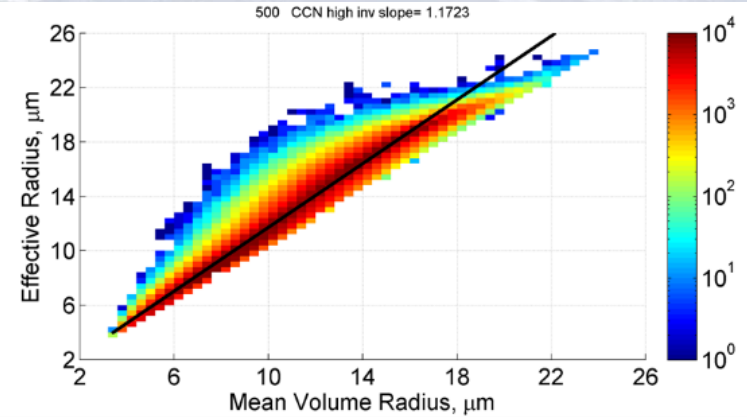
Our simulations of shallow Cu ensembles show:

$$R_{eff} \approx 1.15 \cdot R_v$$

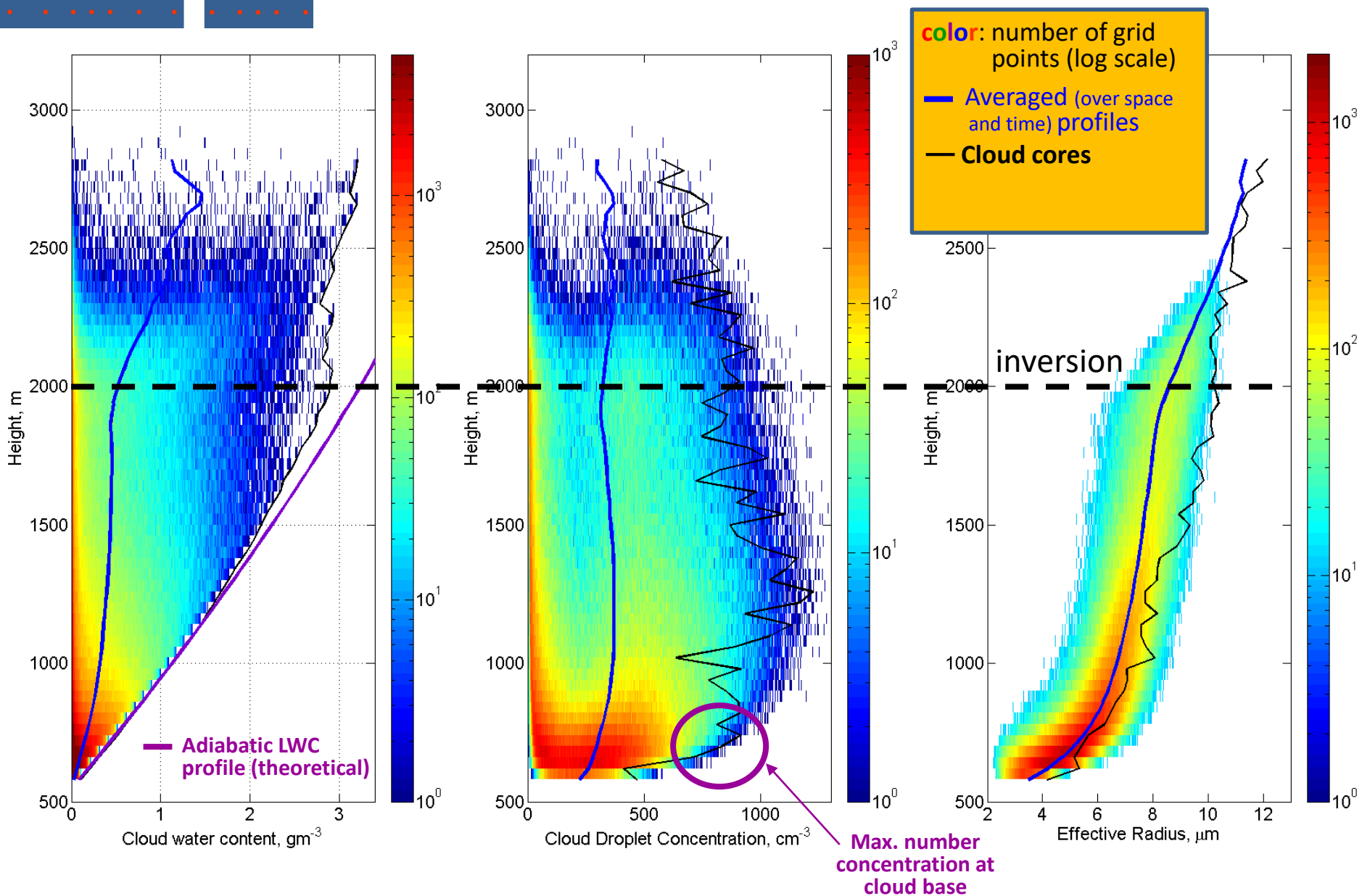
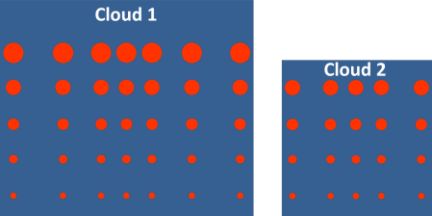
In an “ideal” cloud core:

$$LWC_{ad}(z) = \frac{4\pi\rho_w}{3} NC_{cloud\ base} \left(\frac{R_{eff,ad}(z)}{1.15} \right)^3$$

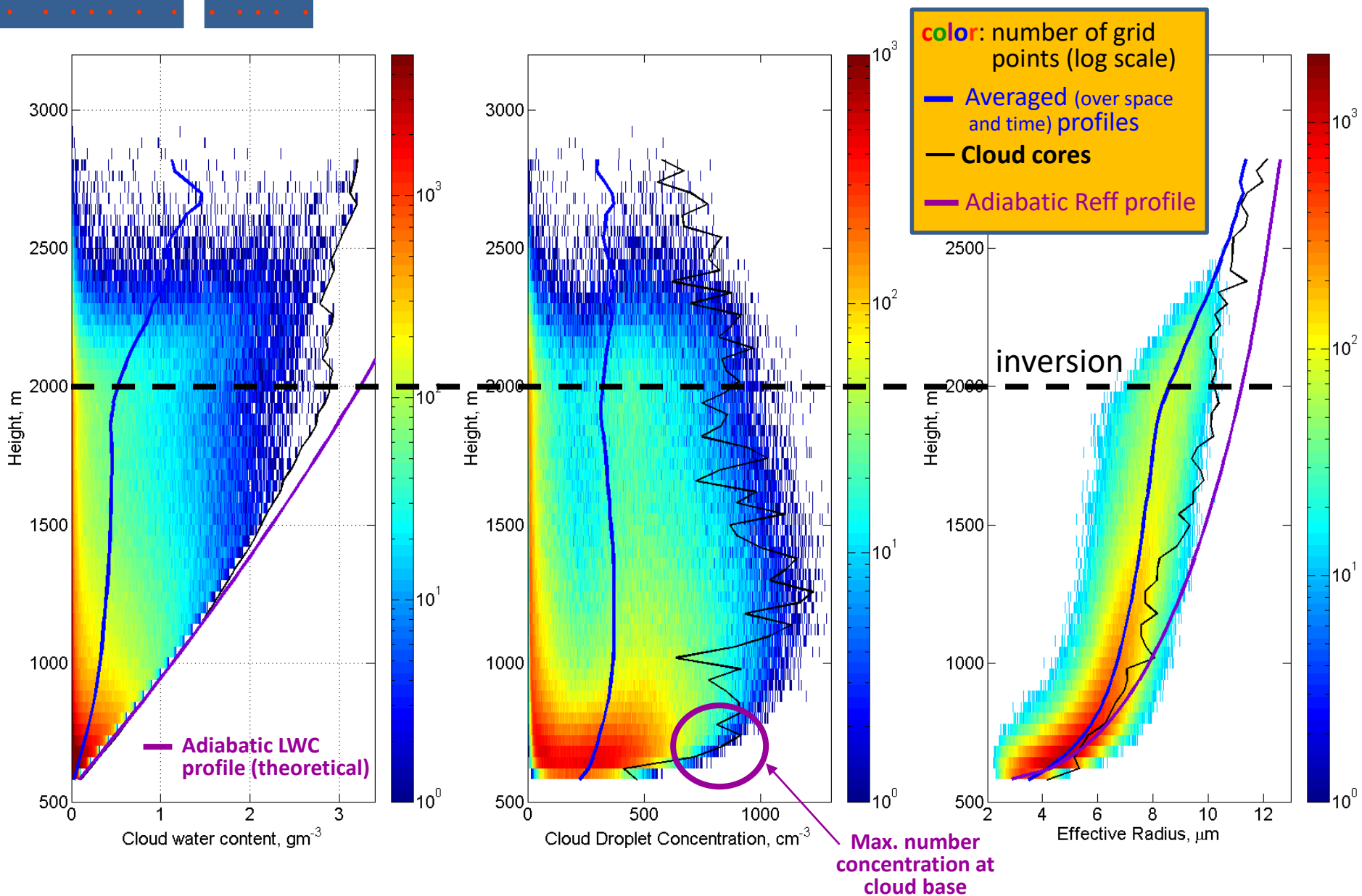
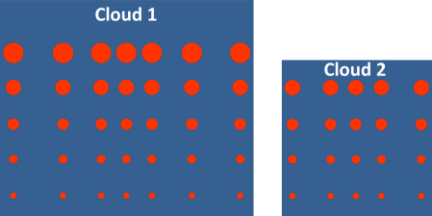
→ Obtain $R_{eff,ad}(z)$



Example of simulation results for 5000 CCN cm^{-3} : scatter over all grid points and times

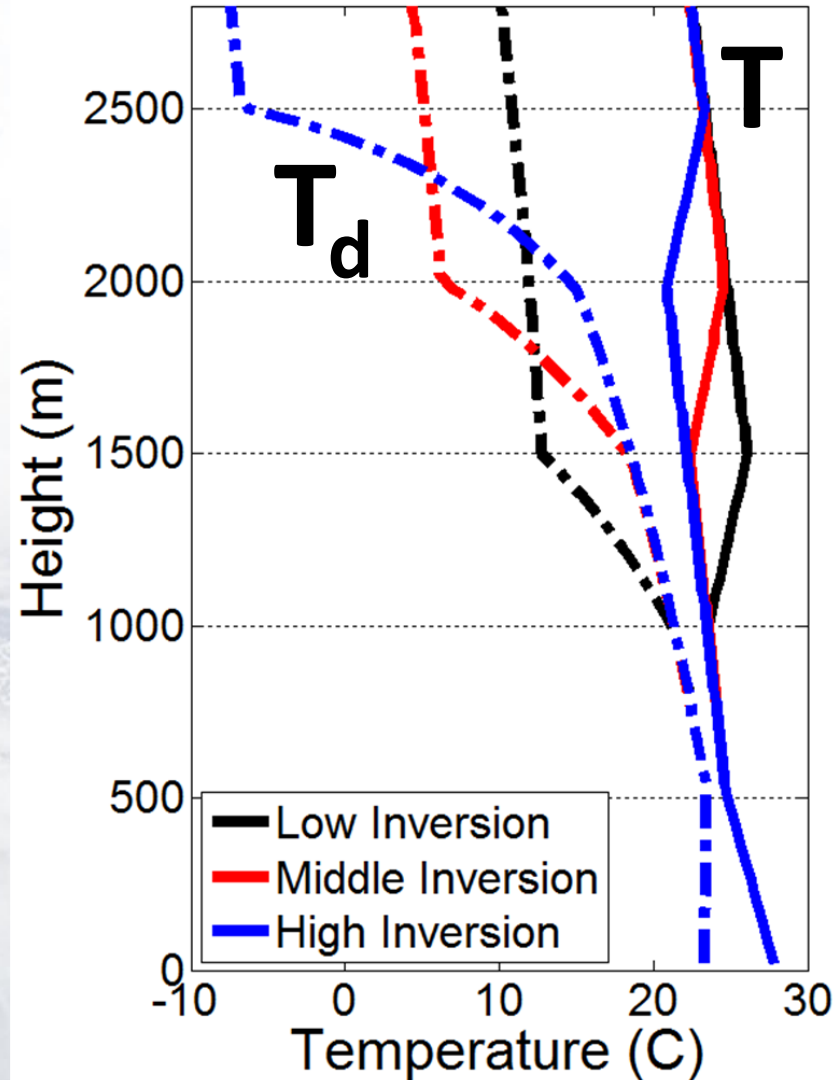


Example of simulation results for 5000 CCN cm^{-3} : scatter over all grid points and times



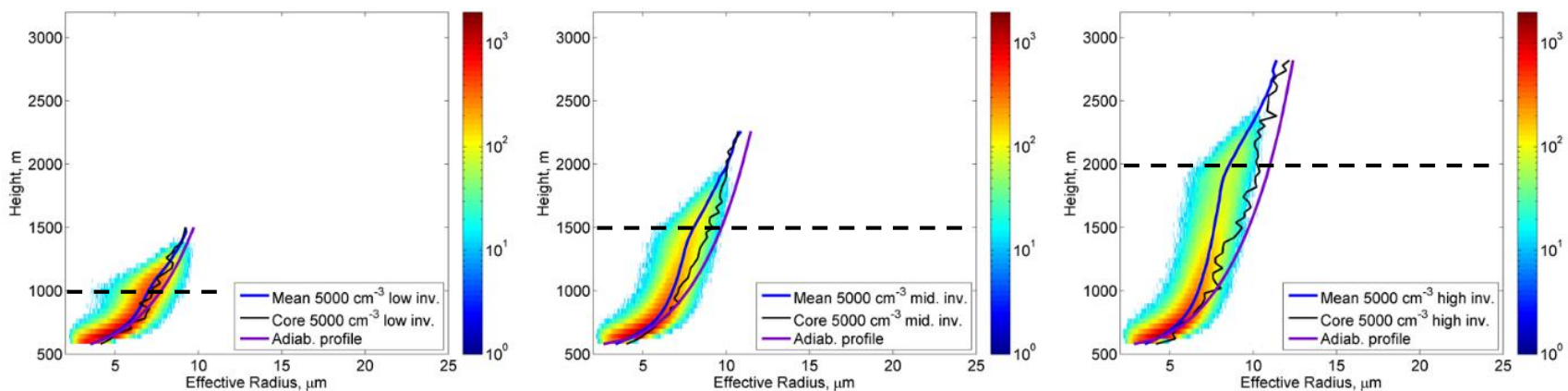
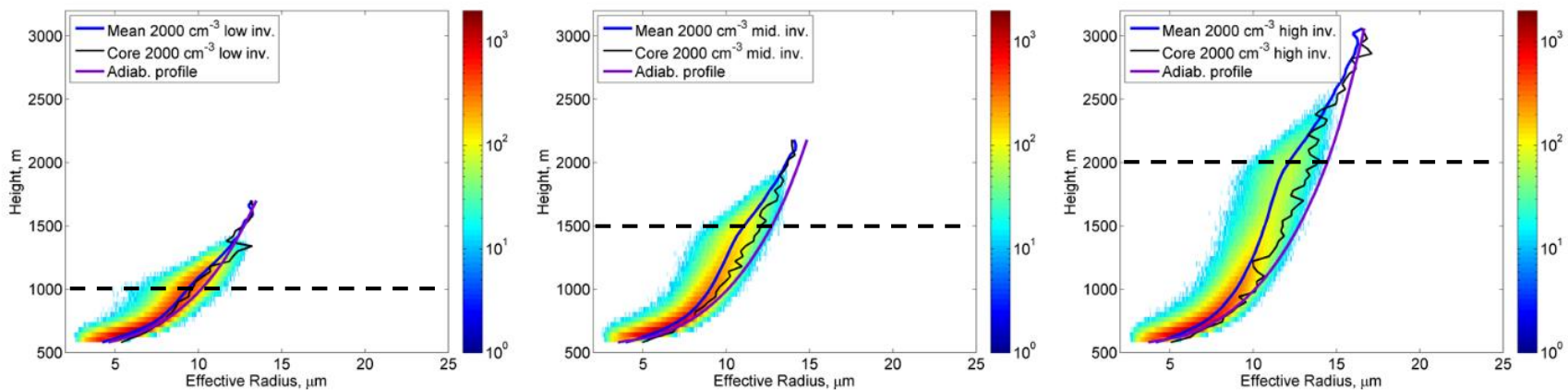
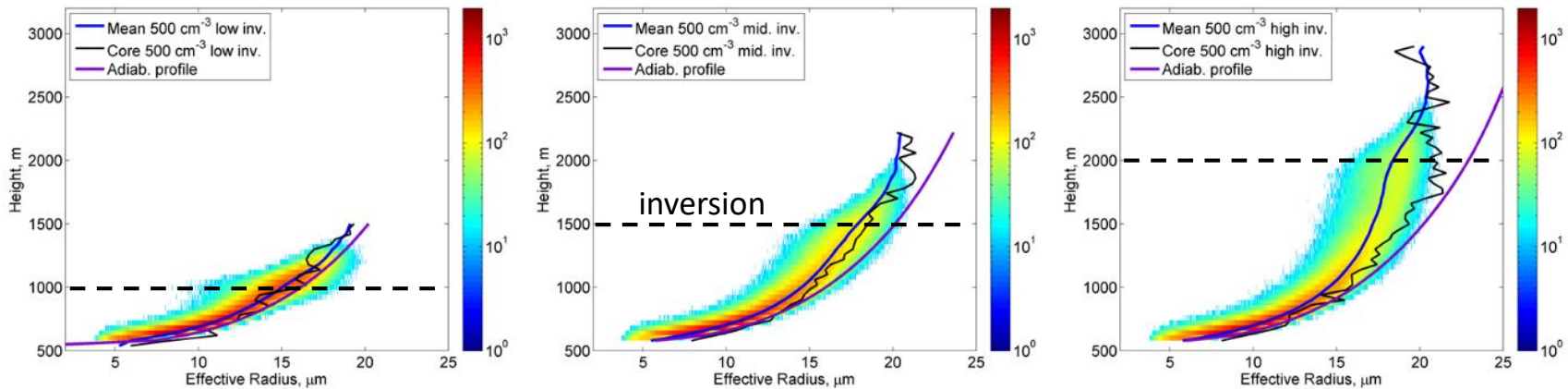
Simulations at different conditions

- **CCN concentrations of 500, 1000, 2000, 3000, 5000 cm^{-3}**
(Only the tails of the CCN distributions are activated)
- **3 different stratifications (inversion at 1000m, 1500m, 2000m)**
- In the very clean (100 and 250 cm^{-3}) experiments there was too much rain, making adiabatic effective radius profile not relevant

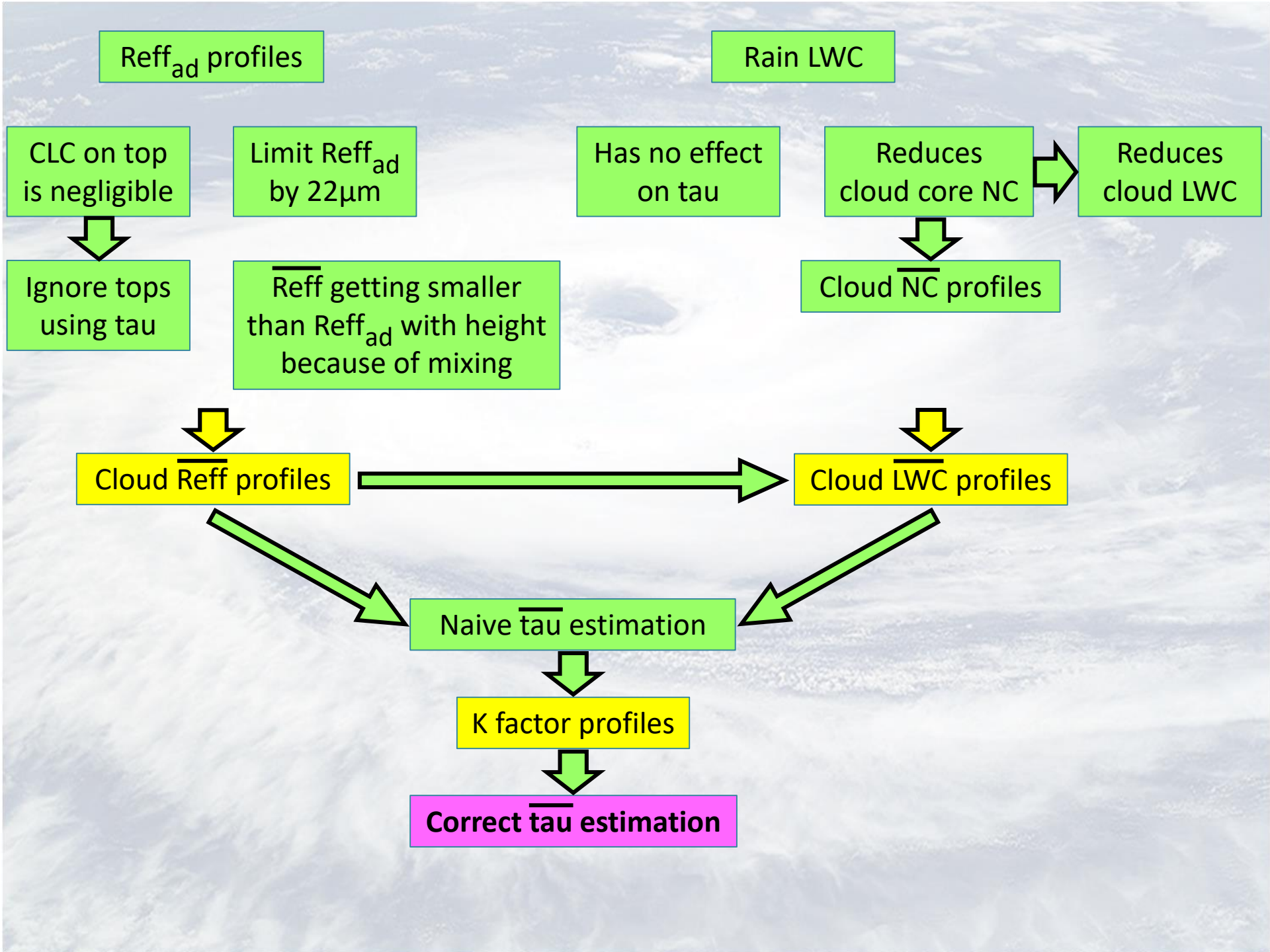


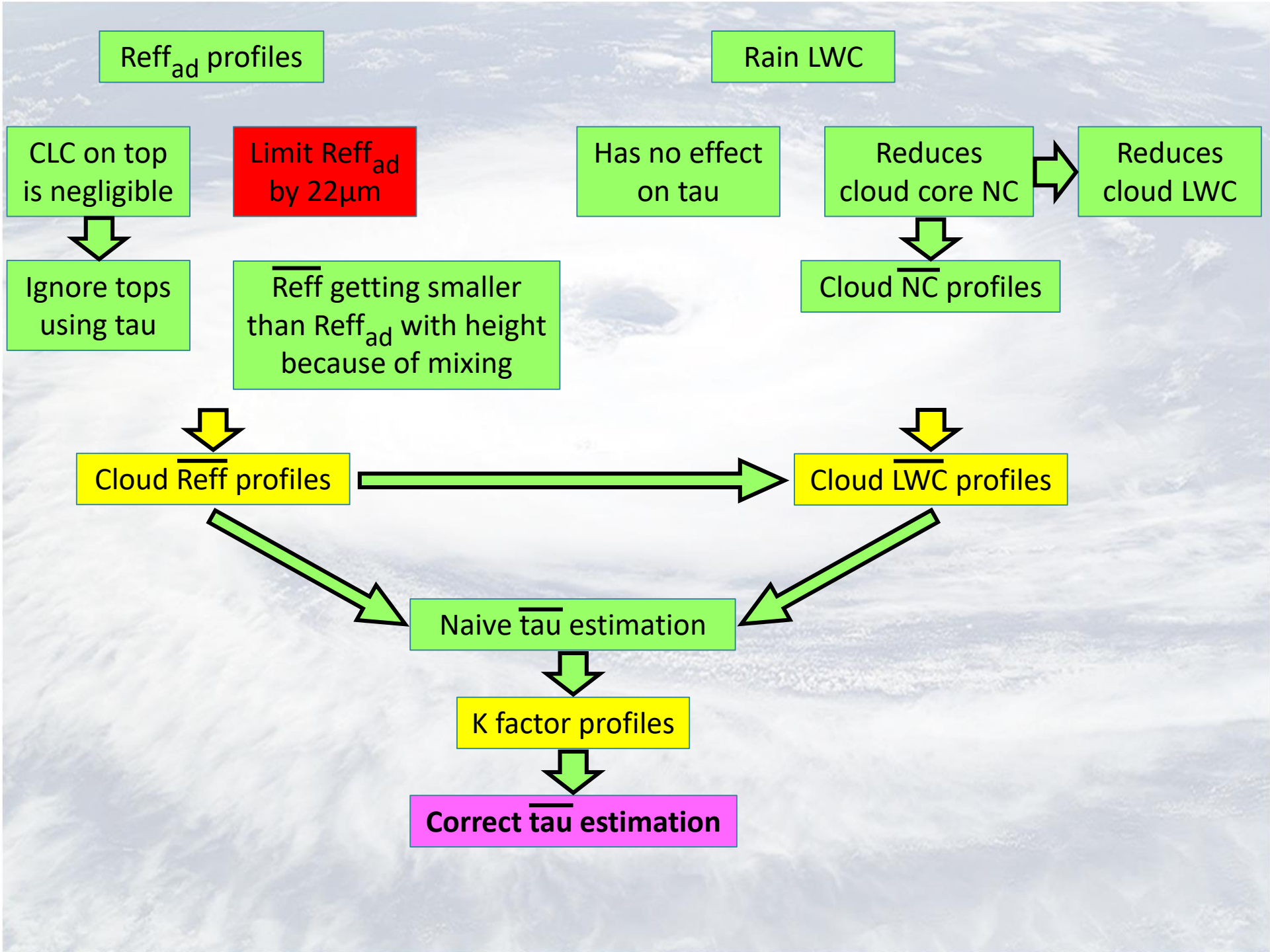
Reff_{ad} profiles in different experiments

Clean

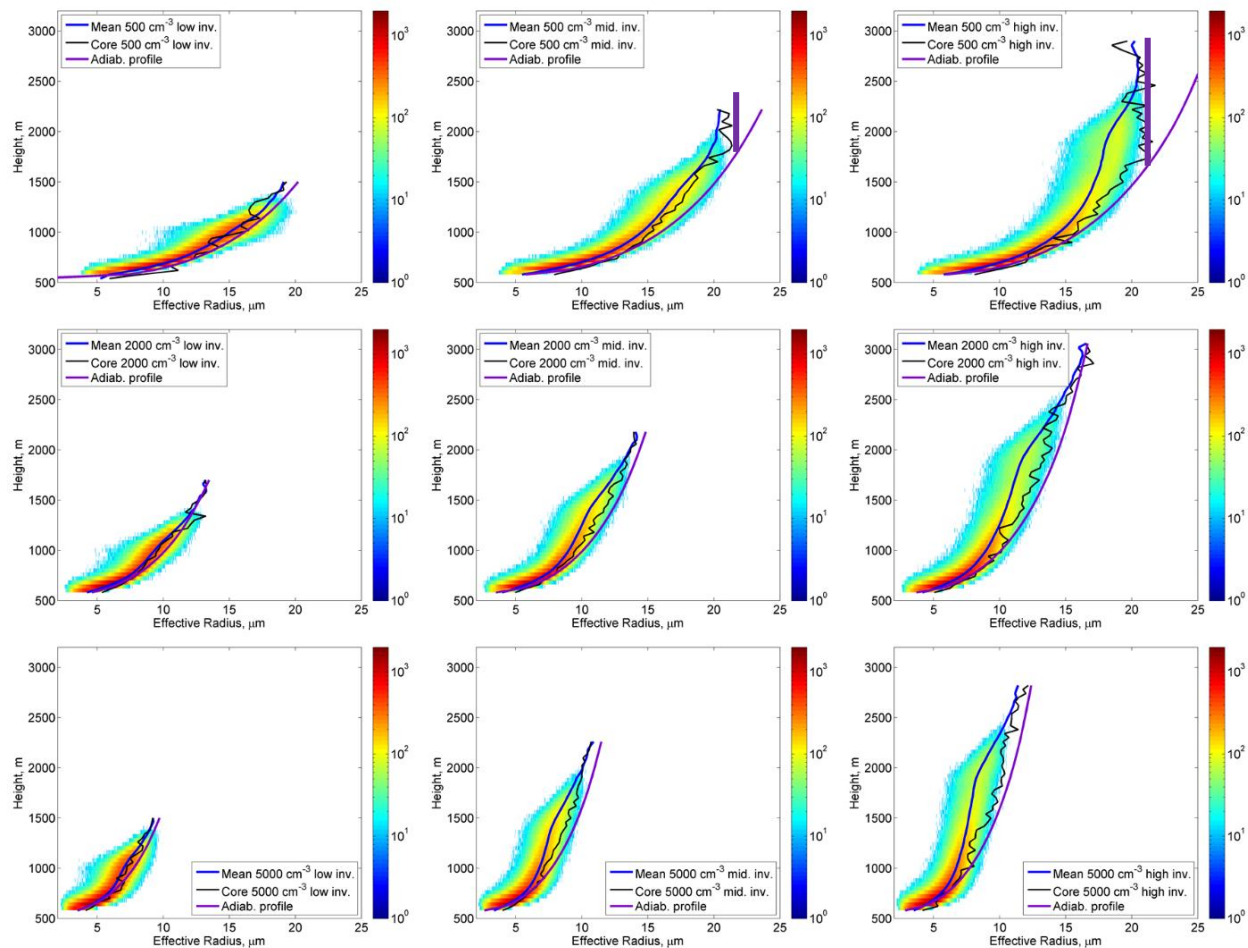


Polluted



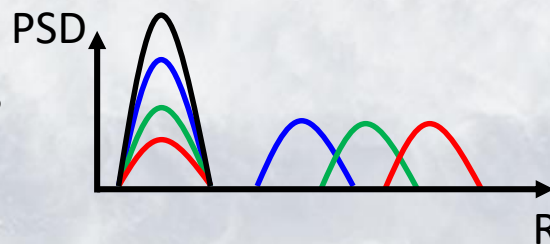


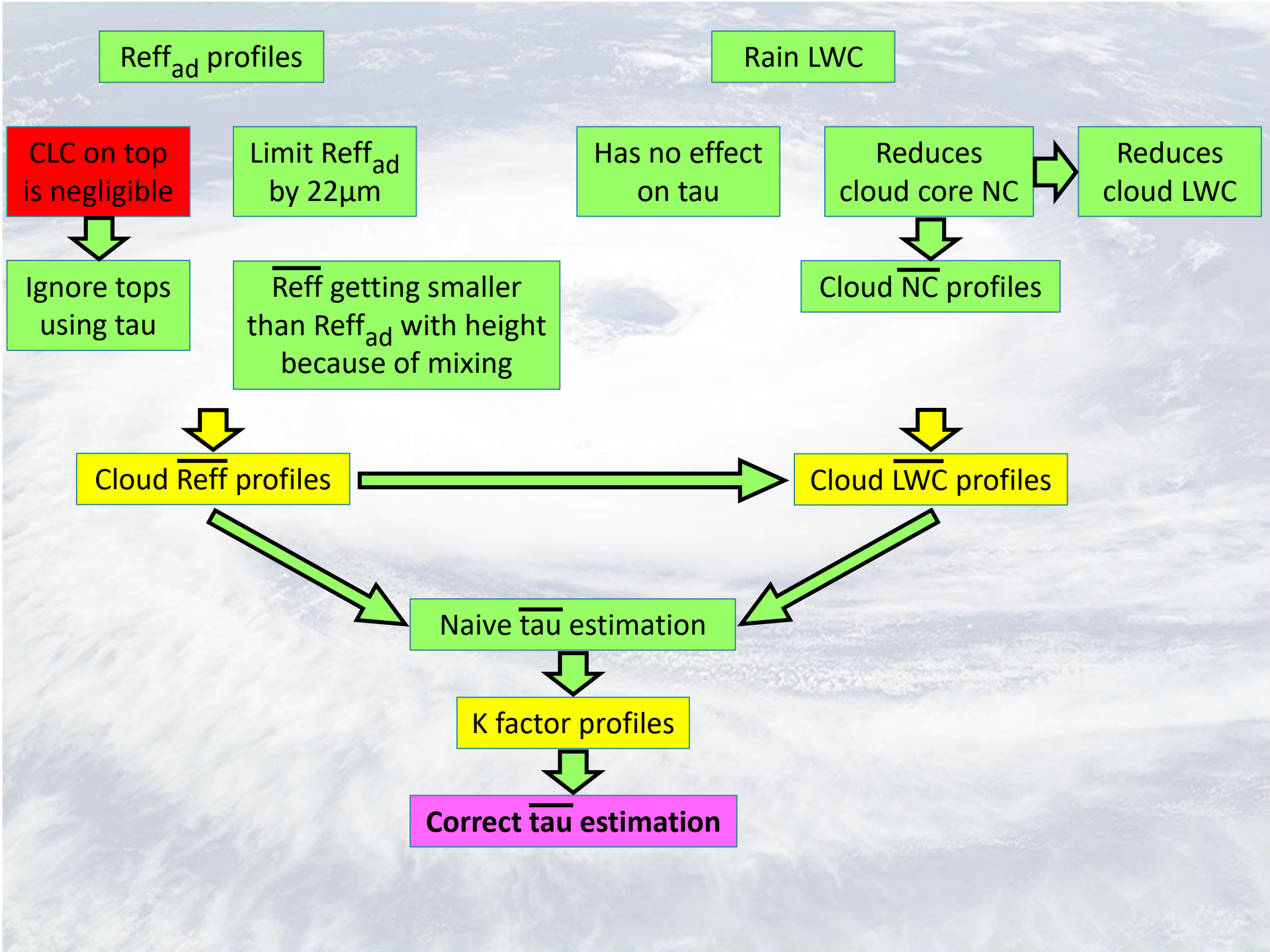
Reff_{ad} profiles in different experiments



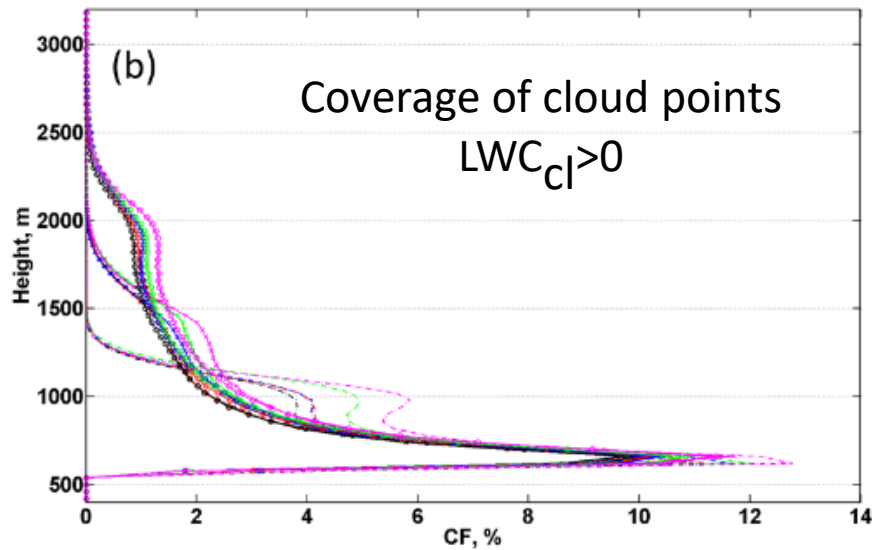
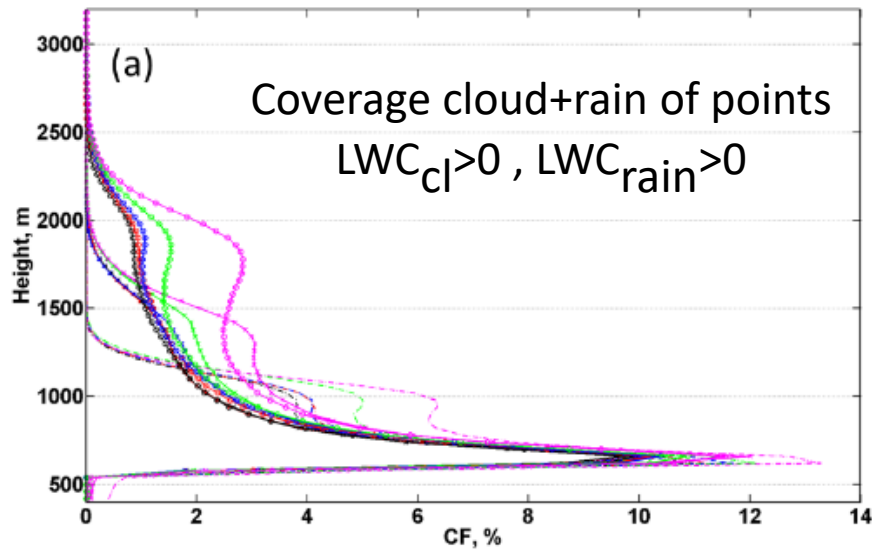
- After ~15 micron the collisions between cloud droplets intensify, which leads to further increase in Reff and to formation of first drizzle.
- When drizzle occurs, it grows via collection of cloud droplets
- This collection is much more efficient than of cloud droplets, limiting them by ~22 micron (“wash out” regime)

In the clean simulations some rain occurs:

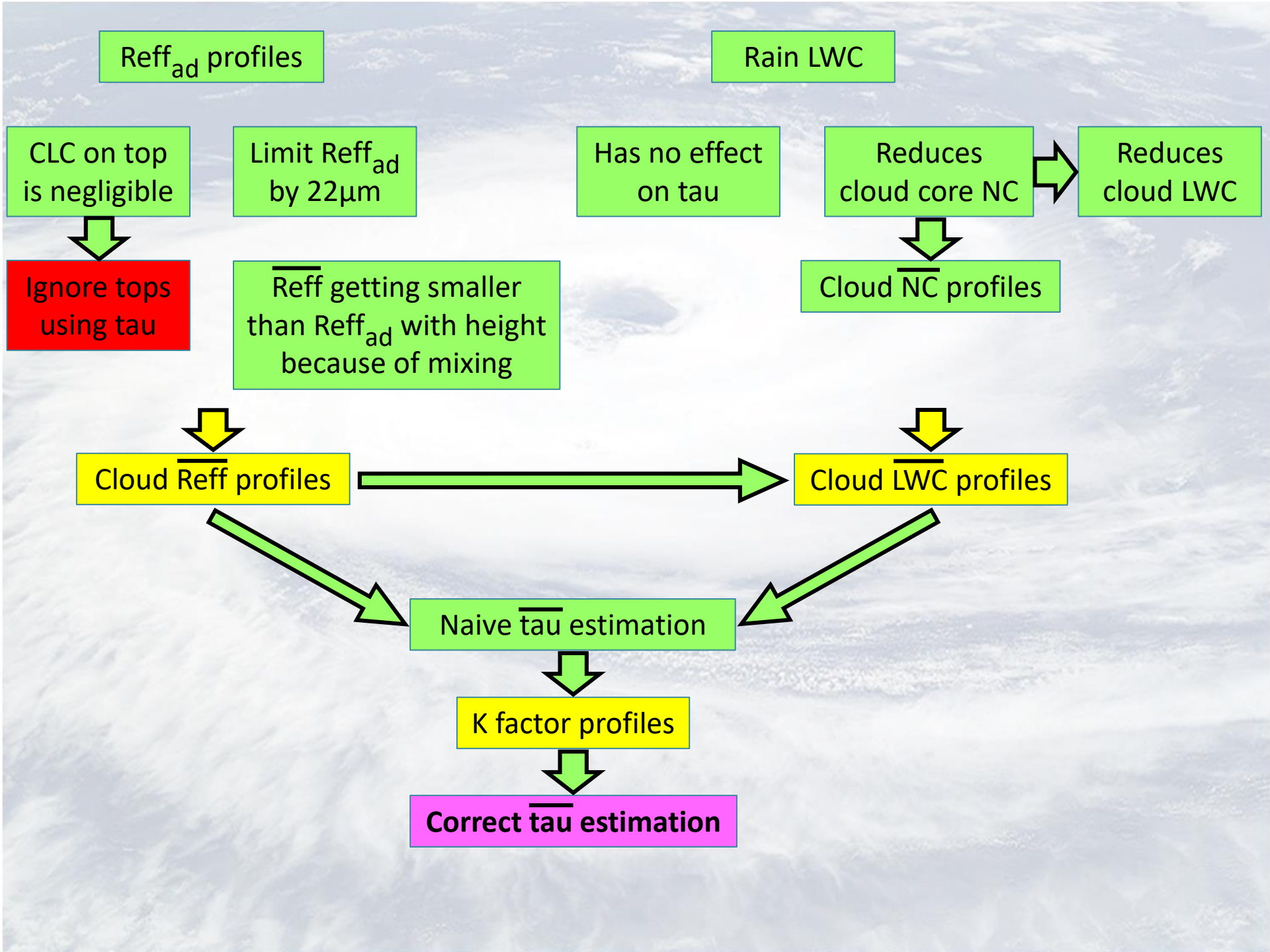




Cloud Fraction in different experiments



- 5000 cm⁻³ low inv.
- 3000 cm⁻³ low inv.
- 2000 cm⁻³ low inv.
- 1000 cm⁻³ low inv.
- 500 cm⁻³ low inv.
- 5000 cm⁻³ mid. inv.
- 3000 cm⁻³ mid. inv.
- 2000 cm⁻³ mid. inv.
- 1000 cm⁻³ mid. inv.
- 500 cm⁻³ mid. inv.
- 5000 cm⁻³ high inv.
- 3000 cm⁻³ high inv.
- 2000 cm⁻³ high inv.
- 1000 cm⁻³ high inv.
- 500 cm⁻³ high inv.



Optical Depth in different experiments

Q - Cloud LWC
 R - Cloud Reff

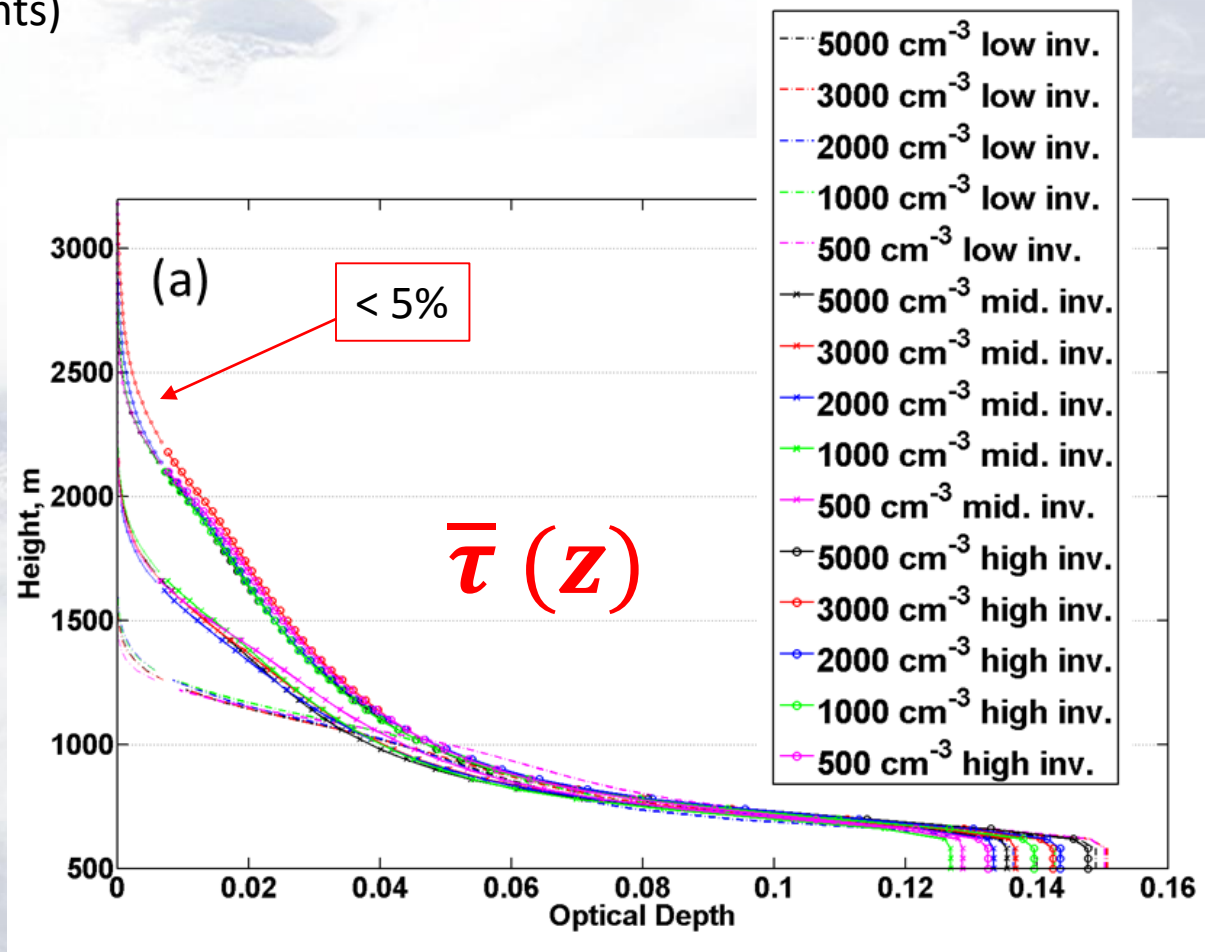
$$\tau(x, y, z) = \int_z^{top} \frac{3}{2\rho_w} \frac{Q(x, y, z')}{R(x, y, z')} dz'$$

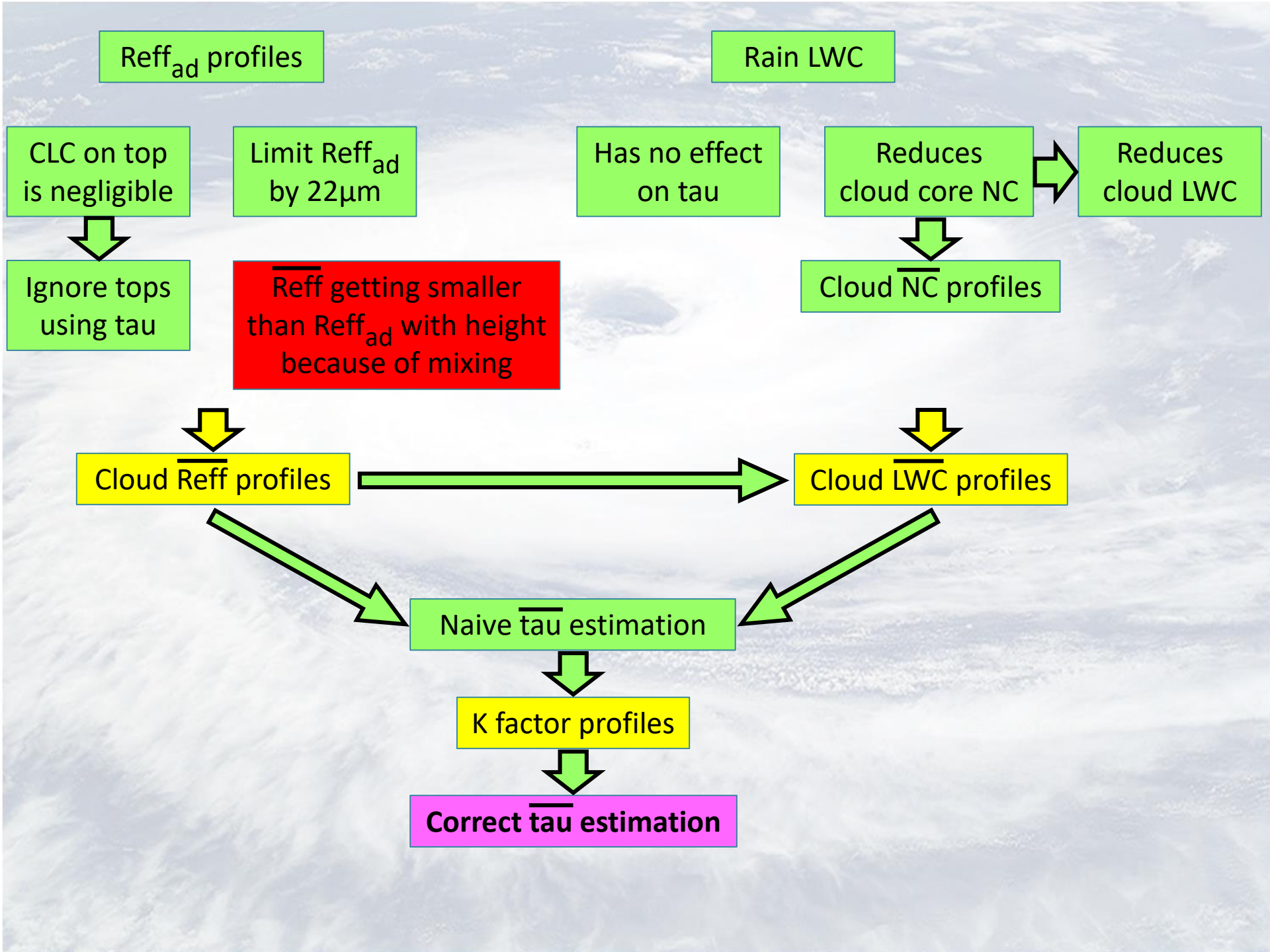
(In geometric apx.)

Mean over entire domain
 (both cloudy and not cloudy points)

➔ $e^{-\bar{\tau}(z)} \equiv \overline{e^{-\tau(x, y, z)}}^{x, y}$

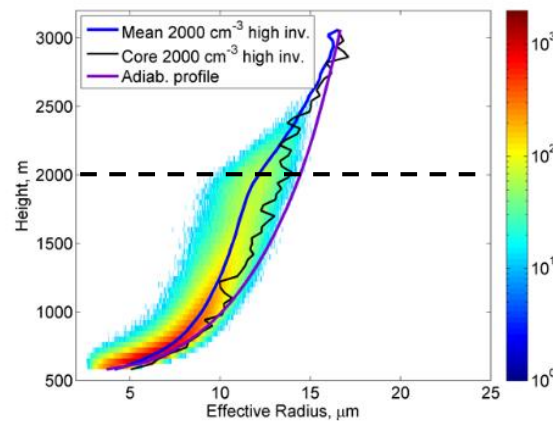
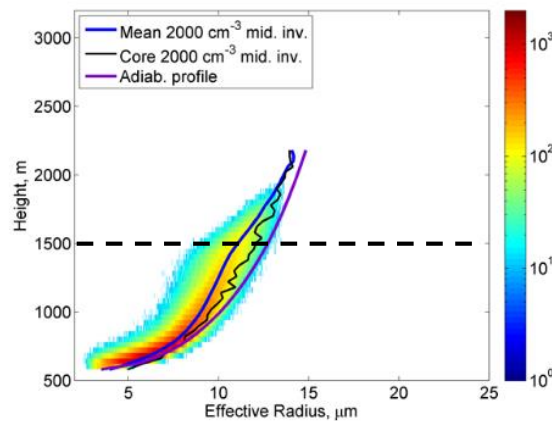
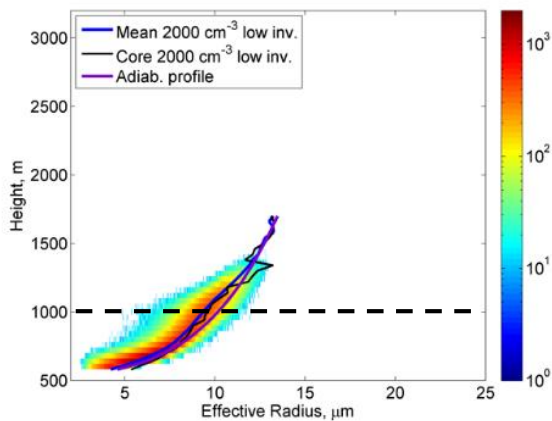
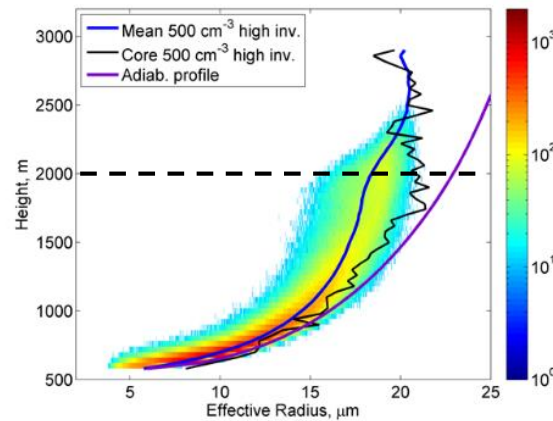
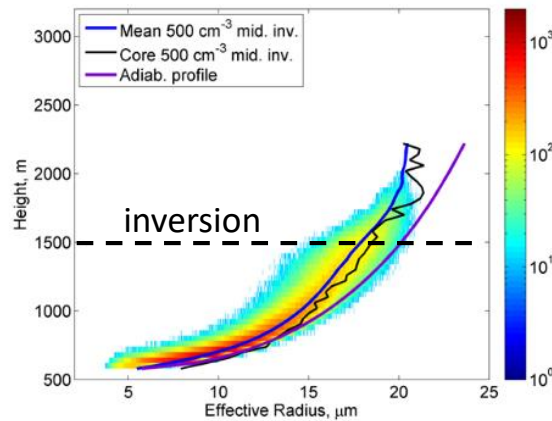
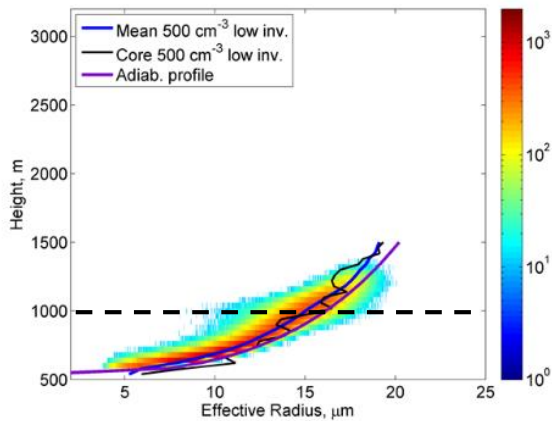
We ignore cloud tops
 because of small
 cloud fraction



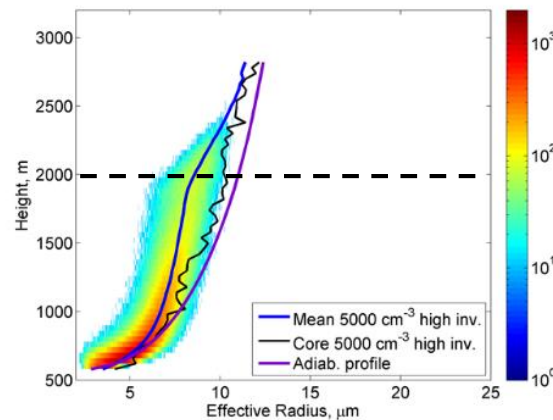
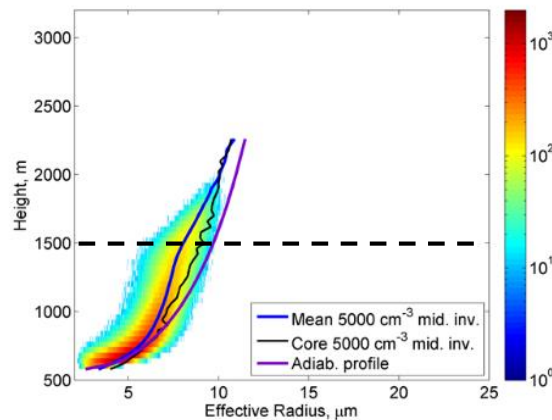
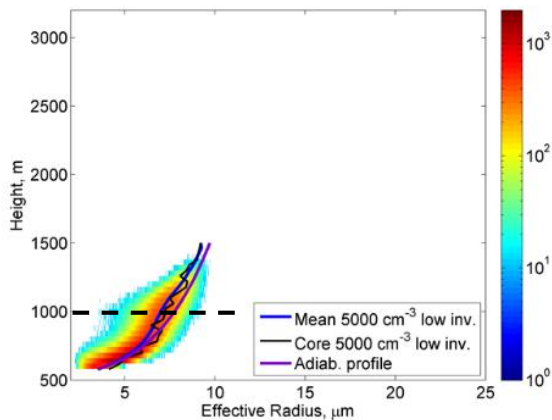


Recall: Reff_{ad} profiles

Clean

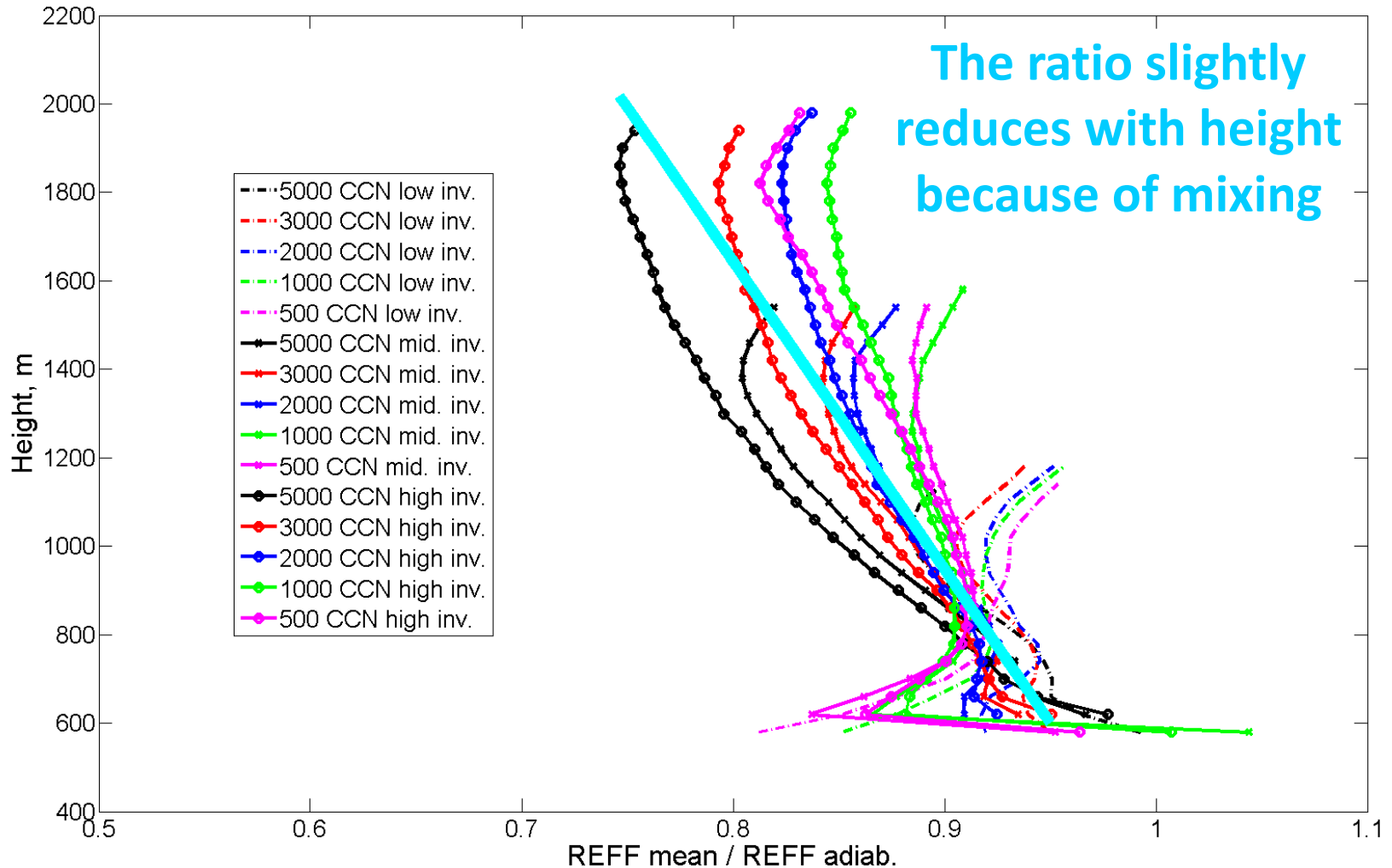


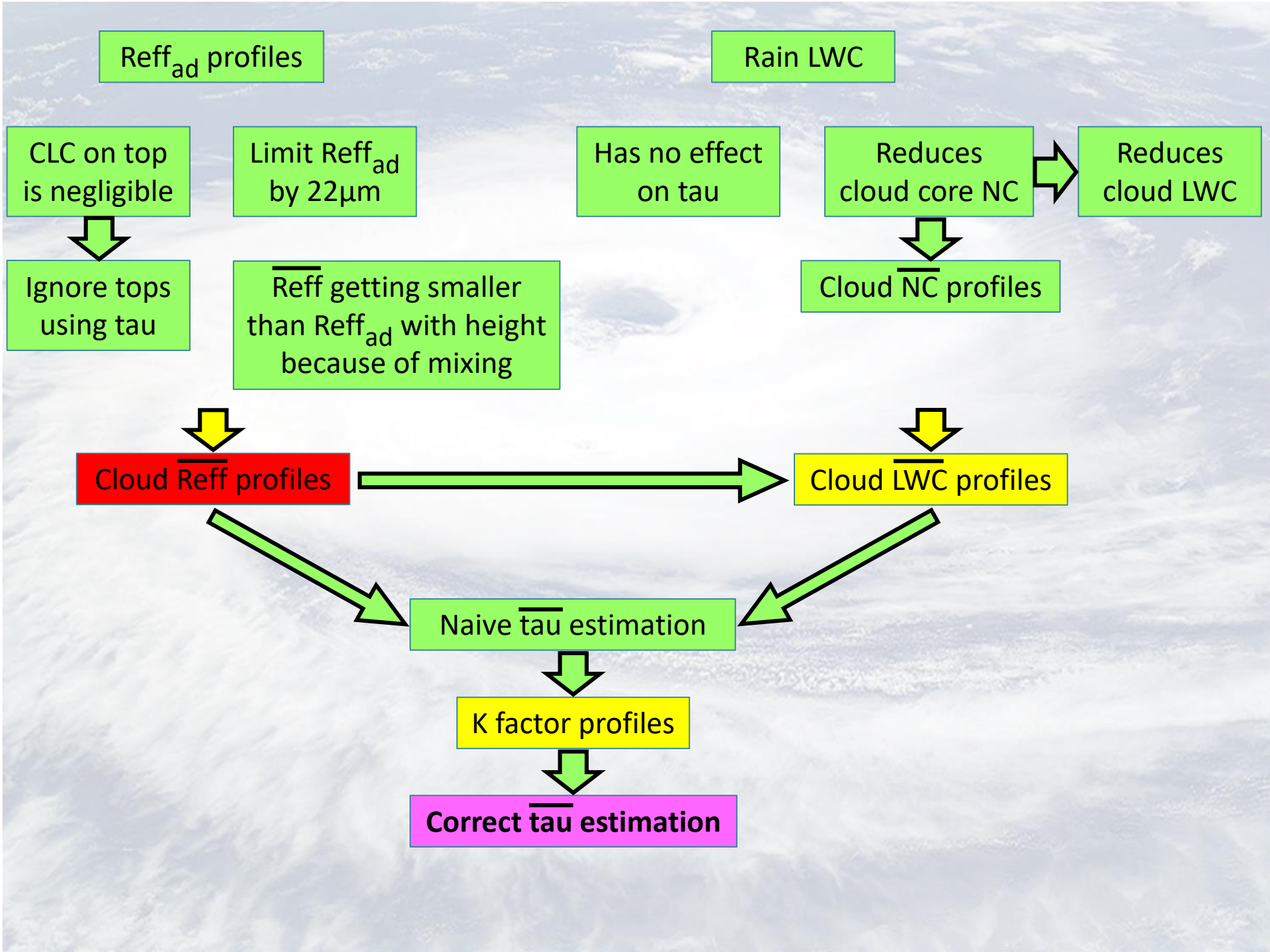
Polluted



Linear fit for the ratio $\overline{\text{Reff}}/\text{Reff}_{\text{ad}}$

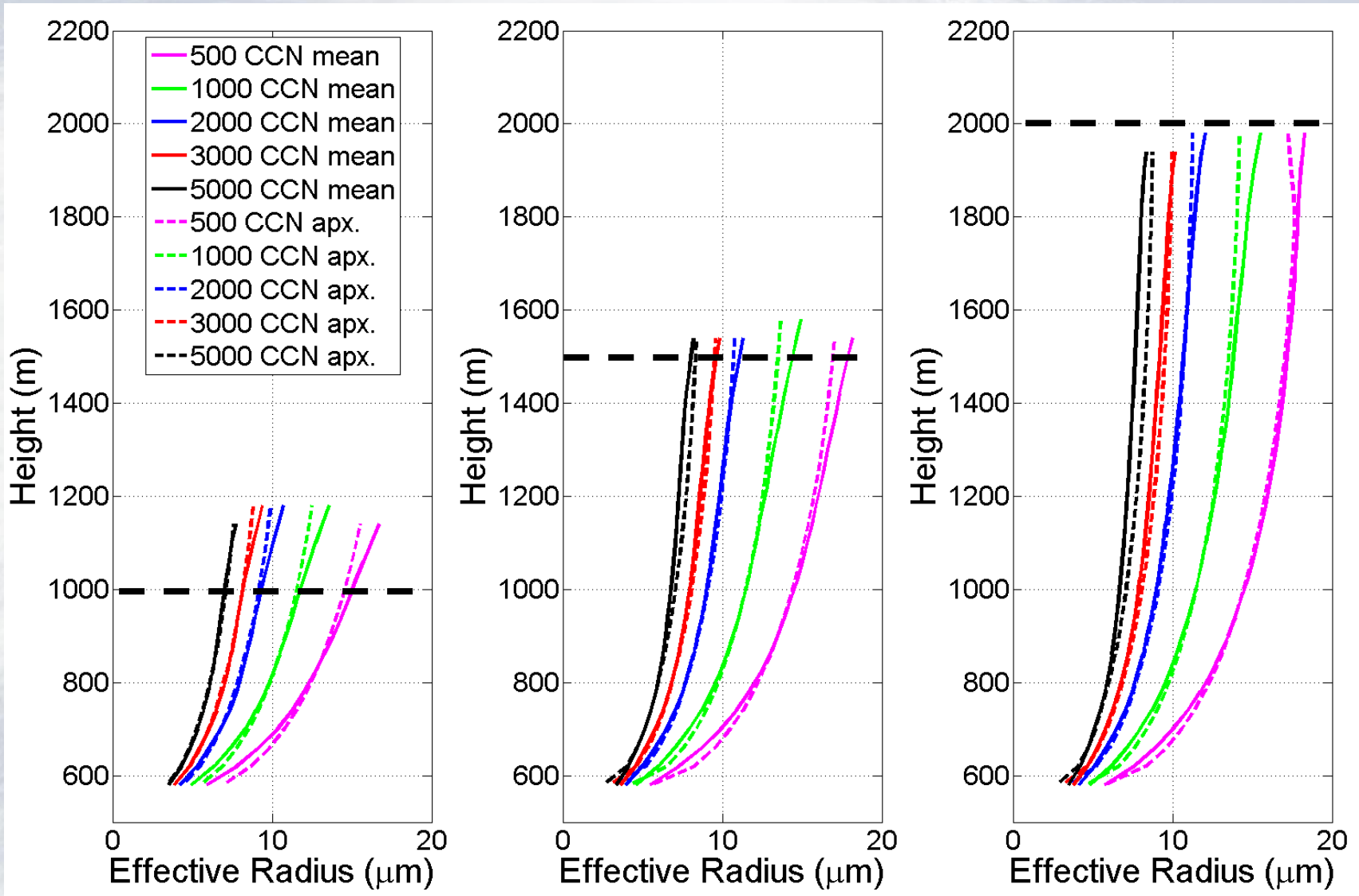
Mean=0.87944 STD=0.048072 ignored levels = 5 % of opt. depth $\text{Reff}_{\text{max}}=22\mu\text{m}$
Fit: $h=-6959.7278(r_e/r_{\text{ad}})+7211.7414$

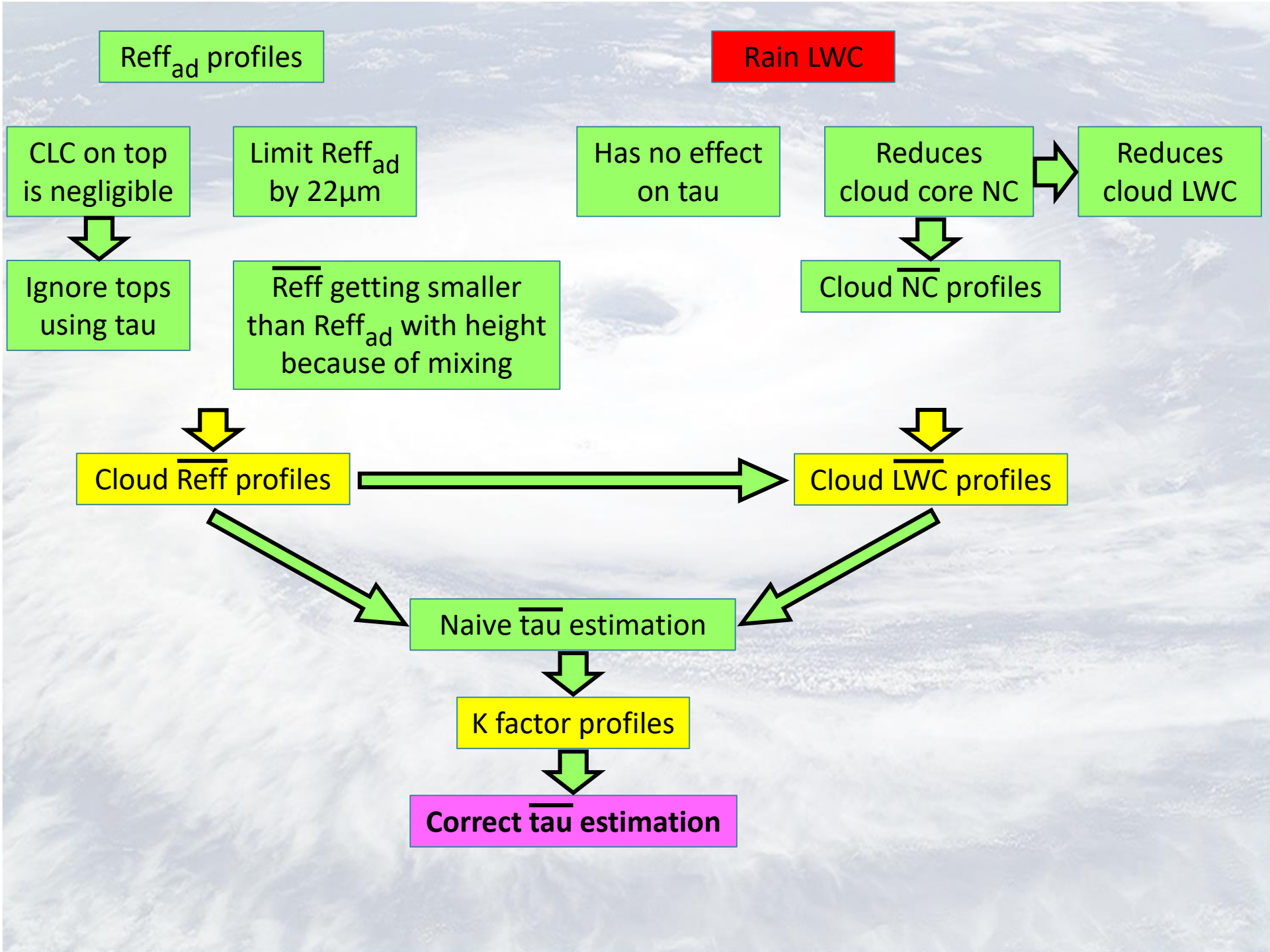




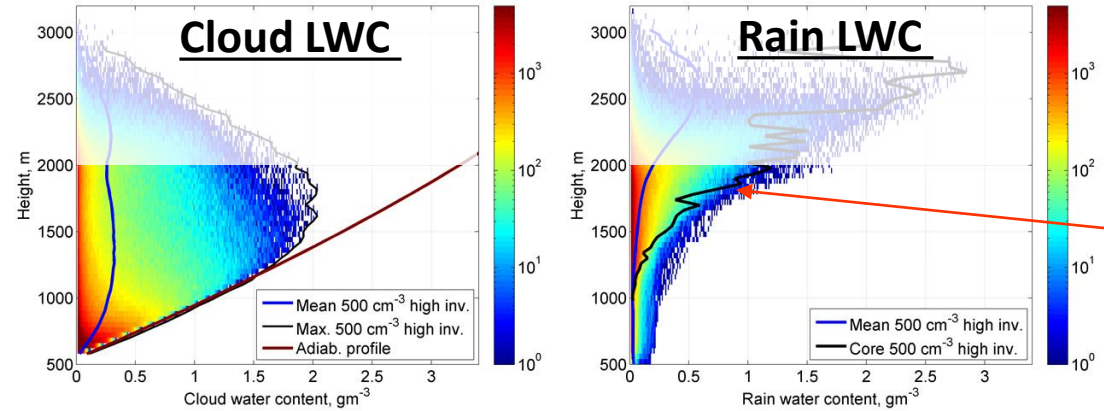
Parametrization for $\overline{\text{Reff}}(z, \text{NC}_{\text{cloud base}})$

The profiles are universal: the smaller clouds behave as lower parts of larger clouds

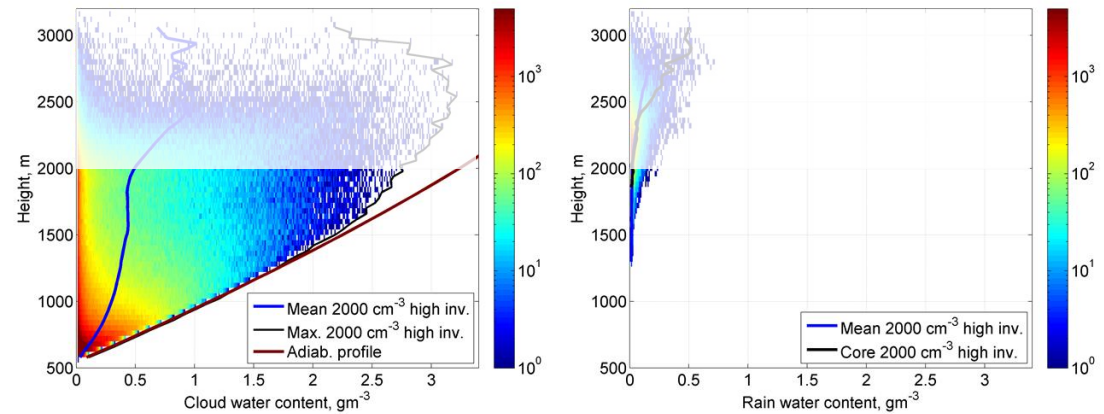




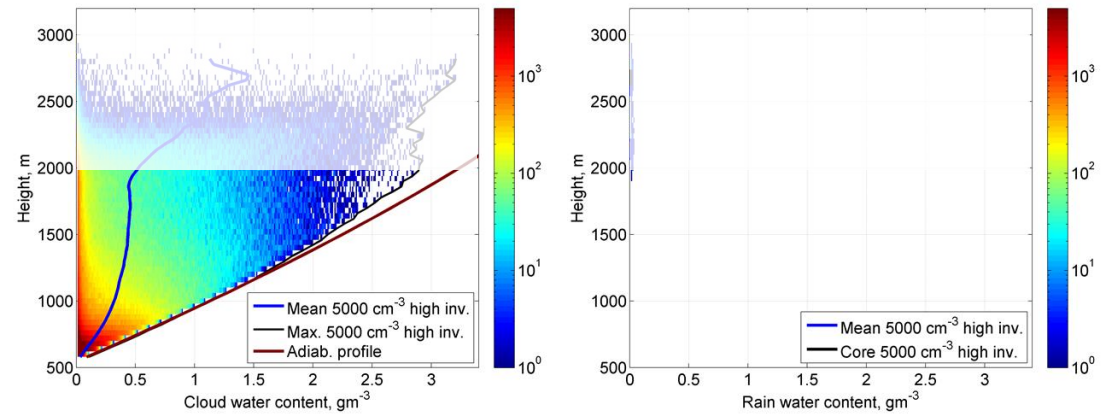
Cloud LWC and Rain LWC in different experiments

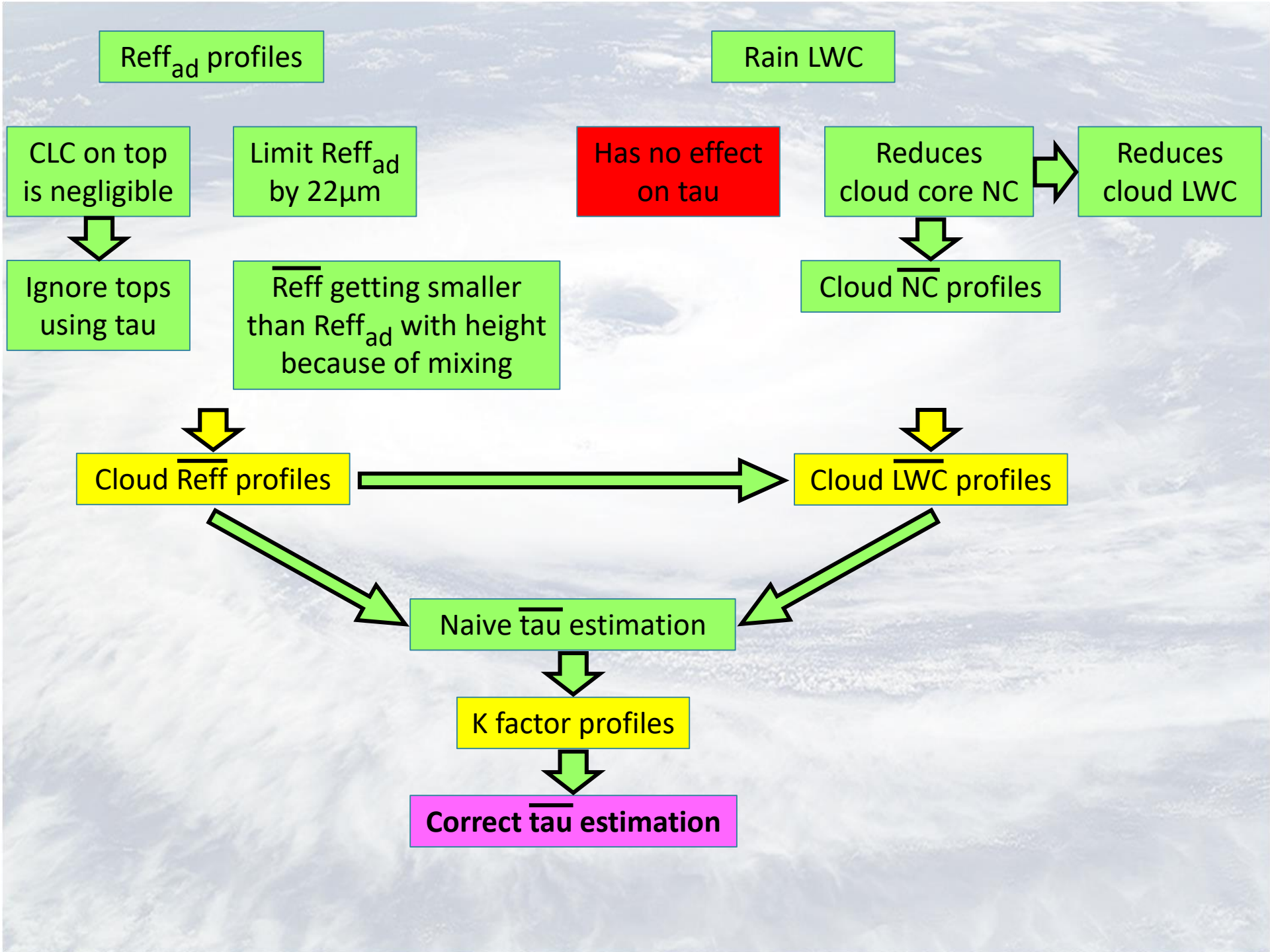


Note that rain forms in cloud cores!



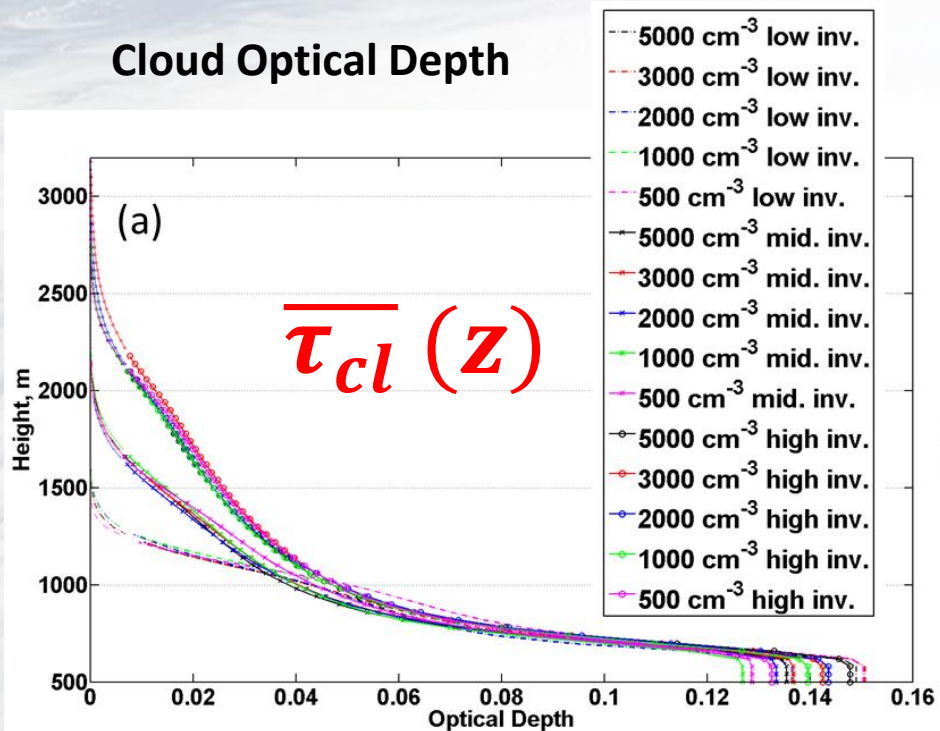
In $\text{CCN}=500$ (and 1000) cm^{-3} experiments there is still significant **rain water content**



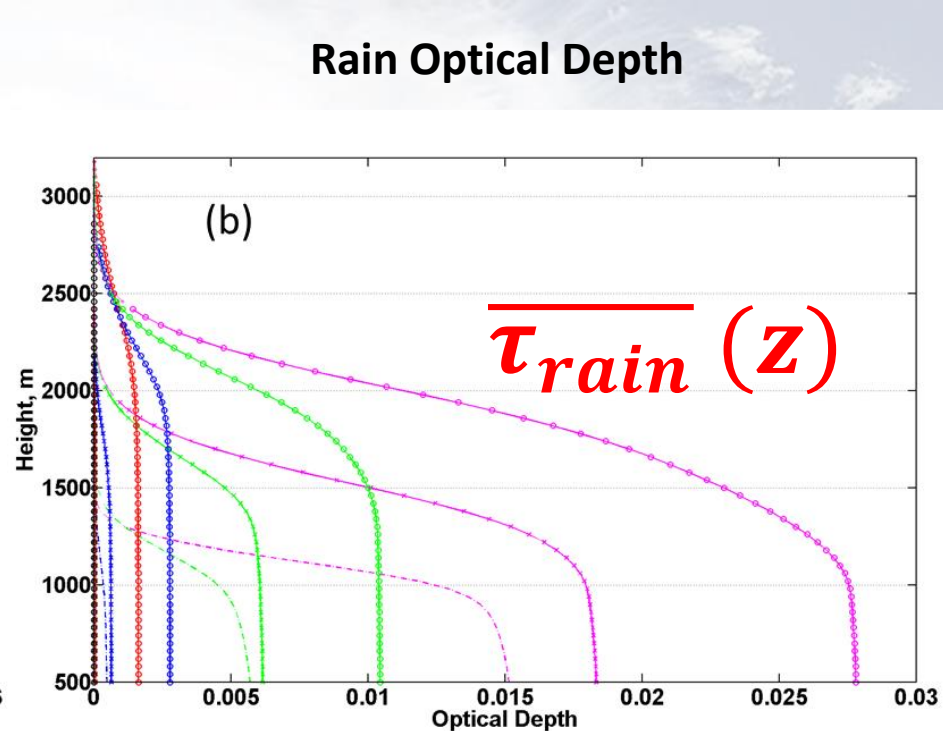


Cloud Optical Depth and Rain OD in different experiments

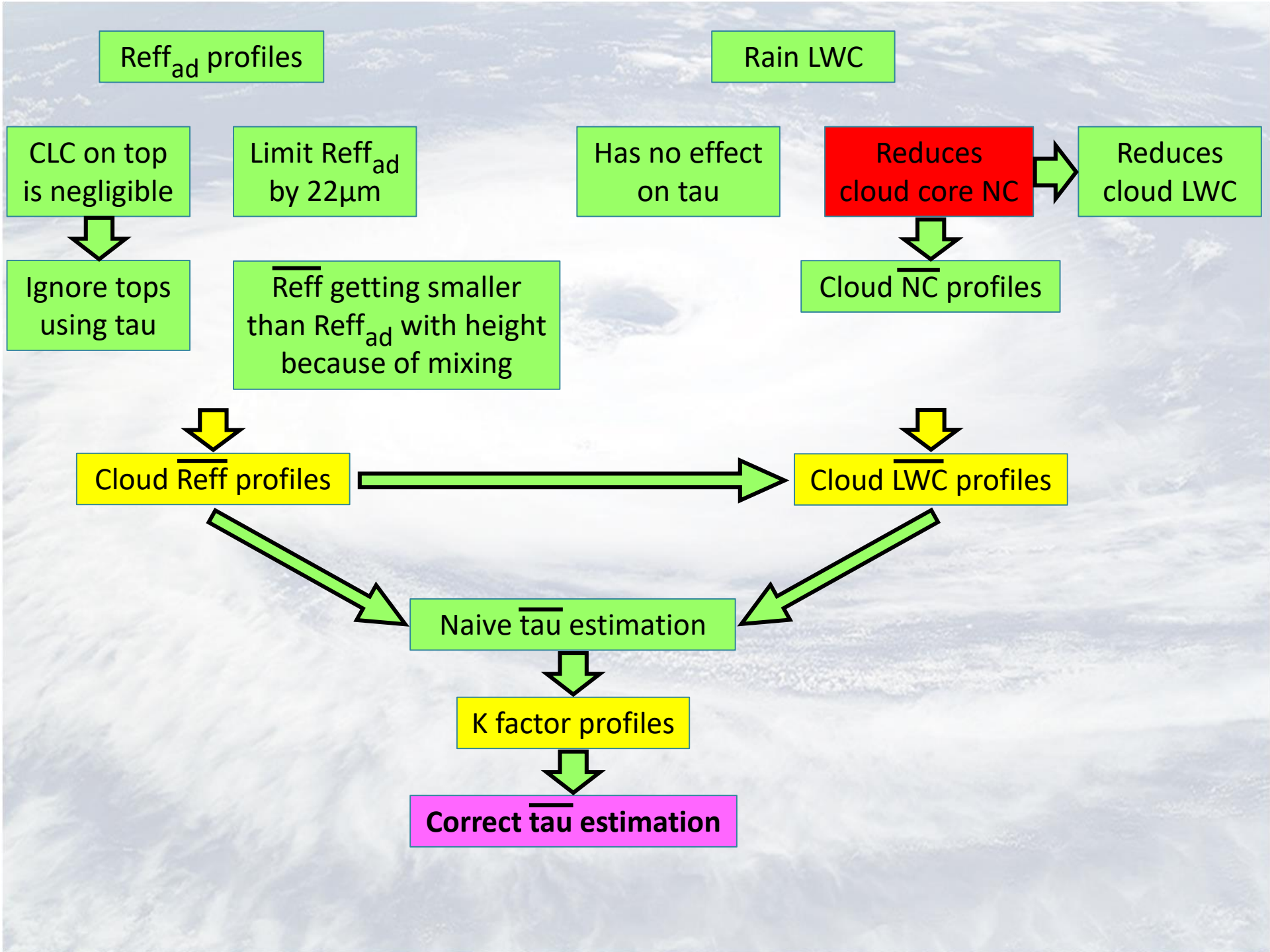
Cloud Optical Depth



Rain Optical Depth

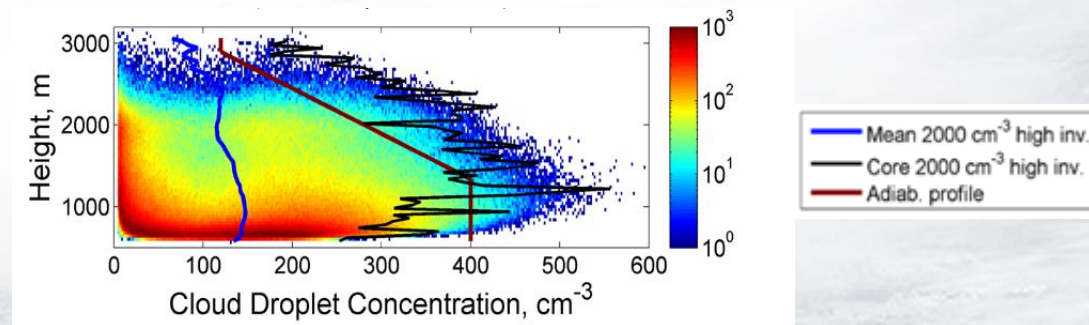
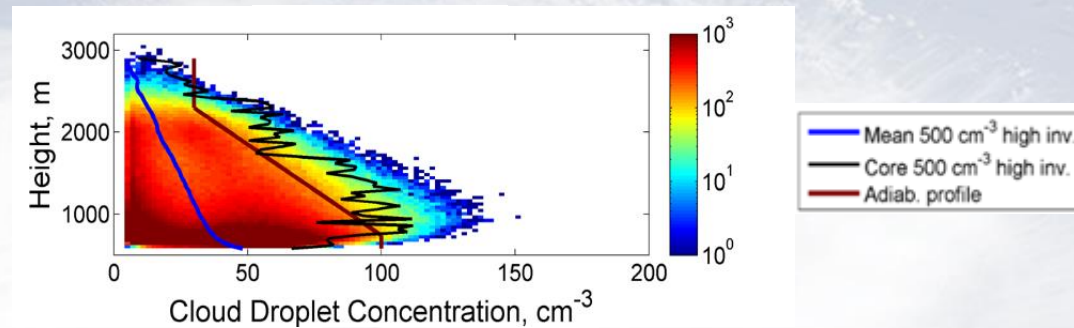


No effect!

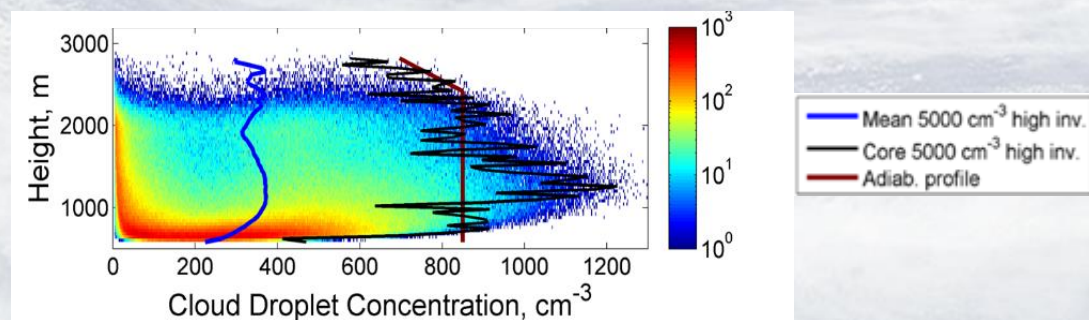


Reduction of cloud core NC with height due to rain

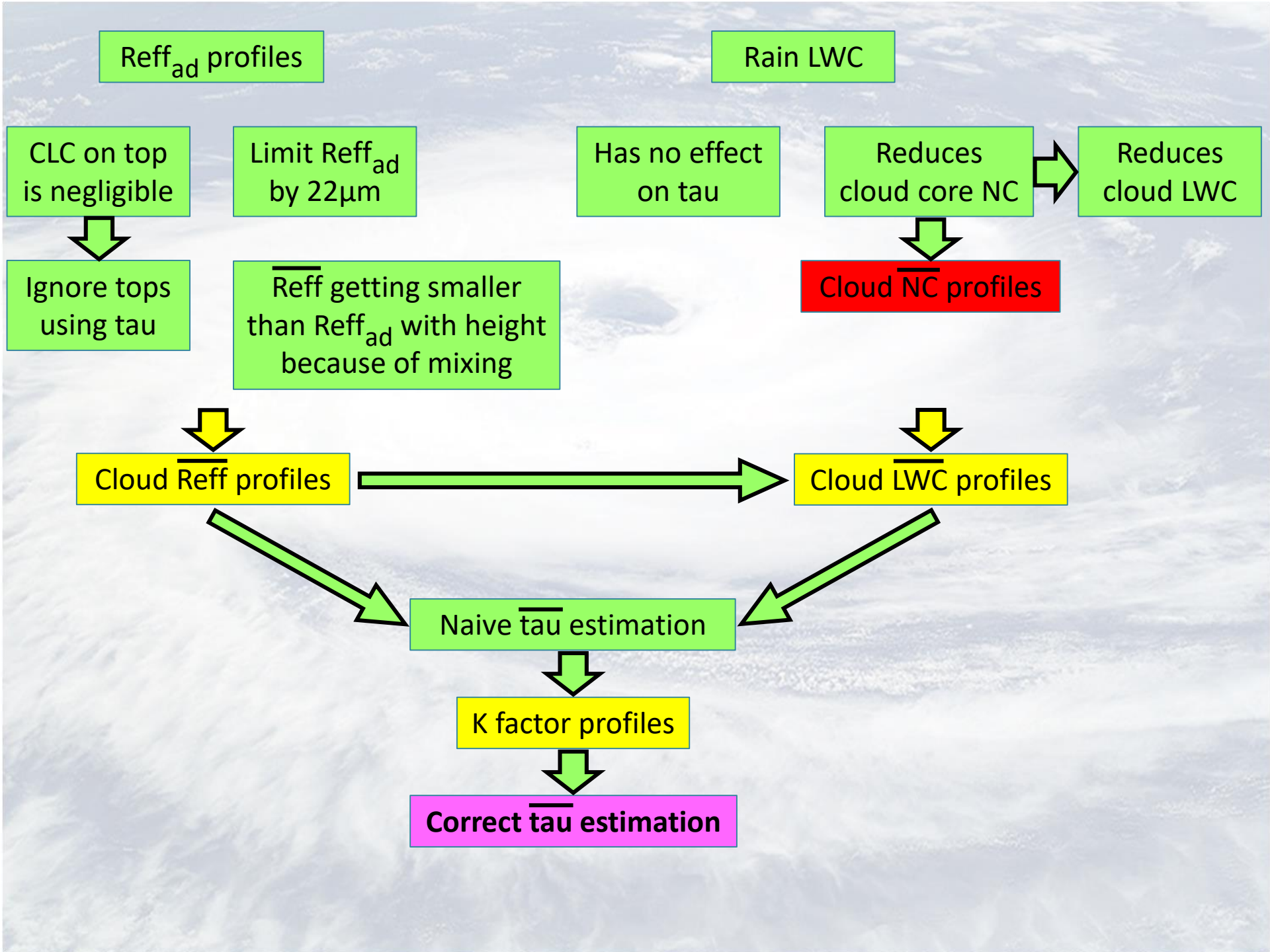
Clean



Polluted



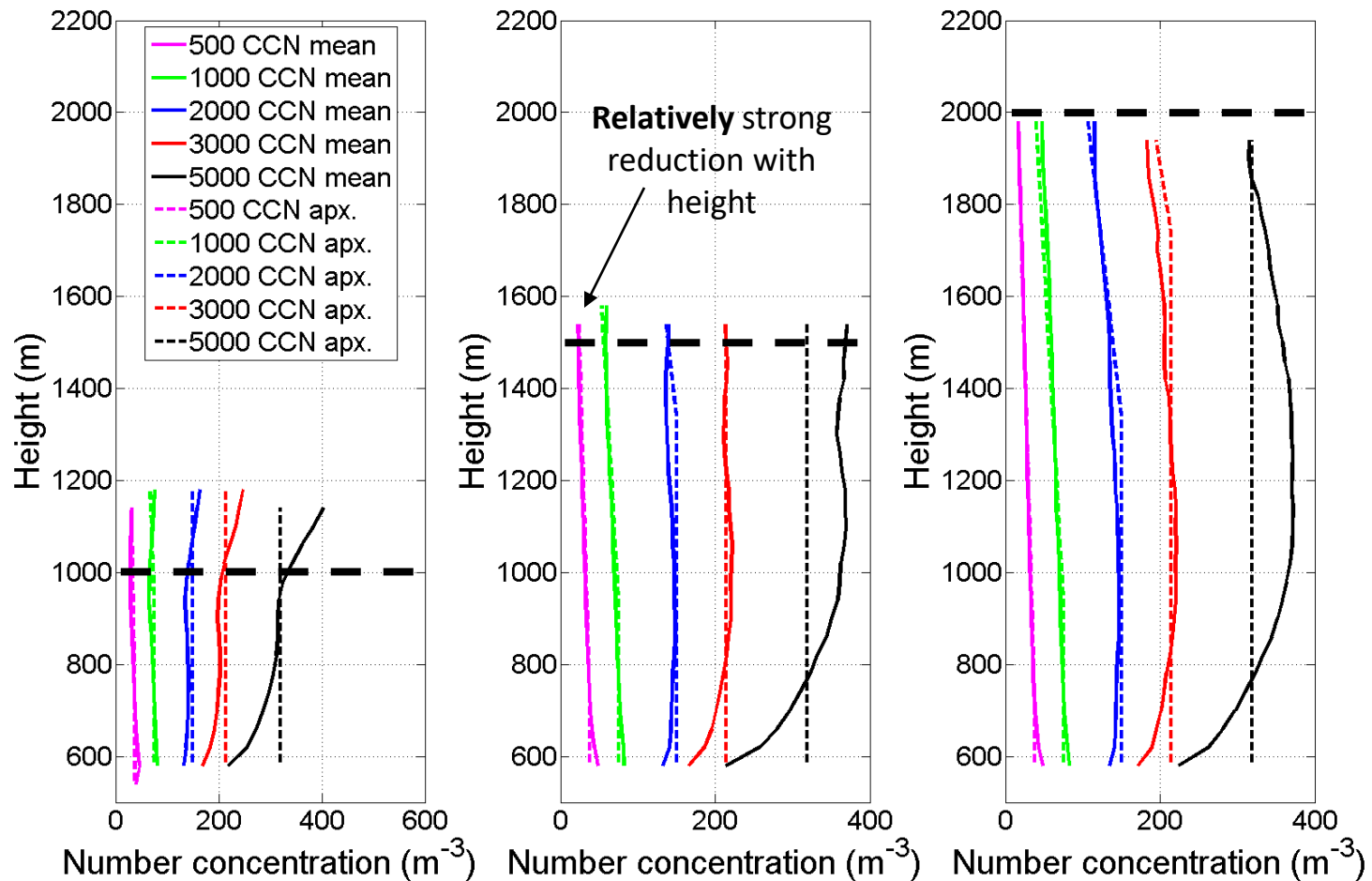
$$NC_{max}(z) = \begin{cases} NC_{cl\ base}, & \text{below the level } z_{12}, \text{ where } r_{e_ad} = 12\mu\text{m} \\ NC_{cl\ base}[1 - \gamma(z - z_{12})], & \text{above the level } z_{12} \end{cases}$$

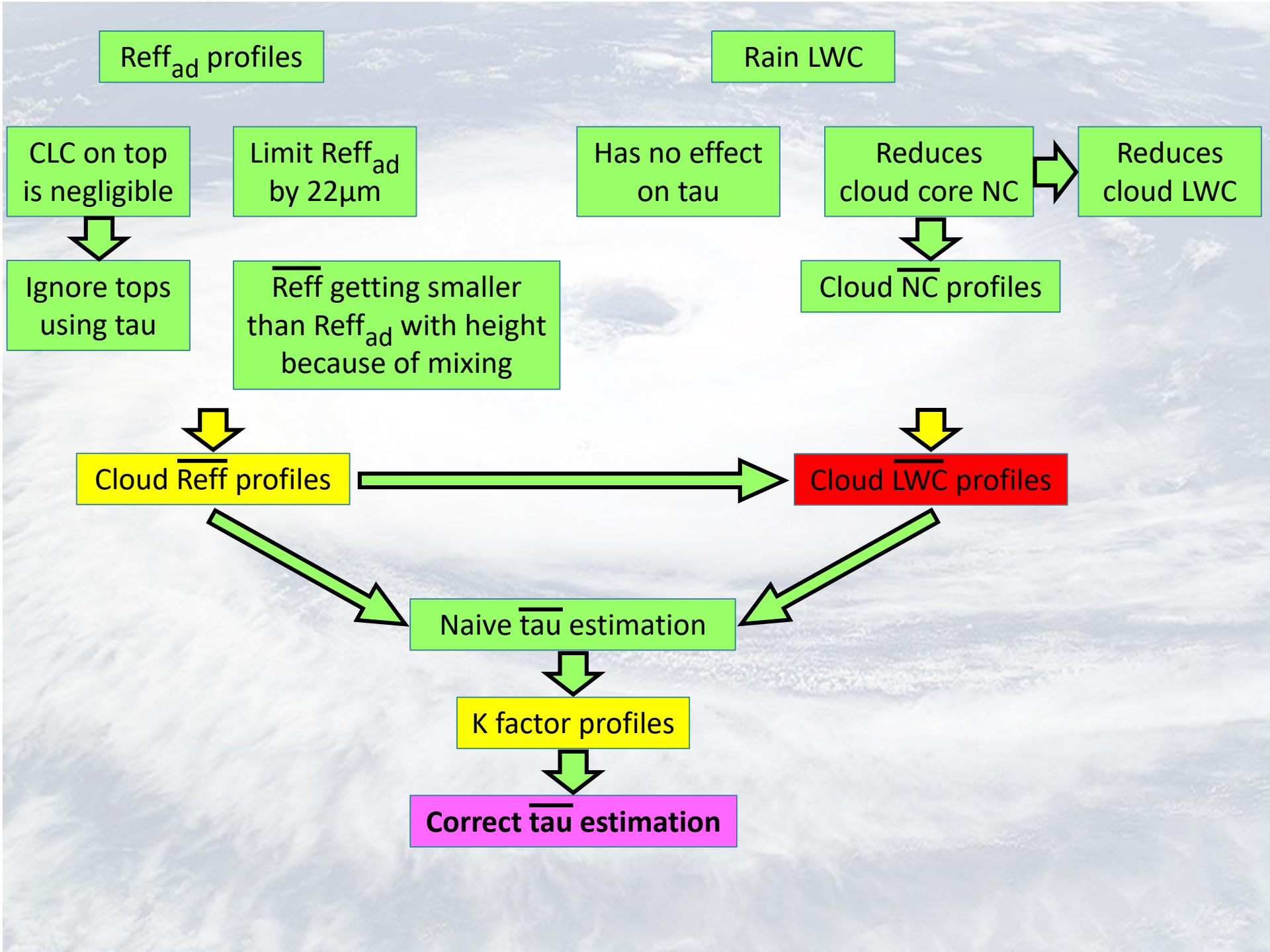


Parametrization for $\overline{NC}(z, NC_{cloud\ base})$

$$\overline{NC}(z) \approx \beta NC_{max}(z)$$

on average (over all heights and simulations) $\beta = 0.38$ with standard deviation of 0.03

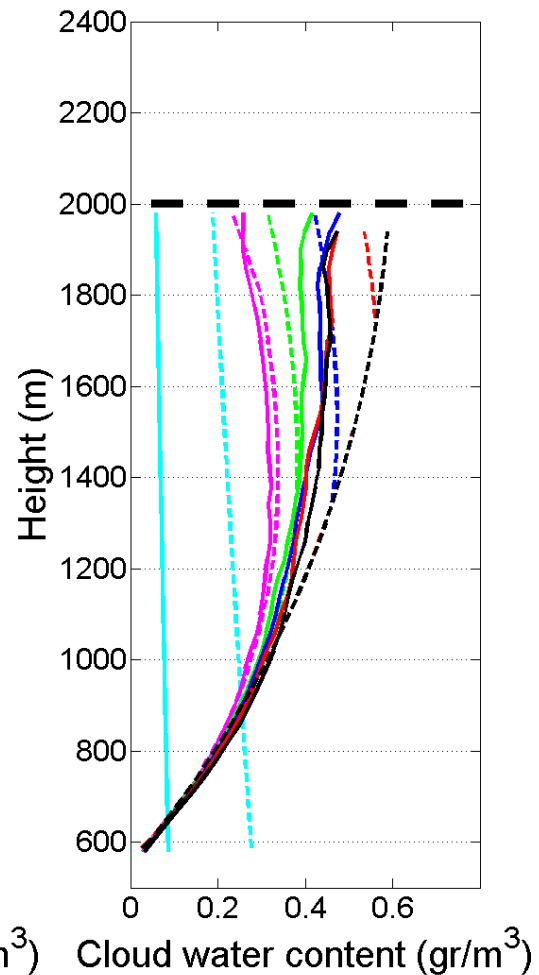
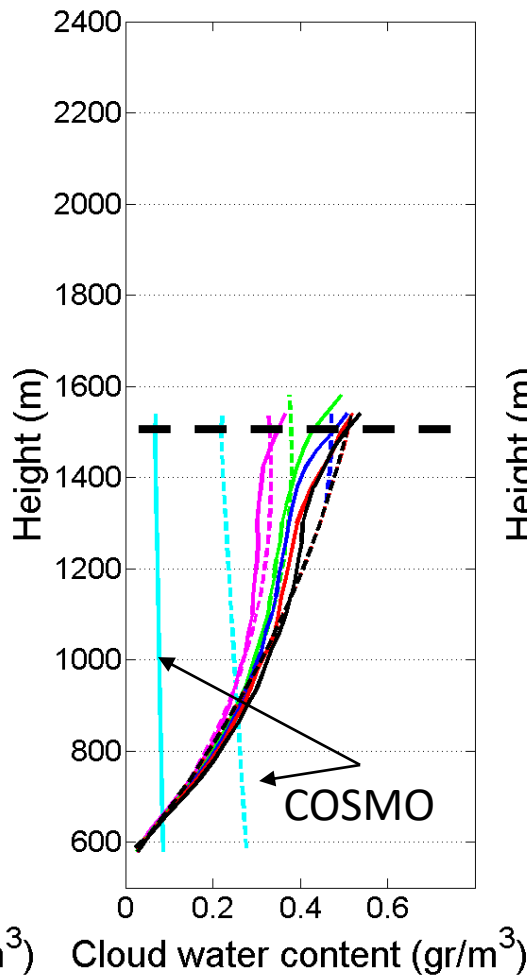
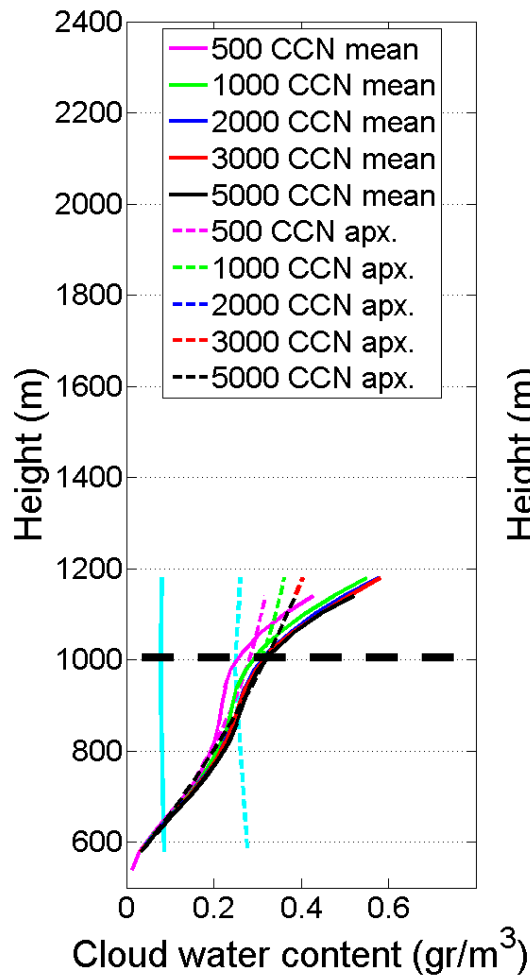




Parametrization for $\overline{LWC}(z, NC_{cloud\ base})$

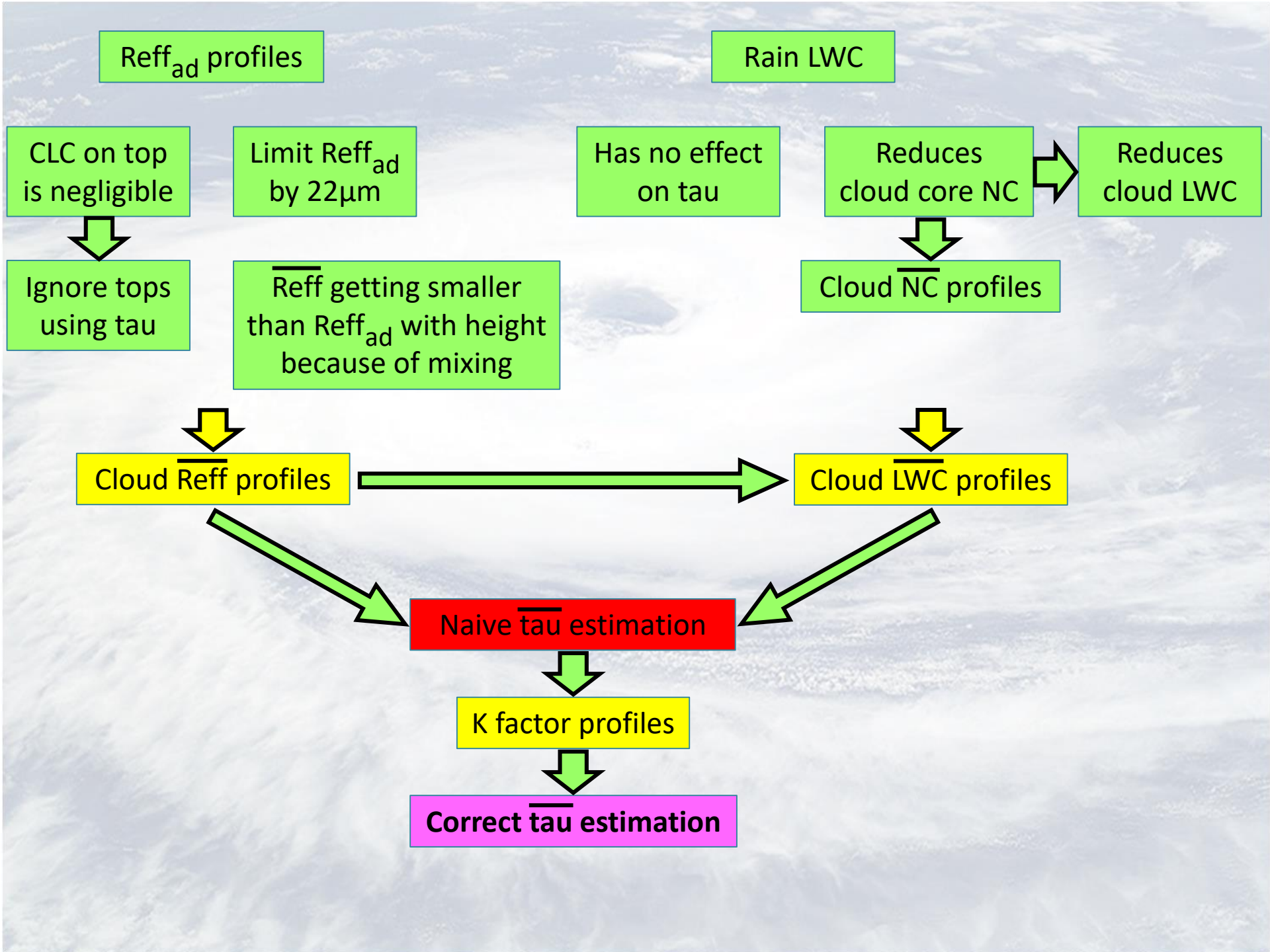
$$\overline{LWC}(z) = \overline{\frac{4}{3} \pi \rho_w N_d(z) r_v^3(z)} = \overline{\frac{4}{3} \pi \rho_w N_d(z) \left(\frac{r_e(z)}{1.15}\right)^3} \approx \frac{4}{3} \pi \rho_w \overline{N_d}(z) \left(\frac{\overline{r_e}(z)}{1.15}\right)^3$$

$\overline{r_e} \approx \text{const horizontally}$



Outline

1. Motivation
2. COSMO new parametrization (**p1**) of SGS cloud properties (for radiation)
3. COSMO new parametrization (**p2**) based on LES simulations
 - A. Simulations design
 - B. Schematic explanation: How should LWC, NC and Reff behave with height?
 - C. Parametrization of mean Reff(z) and LWC(z)
 - D.** Towards the parametrization of the Optical Depth
4. Implementation in COSMO code: (really) first results
5. Summary



Clouds-averaged Optical Depth

Q - Cloud LWC

R - Cloud Reff

$$d\tau(x, y, z) = \frac{3}{2\rho_w} \frac{Q(x, y, z)}{R(x, y, z)} dz$$

Exact Optical Depth

$$e^{-\overline{d\tau}(z)} \equiv \overline{e^{-d\tau(x, y, z)}}^{x, y}$$

Wrong Optical Depth

$$\overline{d\tau}(z) = \frac{3}{2\rho_w} \overline{\left(\frac{Q(x, y, z)}{R(x, y, z)}\right)}^{x, y} dz$$

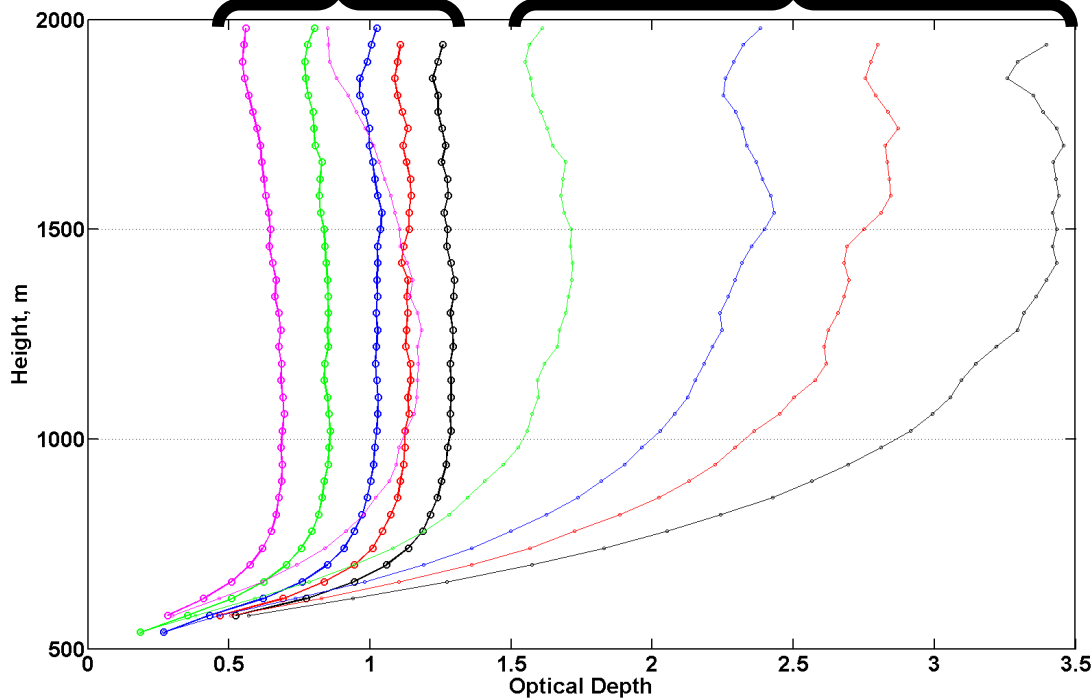
Naive fit to Optical Depth

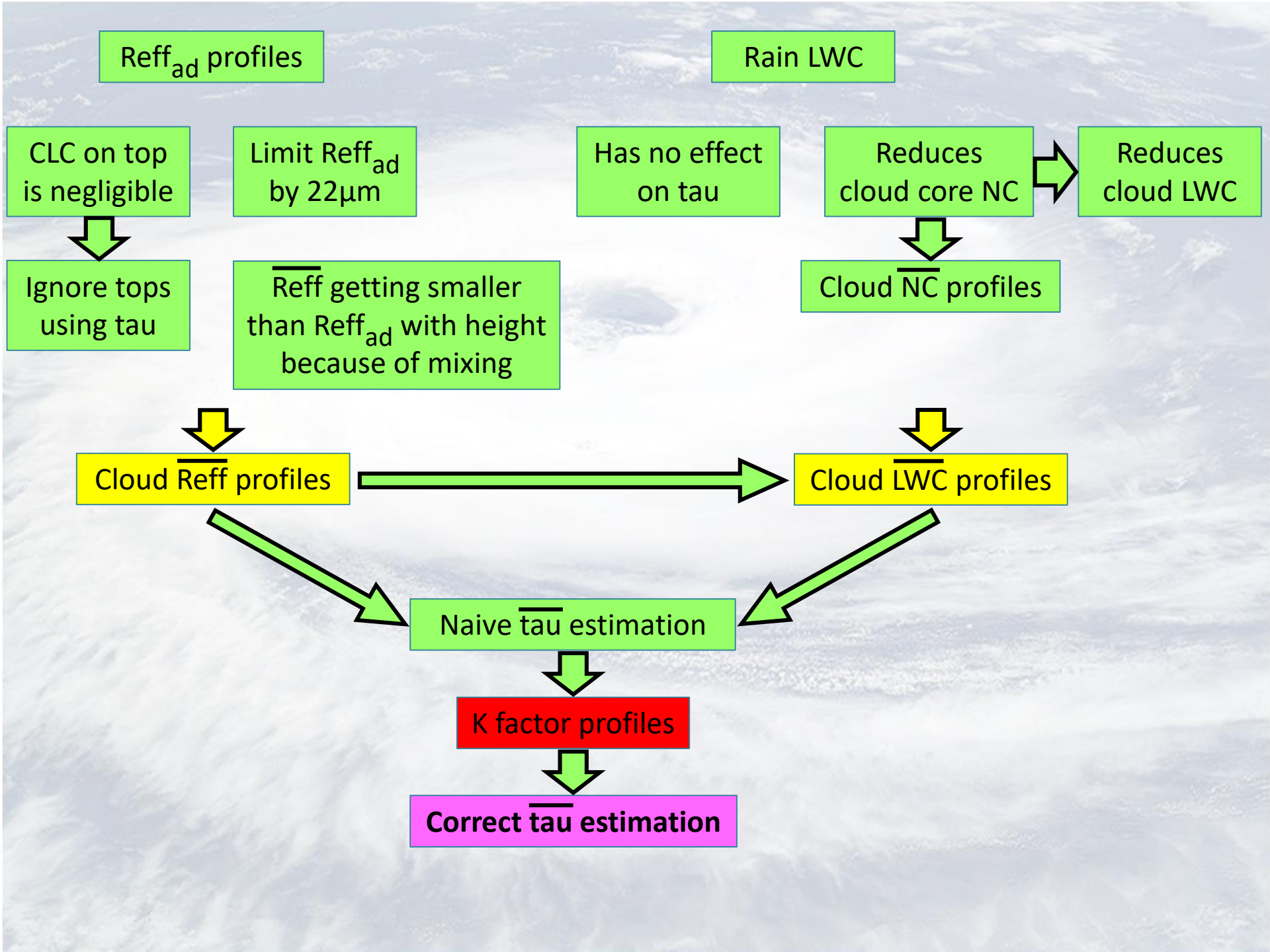
$$\overline{d\tau}(z) = \frac{3}{2\rho_w} \frac{\overline{Q}(z)}{\overline{R}(z)} dz$$

\overline{Q} - Fit for cloud avg. LWC

\overline{R} - Fit for cloud avg. Reff

$\overline{\quad}^{x, y}$
Mean
over
cloudy
points

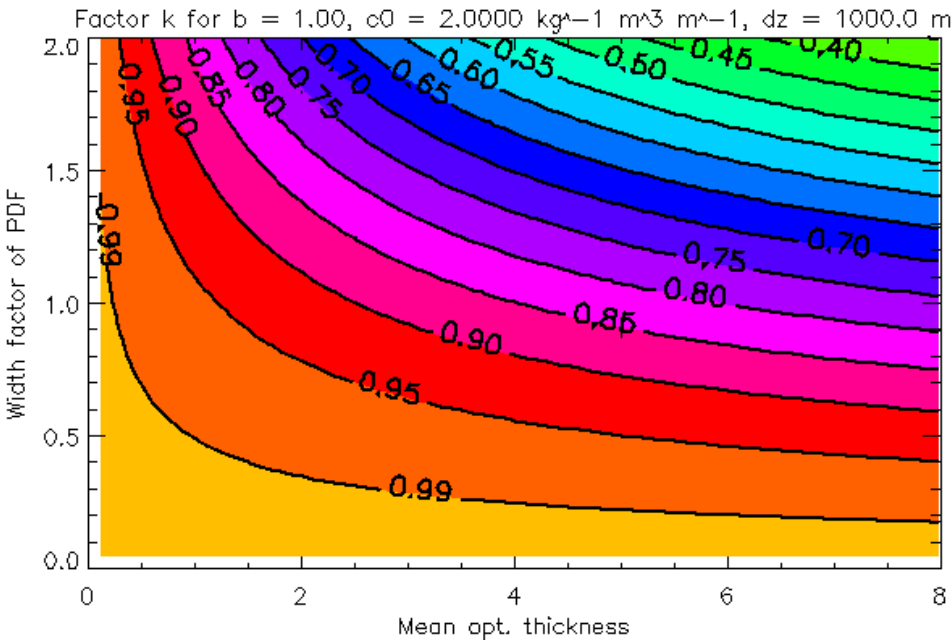




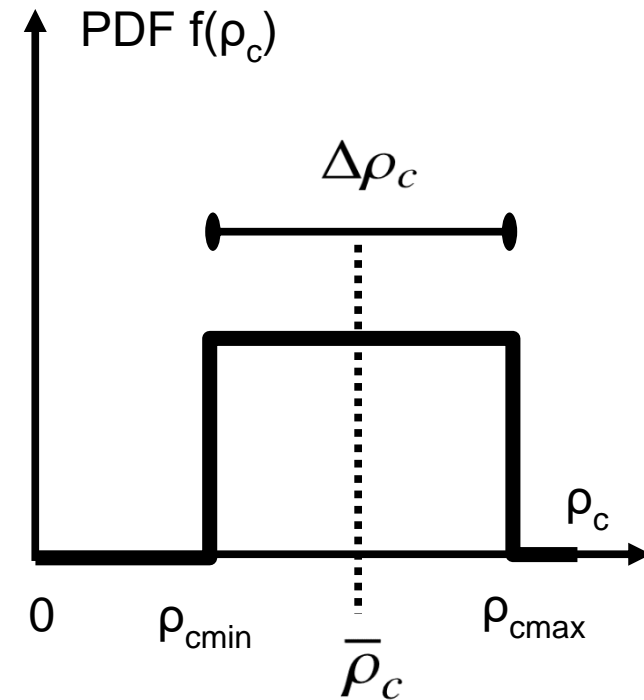
Recall: Subgridscale variability, factor K

$$e^{(-k c_0 \bar{\rho}_c \Delta z)} \stackrel{!}{=} \int_0^{\infty} PDF(\rho_c) e^{(-c_0 \rho_c \Delta z)} d\rho_c$$

$$k = \frac{1}{\bar{\tau} c_0 \bar{\rho}_c \Delta z} \ln \left[\frac{\Delta \rho_c c_0 \Delta z}{\exp(-c_0 \rho_{cmin} \Delta z) - \exp(-c_0 \rho_{cmax} \Delta z)} \right]$$



cloudy grid box ρ_c



$$\text{width factor} = \frac{\Delta \rho_c}{\bar{\rho}_c} \leq 2$$

For higher resolution, $k = 0.5$ seems too low!

Subgridscale variability, factor $K(z, NC_{\text{cloud base}})$

Exact Optical Depth

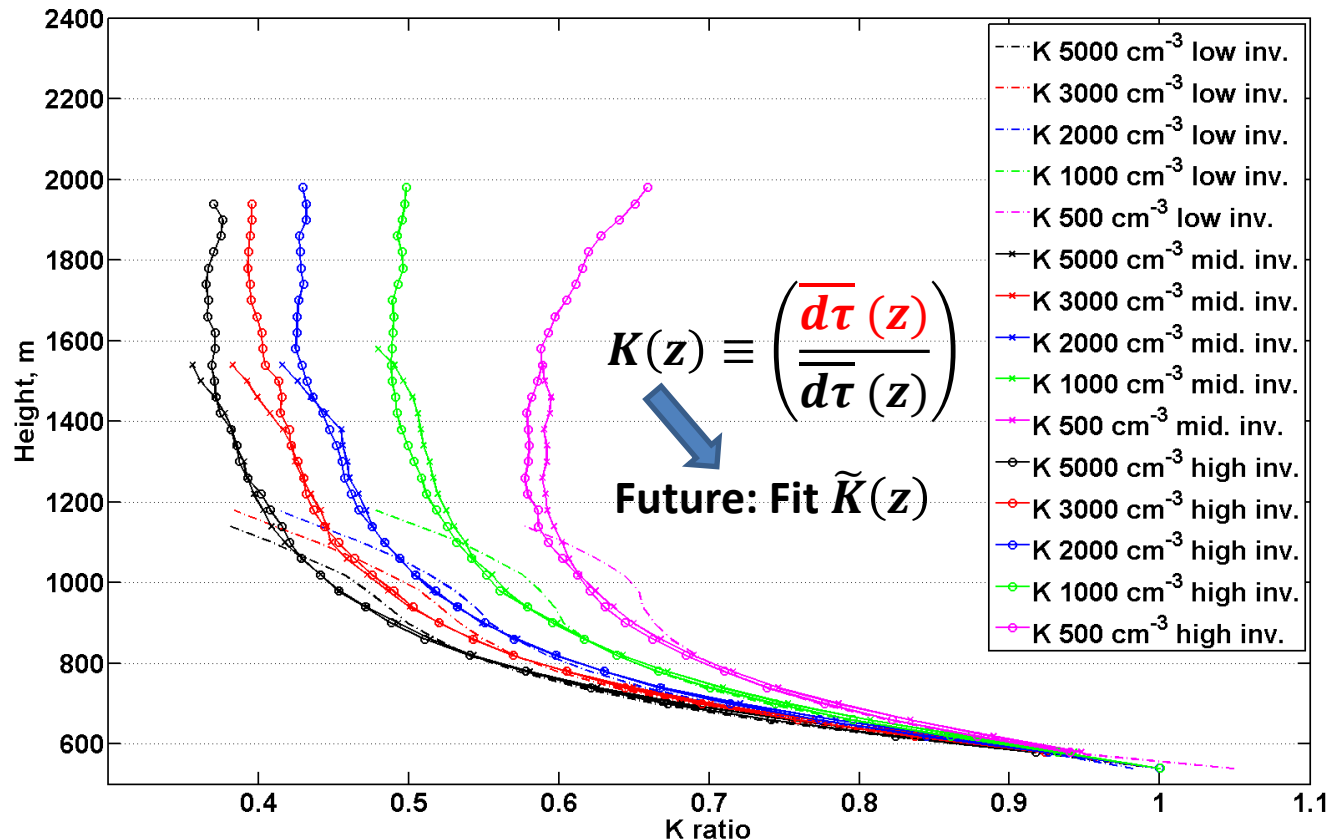
$$e^{-\overline{d\tau}(z)} \equiv \overline{e^{-d\tau(x,y,z)}}^{x,y}$$

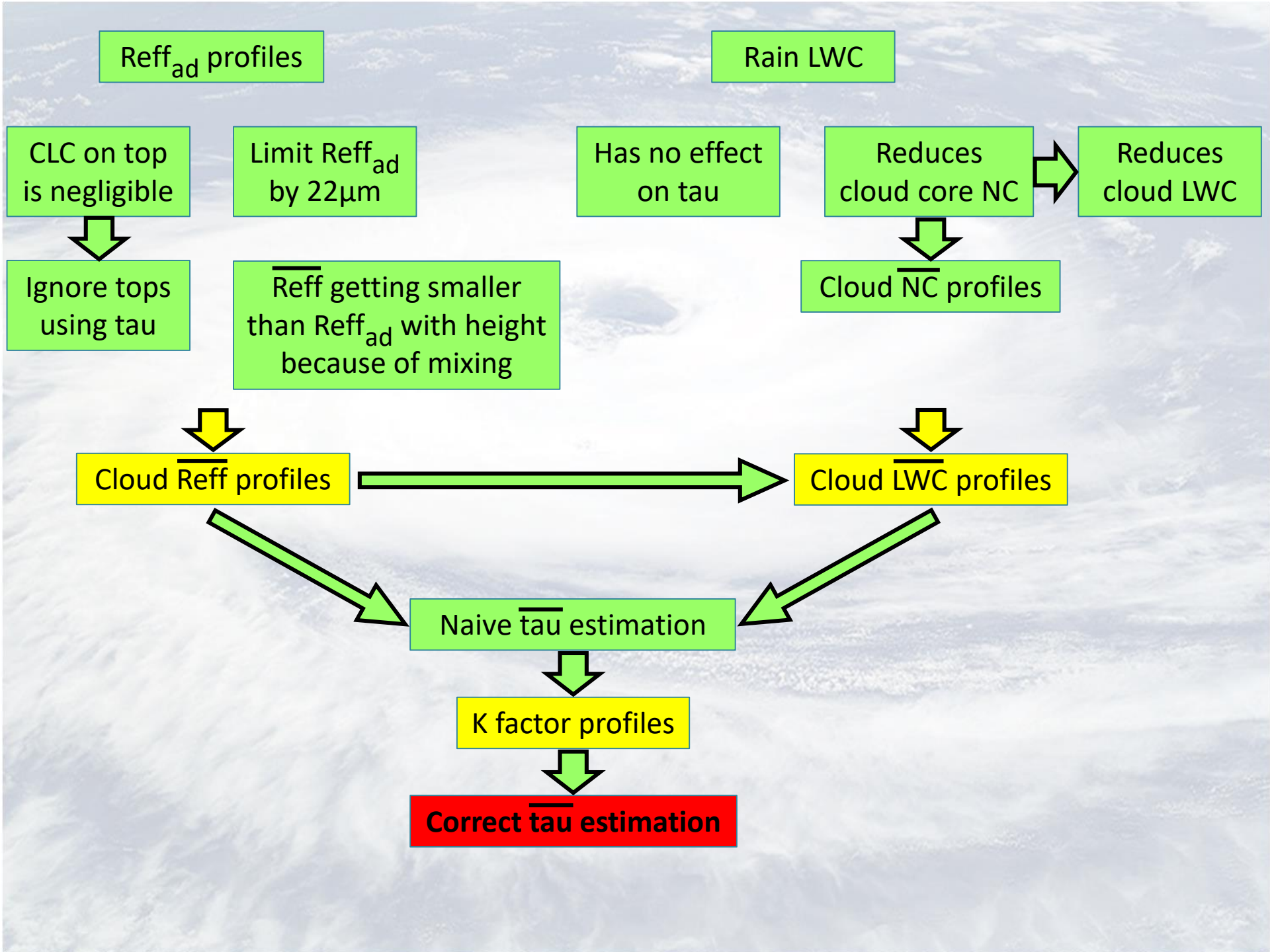
Wrong Optical Depth

$$\overline{d\tau}(z) = \frac{3}{2\rho_w} \overline{\left(\frac{Q(x,y,z)}{R(x,y,z)}\right)}^{x,y} dz$$

Naive fit to Optical Depth

$$\overline{d\tau}(z) = \frac{3}{2\rho_w} \frac{\overline{Q}(z)}{\overline{R}(z)} dz$$





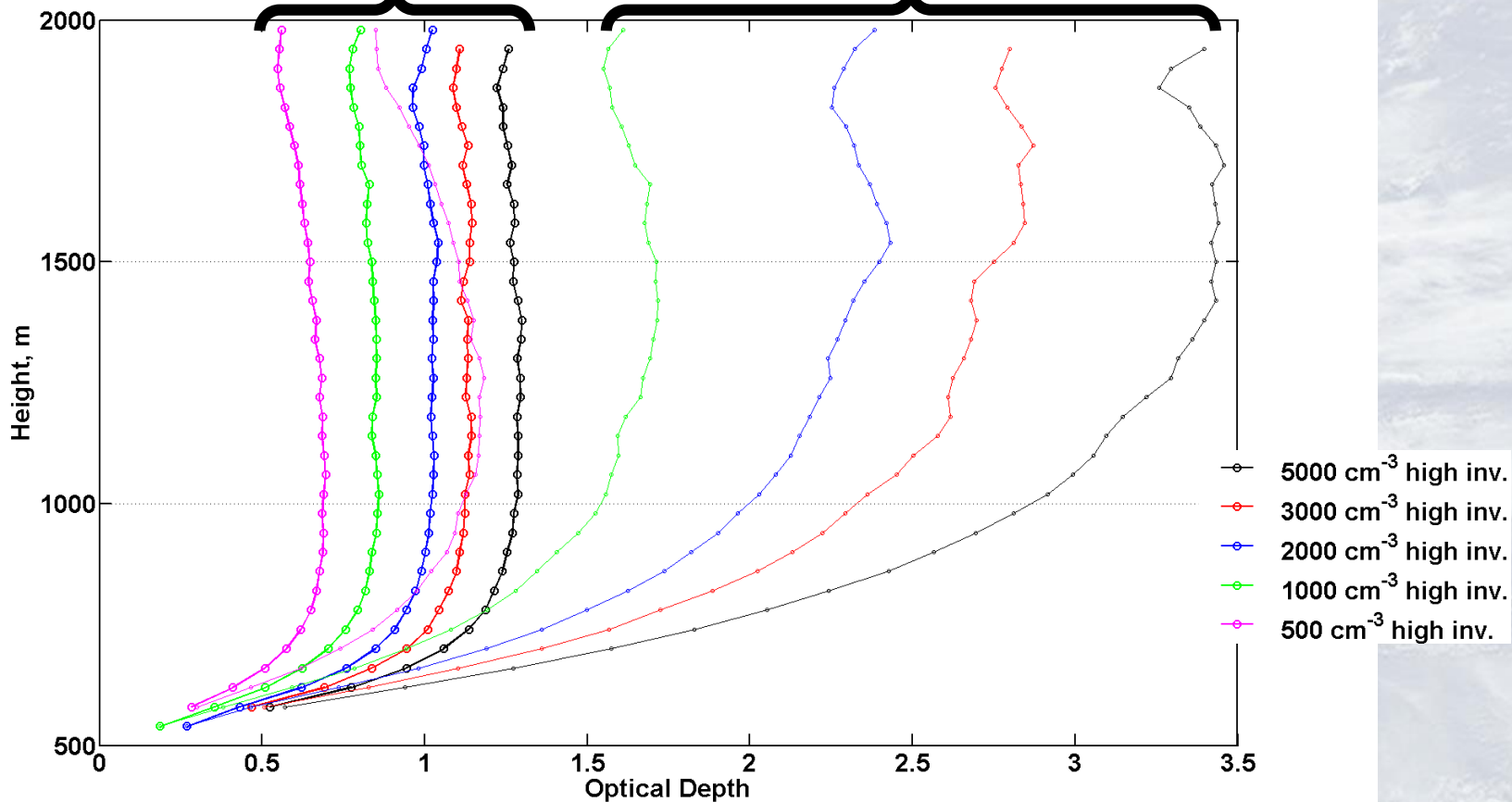
Clouds-averaged Optical Depth

Exact Optical Depth

$$e^{-\overline{d\tau}(z)} \equiv \overline{e^{-d\tau(x,y,z)}}^{x,y}$$

Naive fit to Optical Depth

$$\overline{d\tau}(z) = \frac{3}{2\rho_w} \frac{\overline{Q}(z)}{\overline{R}(z)} dz$$



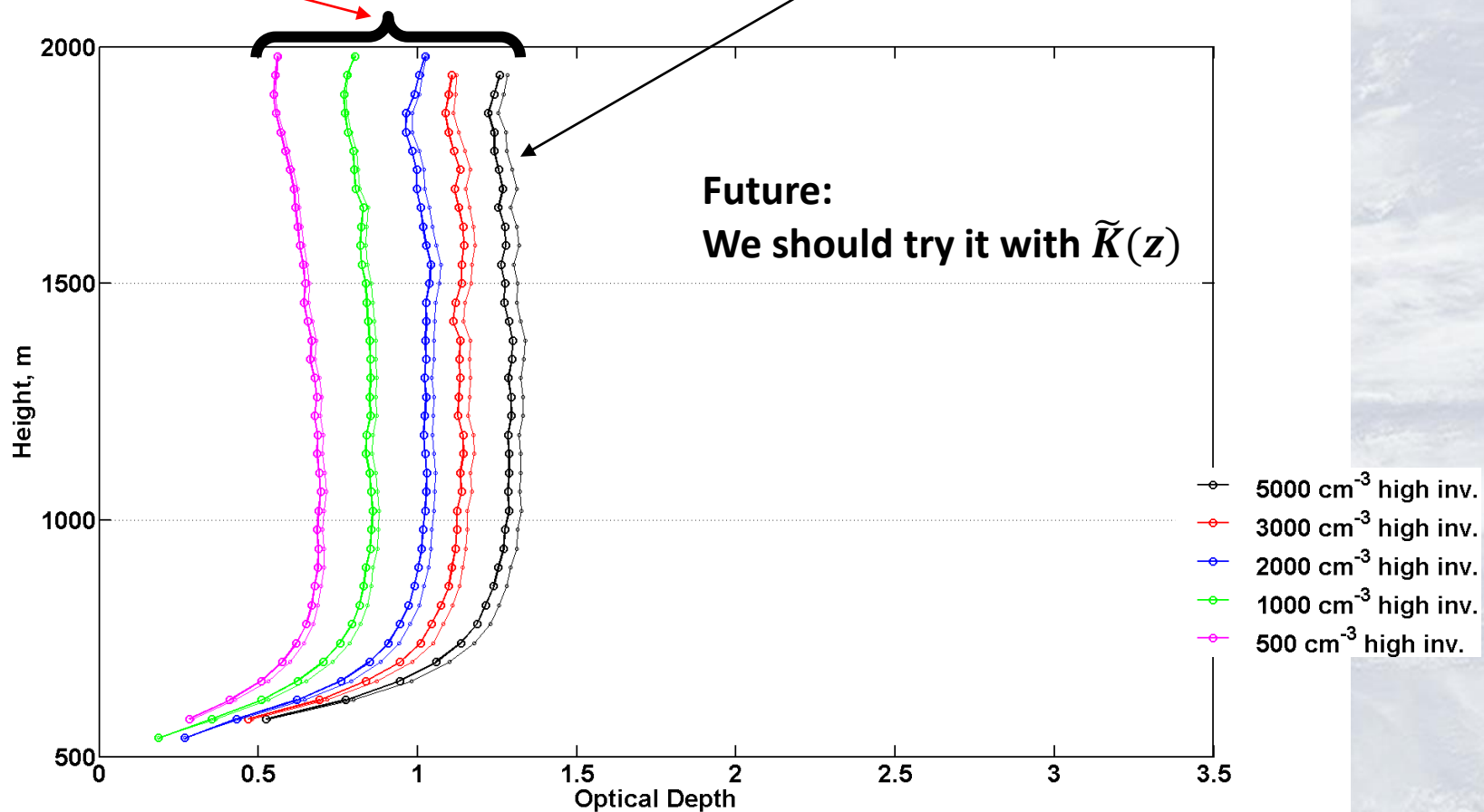
Clouds-averaged Optical Depth

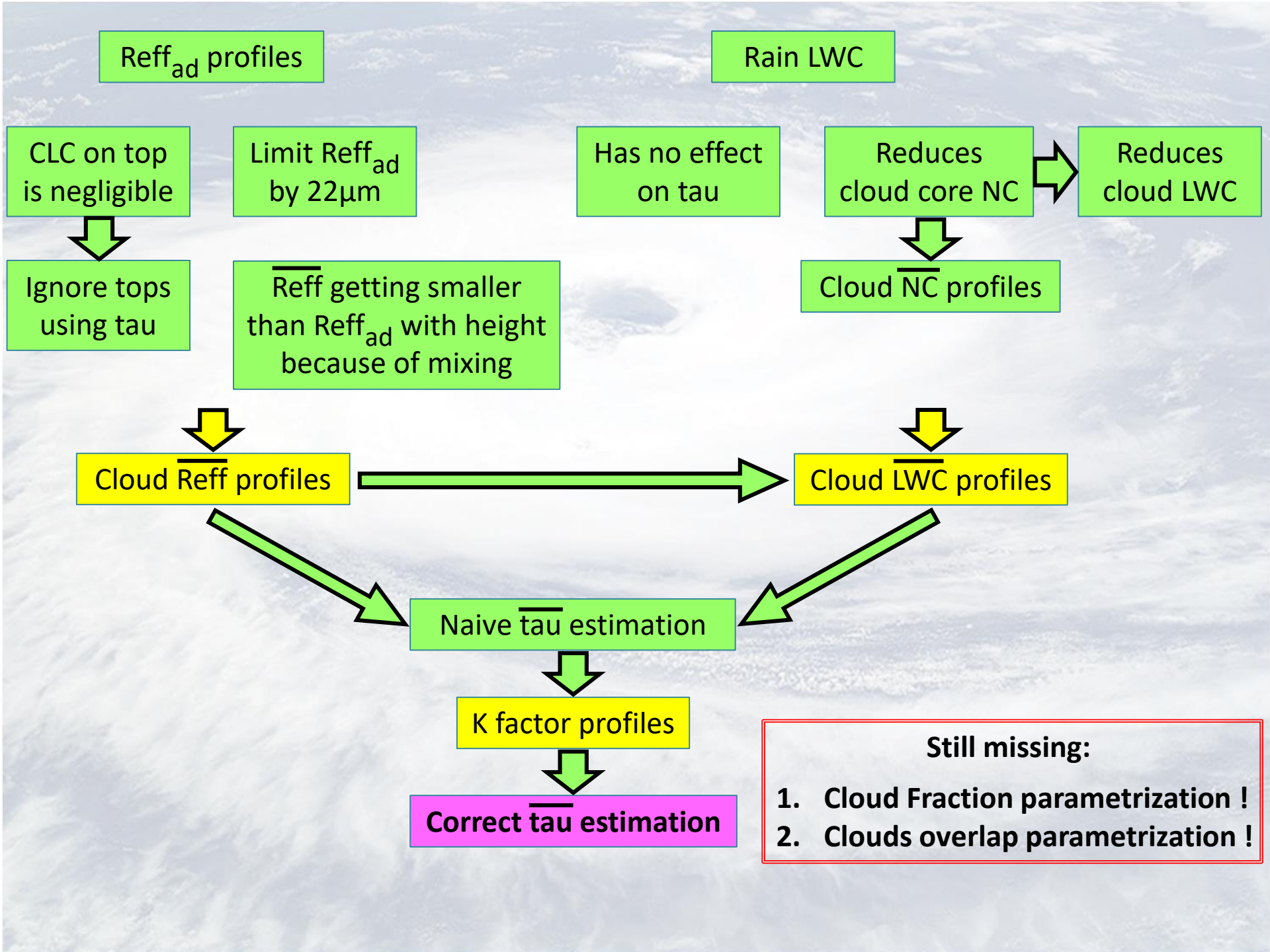
Exact Optical Depth

$$e^{-\overline{d\tau}(z)} \equiv \overline{e^{-d\tau(x,y,z)}}_{x,y}$$

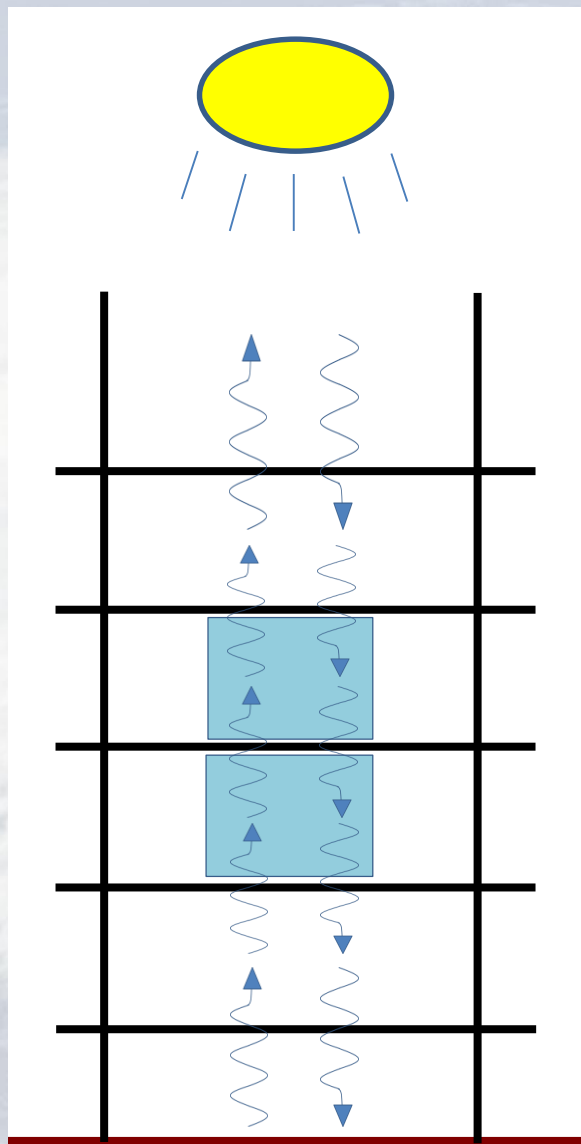
Good fit to Optical Depth

$$K(z) \overline{d\tau}(z) = K(z) \frac{3}{2\rho_w} \frac{\overline{Q}(z)}{\overline{R}(z)} dz$$

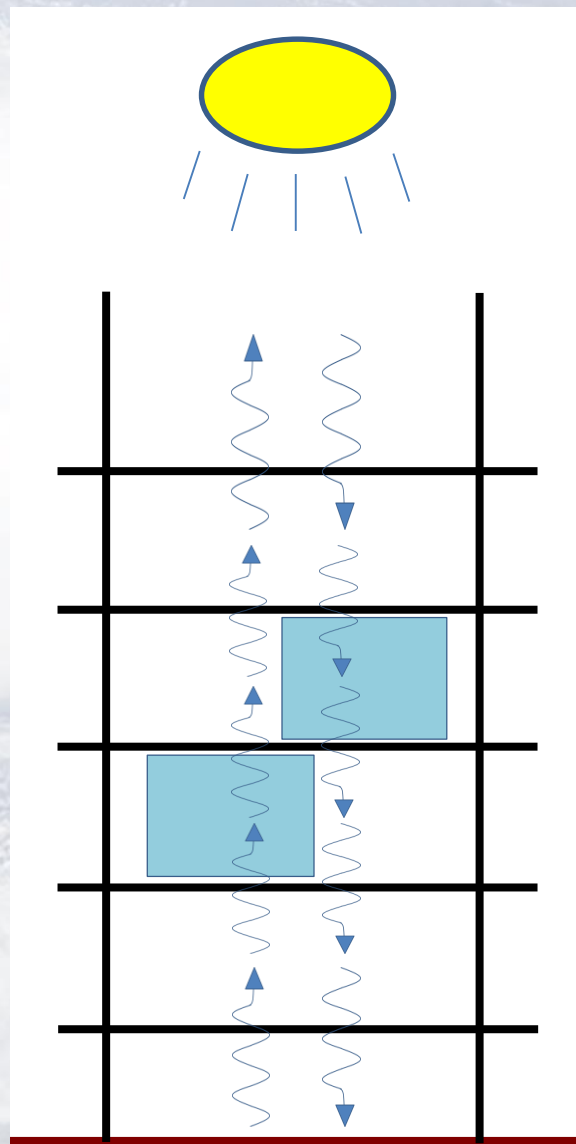




Cloud **overlap** parametrization



Earth

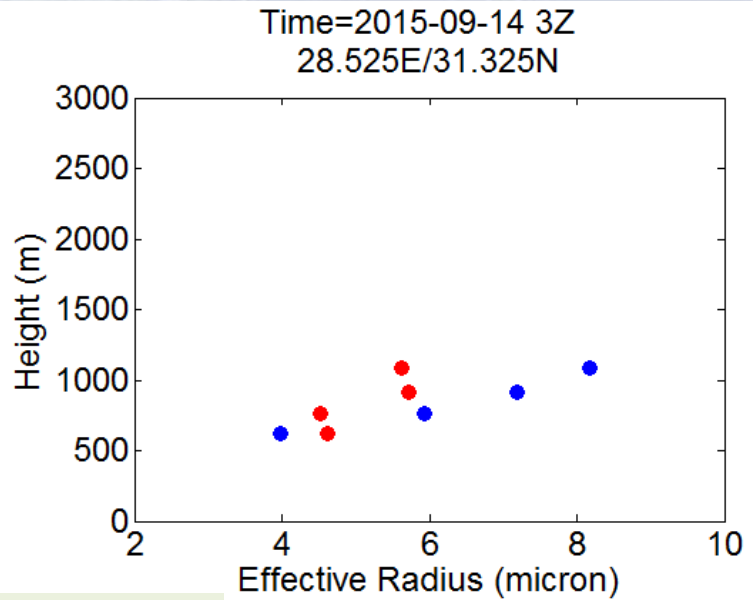
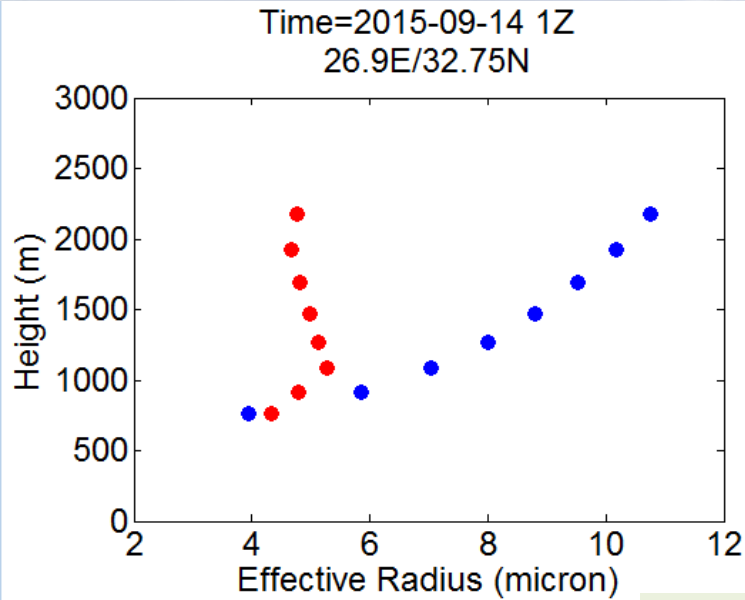


Earth

Outline

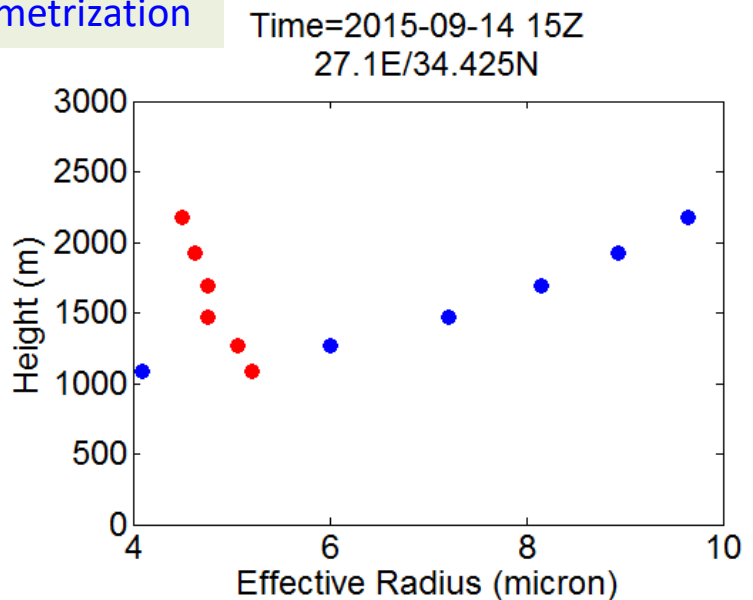
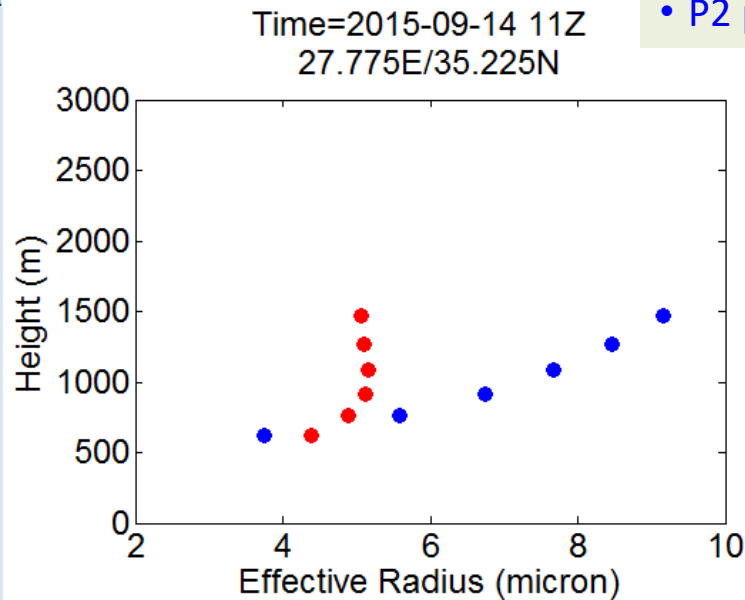
1. Motivation
2. COSMO new parametrization (**p1**) of SGS cloud properties (for radiation)
3. COSMO new parametrization (**p2**) based on LES simulations
 - A. Simulations design
 - B. Schematic explanation: How should LWC, NC and Reff behave with height?
 - C. Parametrization of mean Reff(z) and LWC(z)
 - D. Towards the parametrization of the Optical Depth
4. Implementation in COSMO code: (really) first results
5. Summary

Implementation in COSMO code



• P1 parametrization

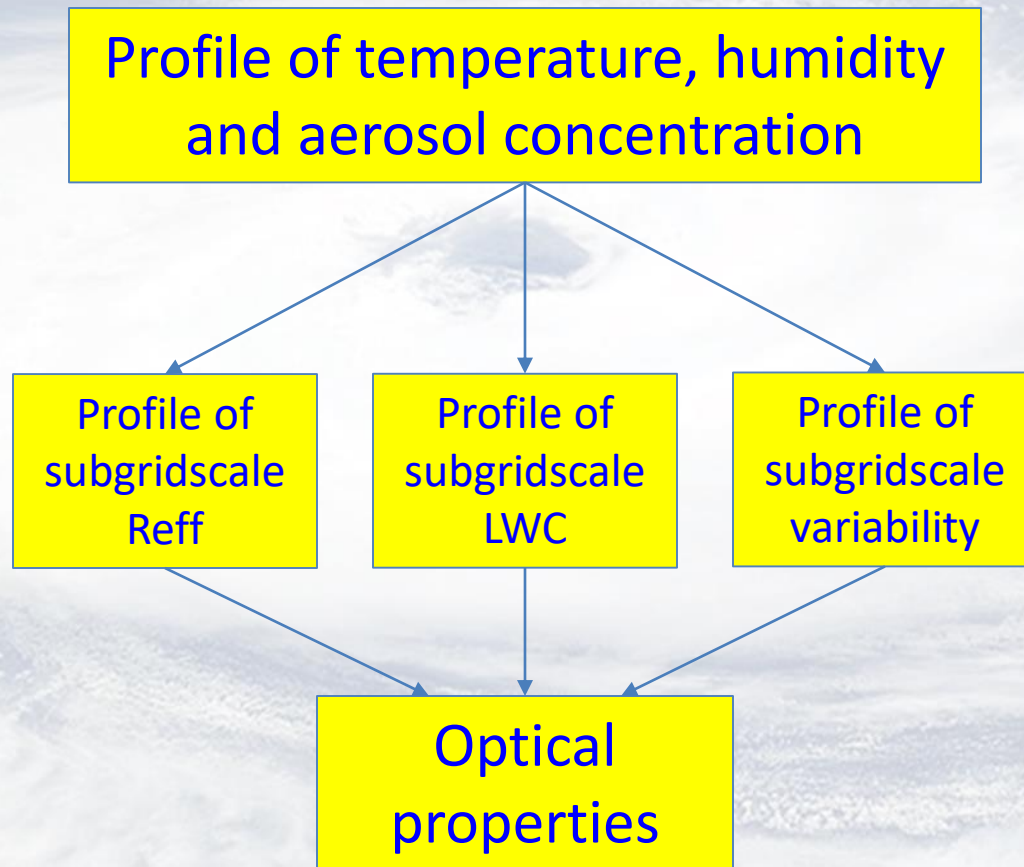
• P2 parametrization



Outline

1. Motivation
2. COSMO new parametrization (**p1**) of SGS cloud properties (for radiation)
3. COSMO new parametrization (**p2**) based on LES simulations
 - A. Simulations design
 - B. Schematic explanation: How should LWC, NC and Reff behave with height?
 - C. Parametrization of mean Reff(z) and LWC(z)
 - D. Towards the parametrization of the Optical Depth
4. Implementation in COSMO code: (really) first results
5. Summary

Summary



Still missing:

Parametrization of
cloud cover

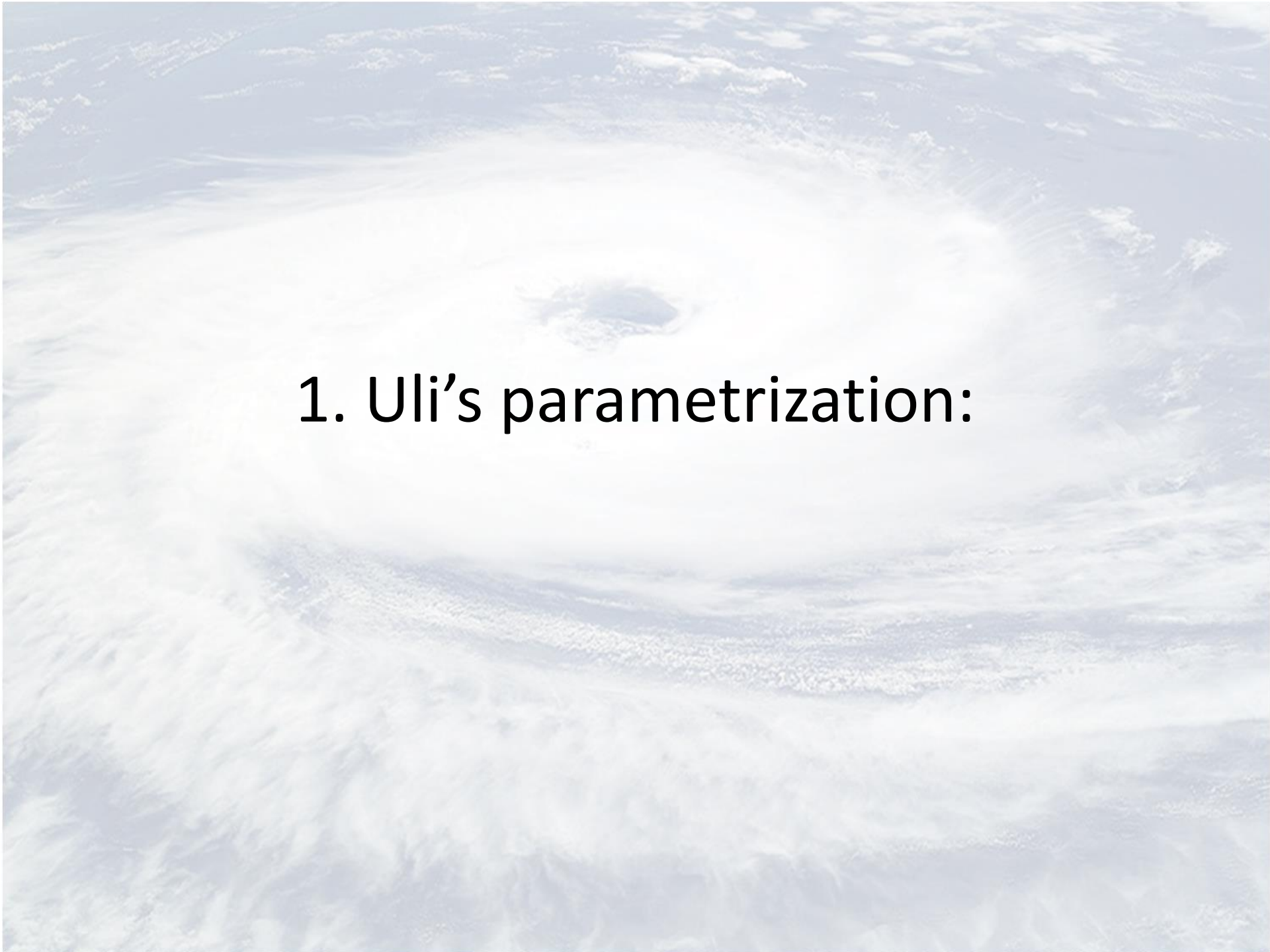
Parametrization of
clouds vertical overlap

An aerial photograph showing a large, circular, light-colored area in the center of a field, possibly a crater or a large hole. The surrounding area is a mix of green and brown, suggesting a natural landscape. The text "Thank you!" is overlaid in the center in a bold, blue font.

Thank you!

An aerial photograph showing a large, circular, light-colored area, possibly a crater or a large-scale geological feature, surrounded by darker, textured terrain. The central area is bright and somewhat featureless, while the surrounding terrain shows various patterns and textures, suggesting a complex geological structure. The text "Additional slides" is overlaid in the center of the image.

Additional slides

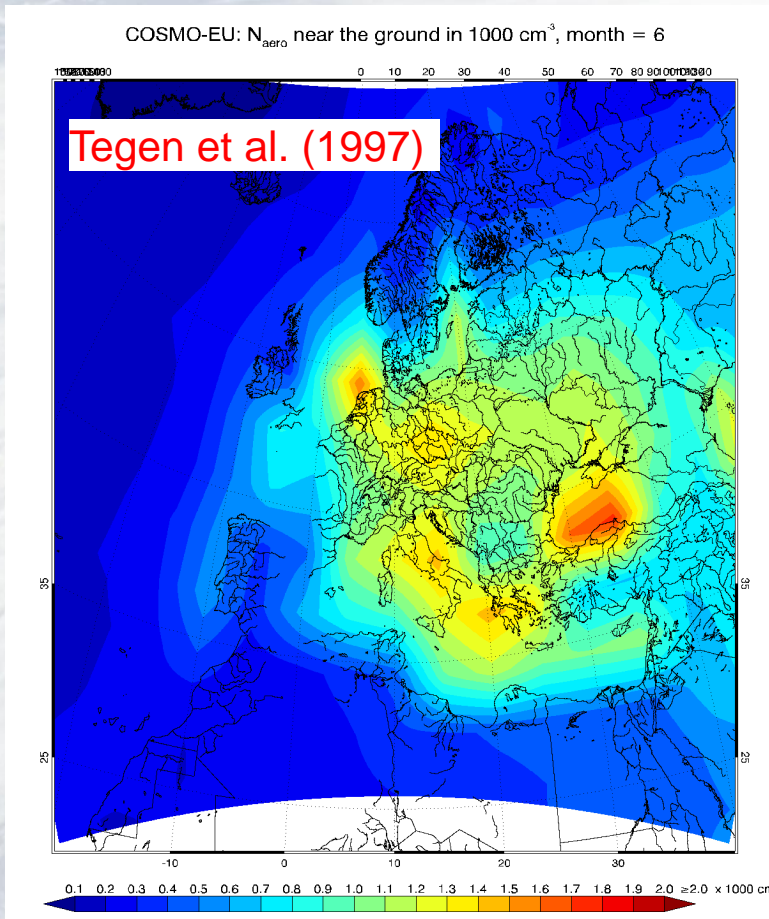
A satellite image of a tropical cyclone, showing a well-defined eye and a dense, swirling cloud structure. The eye is a small, dark, circular area in the center of the storm, surrounded by a thick, white ring of clouds. The outer clouds are more diffuse and spread out, covering a large area of the ocean. The overall appearance is that of a powerful, organized weather system.

1. Uli's parametrization:

Option 2: Tegen / Segal & Khain

- icloud_num_type_rad = 2
 - Cloud nuclei profile $n_{\text{CN}}(z)$ is estimated from Tegen aerosols
 - Activation of n_{CN} to n_{CCN} is estimated from Segal & Khain (2006) parameterization based on the estimated vertical velocity at cloud base
 - n_{C} is assumed equal to n_{CCN}

$n_{CN}(x,y,z)$ from Tegen aerosol climatology



- Tegen climatology is for opt. thicken. τ of 5 aerosol types: **sea salt, sulfuric acid, other organics, black carbon and dust**, where the black carbon is already contained in the „other organics“.
- Assumptions about spec. extinction coefficient β_{ext} , modal radii, aerosol bulk density and soluble fraction η lead to total N_{CN} number per area. Assumption of an exponentially decreasing vertical profile (in terms of mass fraction!) leads to 3D CN concentrations:

$$N_{CN} = \sum_{i=1}^4 \frac{3 \tau_i \eta_i}{4 \pi \beta_{ext,i} \bar{r}_{mode,i}^3 \rho_{bulk,i}}$$

$$N_{CN} = \int_0^{z_{max}} n_{CN}(z) \rho_0(z) dz$$

$$\rho_0(z) = \rho_{00} \exp\left(-\ln 2 \frac{z}{\Delta z_{\rho,1/2}}\right)$$

	i	η	β_{ext} $\text{m}^2 \text{kg}^{-1}$	\bar{r}_{mode} μm	ρ_{bulk} kg m^{-3}
dust	1	0.1	1500	1.0	3000
organics	2	0.9	8000	0.08	2000
SO ₄	3	1	8000	0.08	2000
sea salt	4	0.9	200	0.5	3000

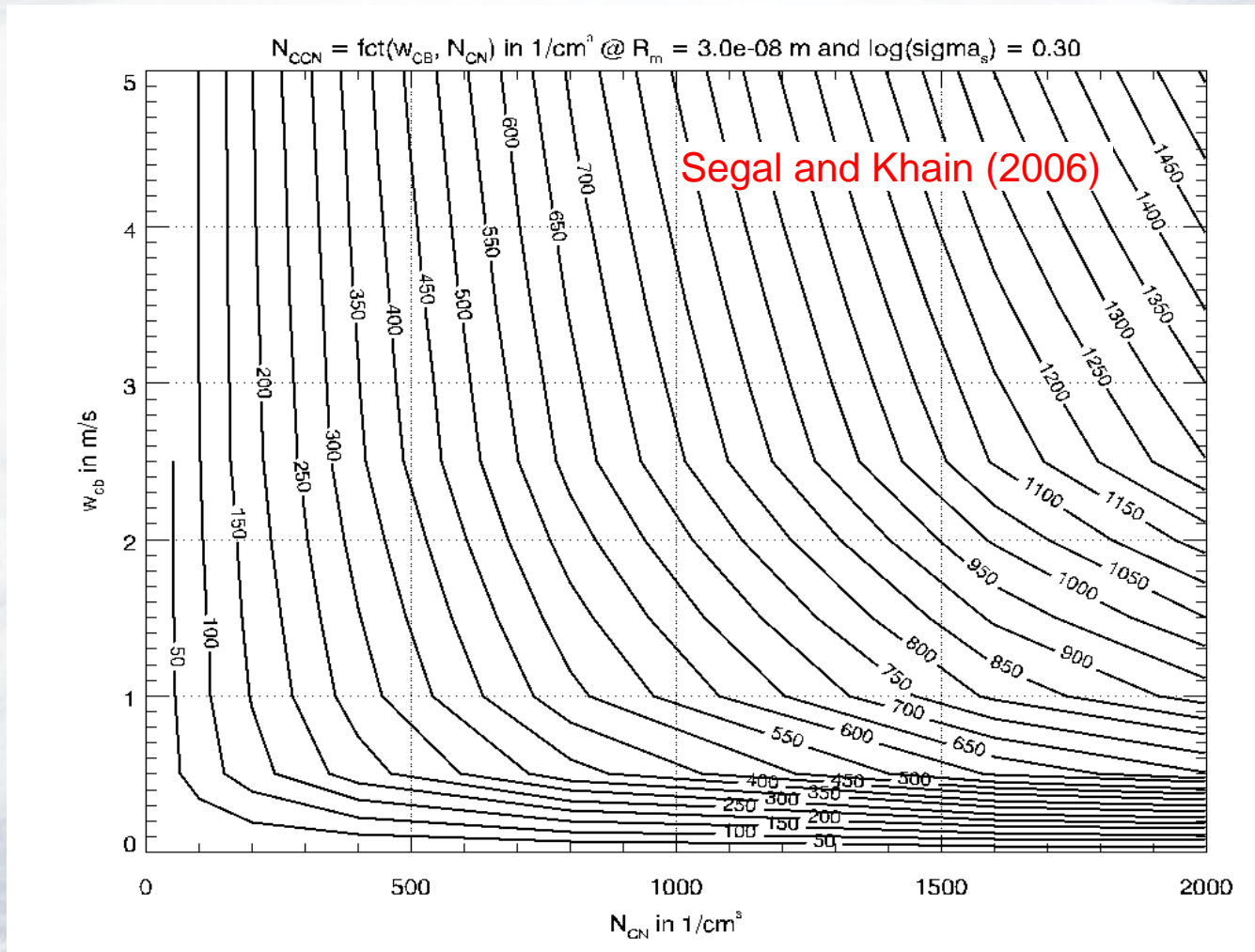
$$n_{CN}(z) = n_{CN,0} \begin{cases} \exp\left(-\frac{z-z_0}{\Delta z_{1/e}}\right) & \text{if } z > z_0 \\ 1 & \text{else} \end{cases} \quad [\text{kg}^{-1}]$$

$$\Rightarrow n_{CN,0} = N_{CN} \left\{ \rho_0(z_0) \left[\frac{\Delta z_{\rho,1/2}}{\ln 2} \left(\exp\left(\ln 2 \frac{z_0}{\Delta z_{\rho,1/2}}\right) - 1 \right) + \Delta z_{eff,1/e} \left(1 - \exp\left(\frac{z_0 - z_{max}}{\Delta z_{eff,1/e}}\right) \right) \right] \right\}^{-1}$$

$$\text{with } \Delta z_{eff,1/e} = \left(\frac{1}{\Delta z_{1/e}} + \frac{\ln 2}{\Delta z_{\rho,1/2}} \right)^{-1}$$

$n_{CCN}(x,y,z)$ from Tegen / Segal & Khain

... + Updraft-based activation parameterization of n_{CCN} :



$n_{CCN}(x,y,z)$ from Tegen / Segal & Khain

→ Parameterized after Segal and Khain (2006) as function of n_{CN} and w_{cb} at cloud base, where mean radius and width of an assumed log-normal aerosol distribution is assumed constant (2D lookup tables)

→ In „active“ clouds ($w_{nuc} > w_{cb,min}$ and $q_c > 0$ or $clc_con > 0$ over several adjacent height layers), activation is at cloud base and n_{CN} decreases exponentially above cloud base (→ autoconversion, accretion).

→ All other grid points: derive n_c from lookup table based on local n_{CN} and w_{nuc}

→ Let $n_{CCN,SK}$ be the lookup table, then:

$$n_C(z) = \begin{cases} n_{CCN,SK}(n_{CN}(z_{cb}), w_{nuc}(z_{cb})) \exp\left(-\frac{z-z_{cb}}{\Delta z_{a,1/e}}\right) & \text{if } w \geq w_{cb,min} \wedge q_C(z) > 0 \wedge z \geq z_{cb} \\ n_{CCN,SK}(n_{CN}(z), \max[w_{nuc}(z), w_{cb,min}]) & \text{else} \end{cases} \quad [\text{kg}^{-1}]$$

→ Effective updraft speed w_{nuc} for nucleation, including turbulence, radiative cooling an parameterized convection:

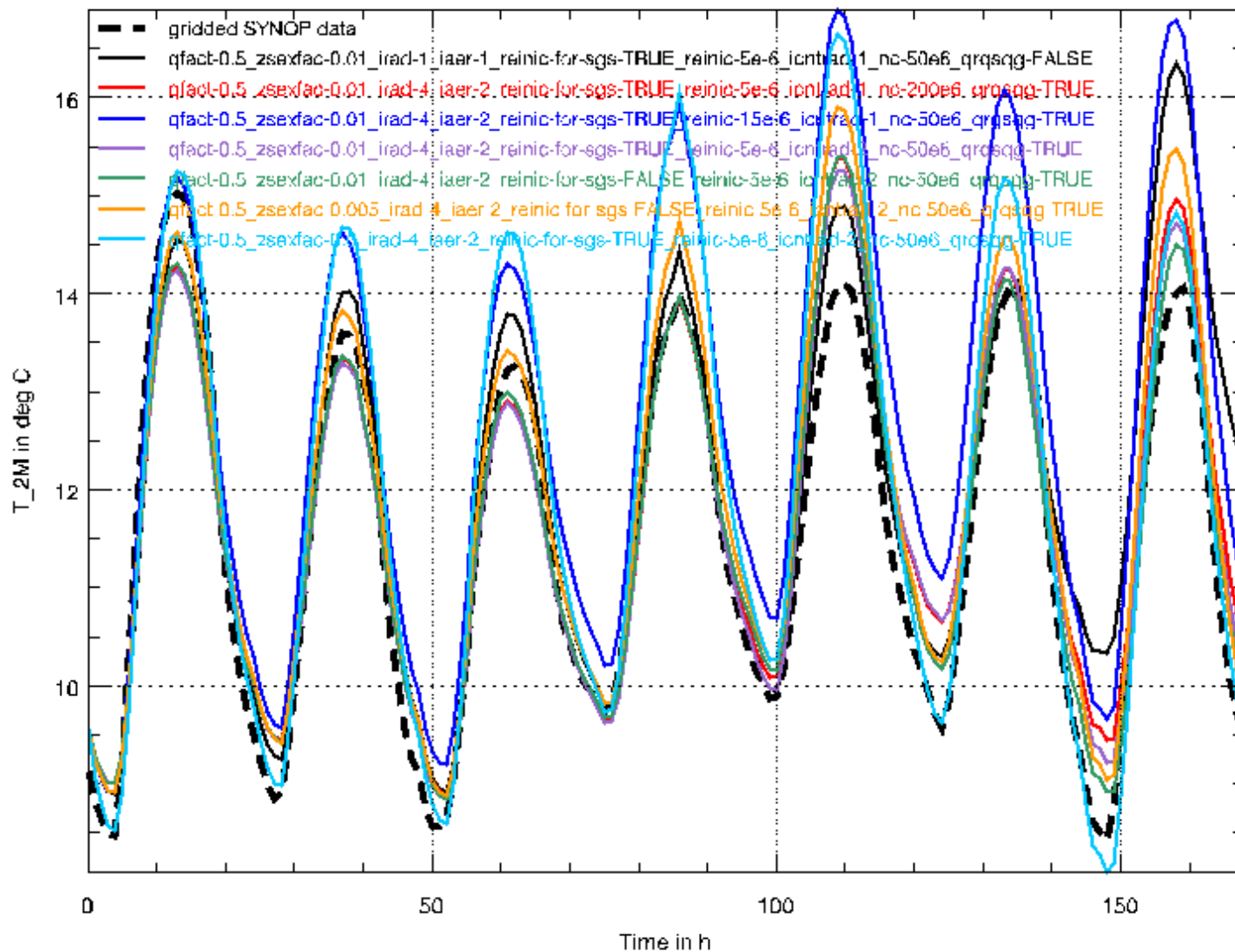
$$w_{eff} = \bar{w} + 0.7 \sqrt{\frac{2TKE}{6}} - \frac{c_p}{g} \frac{\partial T}{\partial t} \Big|_{\text{radiation}}$$

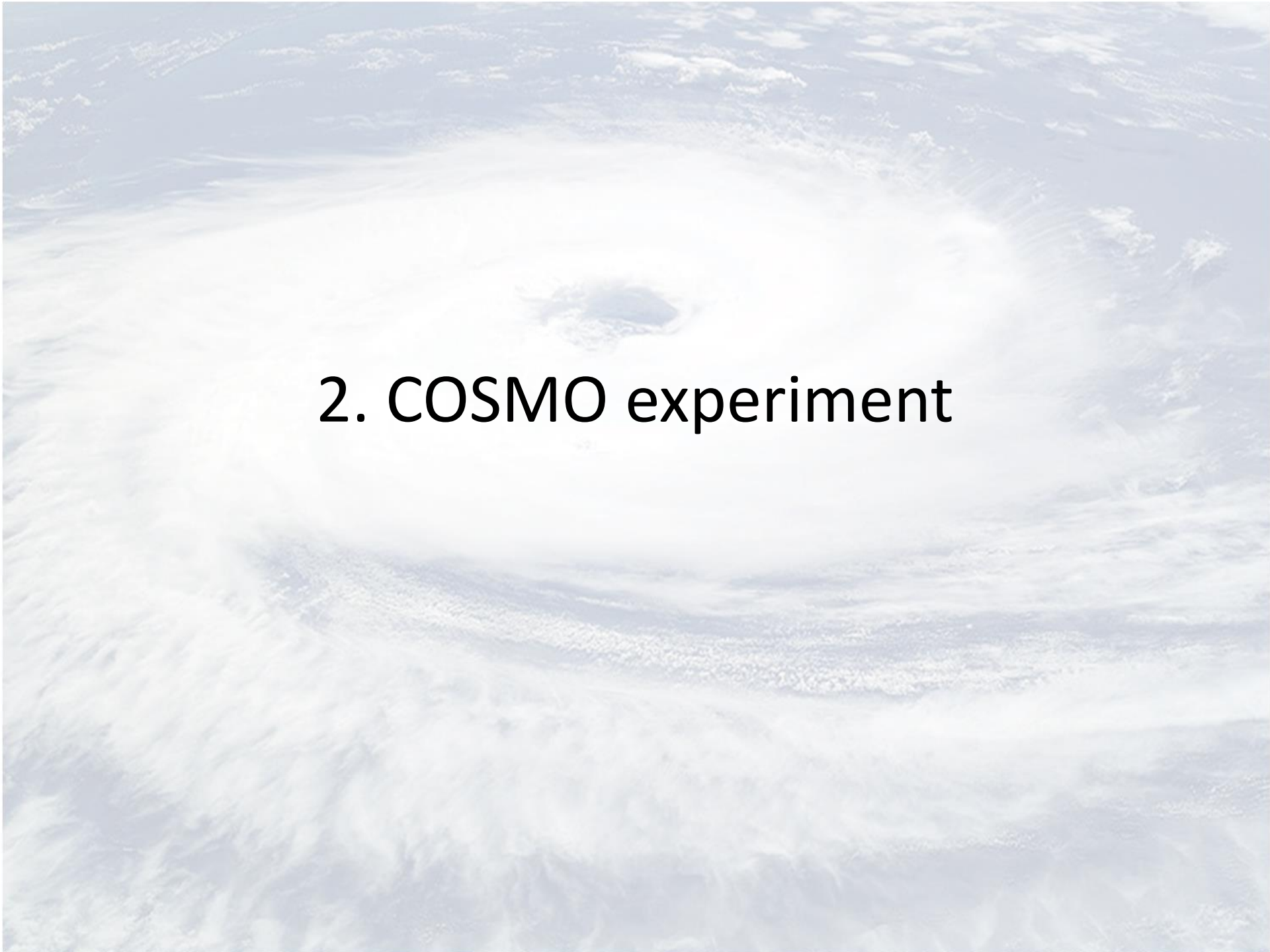
$$w_{nuc} = \max[w_{eff}, w^*]$$

$$w^* = \left(-g z_{topcon} \frac{\overline{w' \Theta'_{v,S}}}{\overline{\Theta_{v,S}}} \right)^{1/3} \quad (\text{convective velocity scale after Deardorff})$$

→ z_{top_con} : PBL height as determined from $\Theta_v < \Theta_{v,surf} + 0.5$ K, or upper bound of lowest continuous „ clc_con “ layer

Timeseries of mean T_{2M} over SYNOP-masked domain



An aerial photograph of a large, circular, light-colored crater or impact site in a desert landscape. The crater is the central focus, surrounded by a dark, rocky rim. The surrounding terrain is a mix of light-colored sand and darker, rocky areas. The text "2. COSMO experiment" is overlaid in the center of the image.

2. COSMO experiment

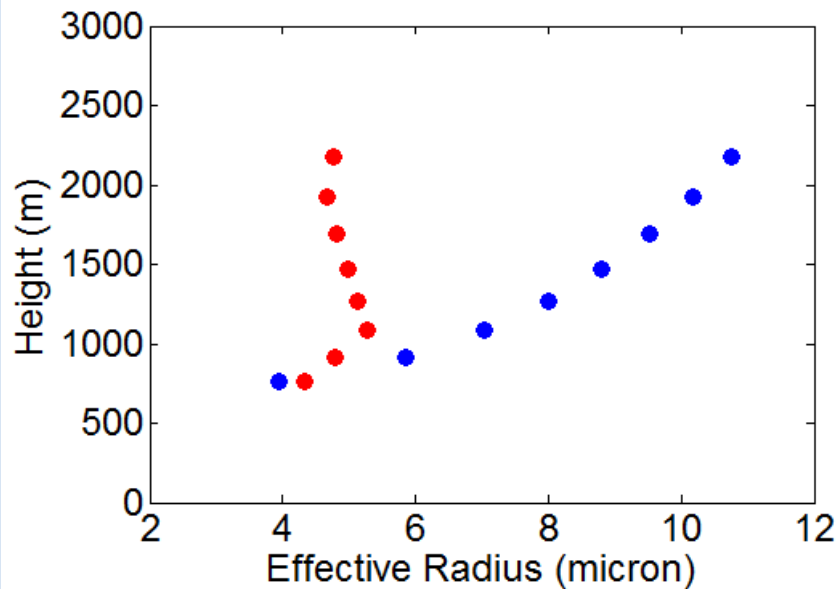
In the test version, these 3 are calculated anyway (even if `luse_qc_adiab_for_reffc_sgs=FALSE`):

- $\text{reff_sam} - \text{reff_avg_fact} * \text{refftc} \% \text{r_eff}$
- $\text{lwc_sam} - \text{lwc_avg_fact} * \text{lwc_adiab}$
- $\text{lwc_sam_avg} - \text{lwc_avg_fact} * \text{lwc_adiab} * (\text{radqc_fact} * \text{zclc})$

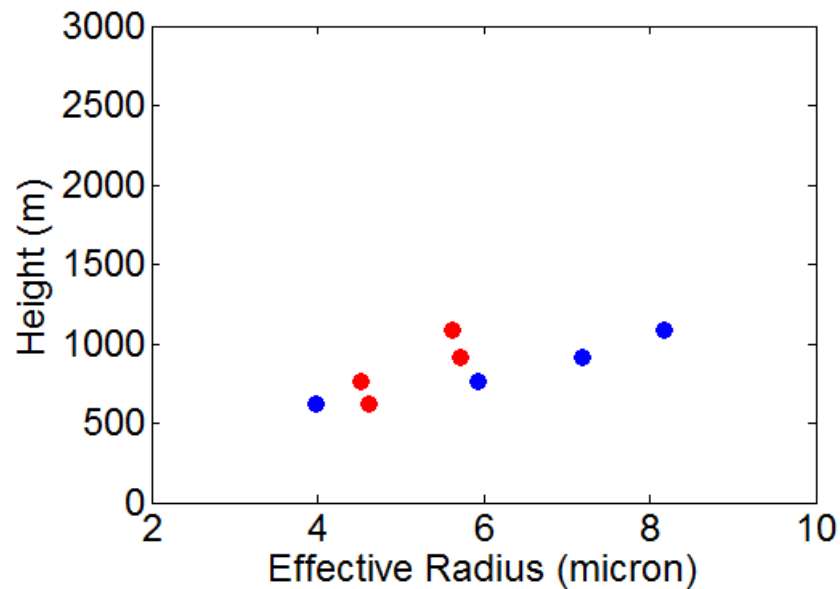
2 versions:

1. “SAM” version (with `luse_qc_adiab_for_reffc_sgs=TRUE`)
2. “no-SAM” version (with `luse_qc_adiab_for_reffc_sgs=FALSE`)

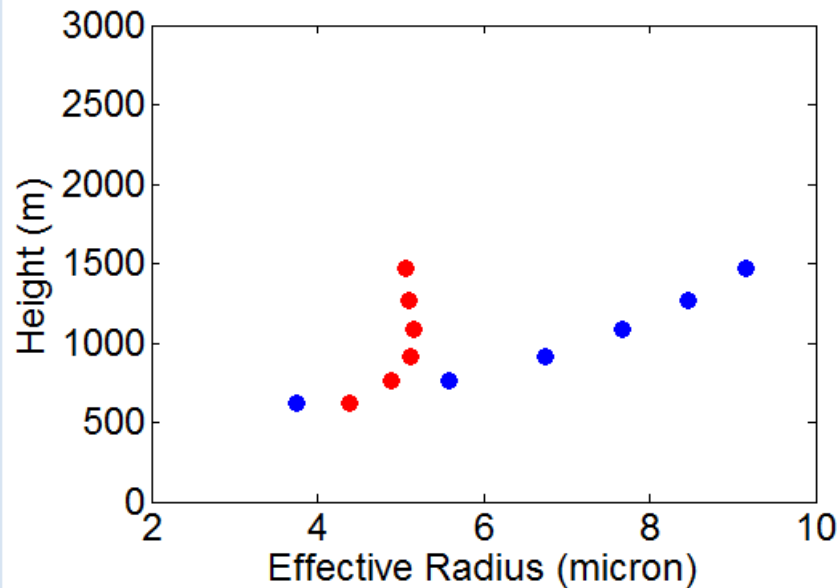
Time=2015-09-14 1Z
26.9E/32.75N



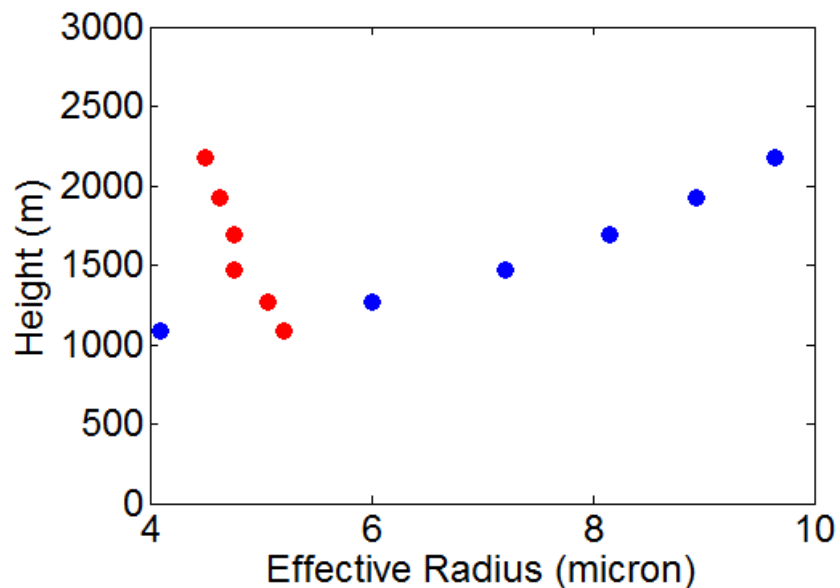
Time=2015-09-14 3Z
28.525E/31.325N



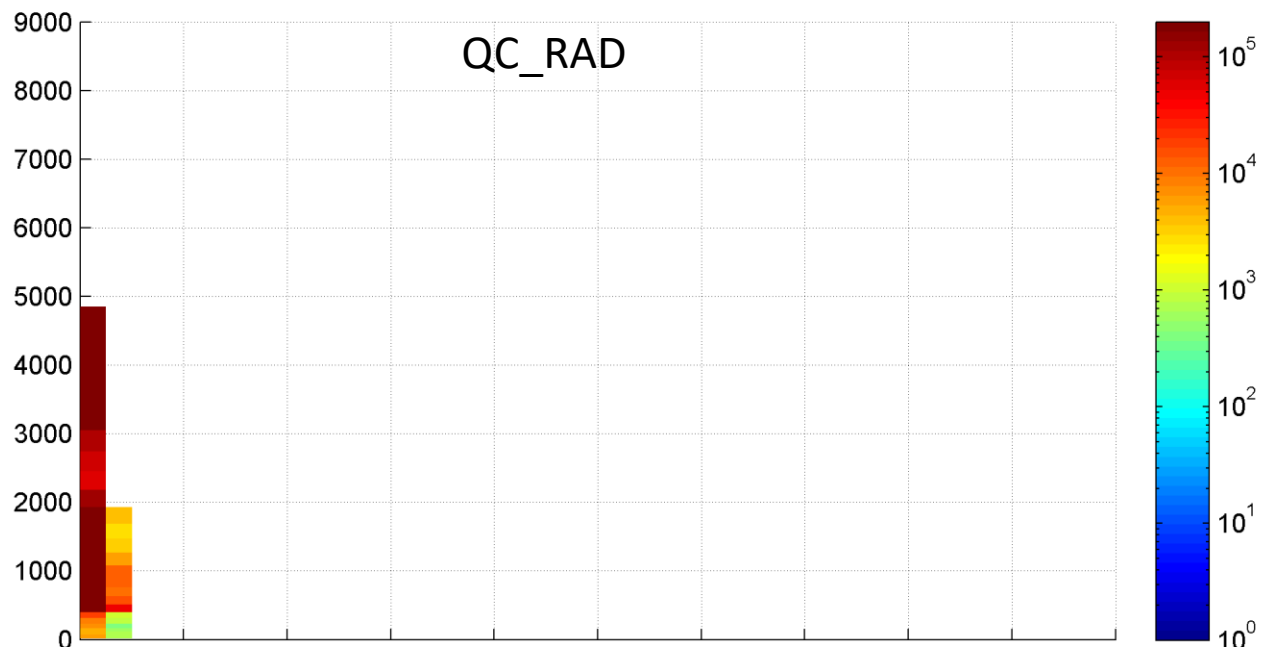
Time=2015-09-14 11Z
27.775E/35.225N



Time=2015-09-14 15Z
27.1E/34.425N

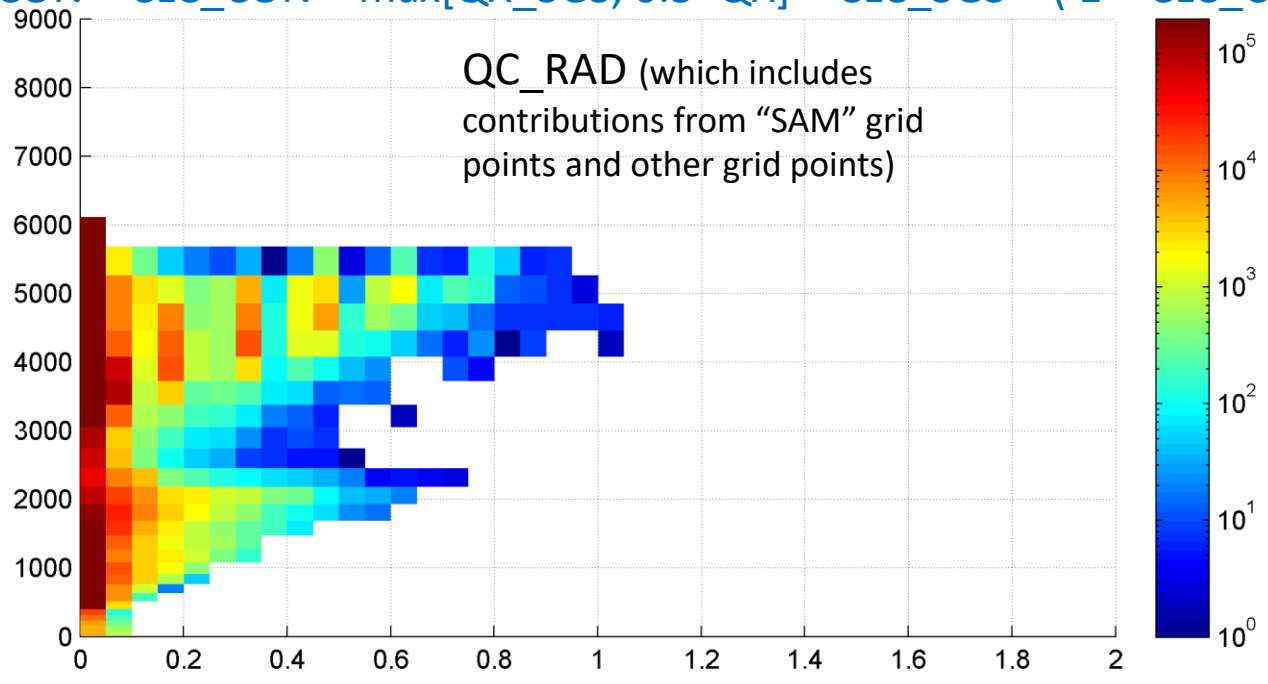


Grid-averaged

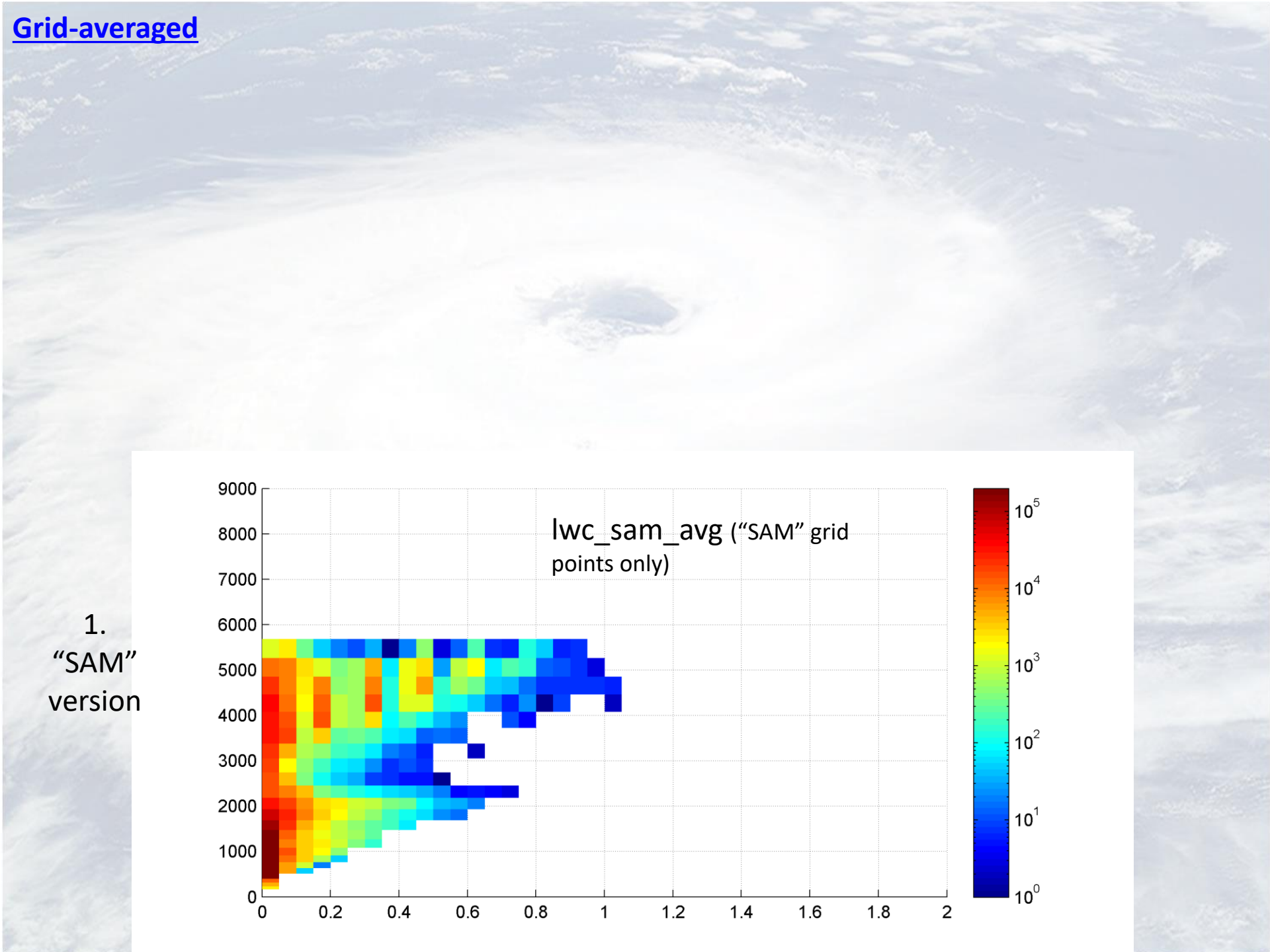


2.
"no-SAM"
version

$$QX_RAD = QX_CON * CLC_CON + \max[QX_SGS, 0.5 * QX] * CLC_SGS * (1 - CLC_CON)$$

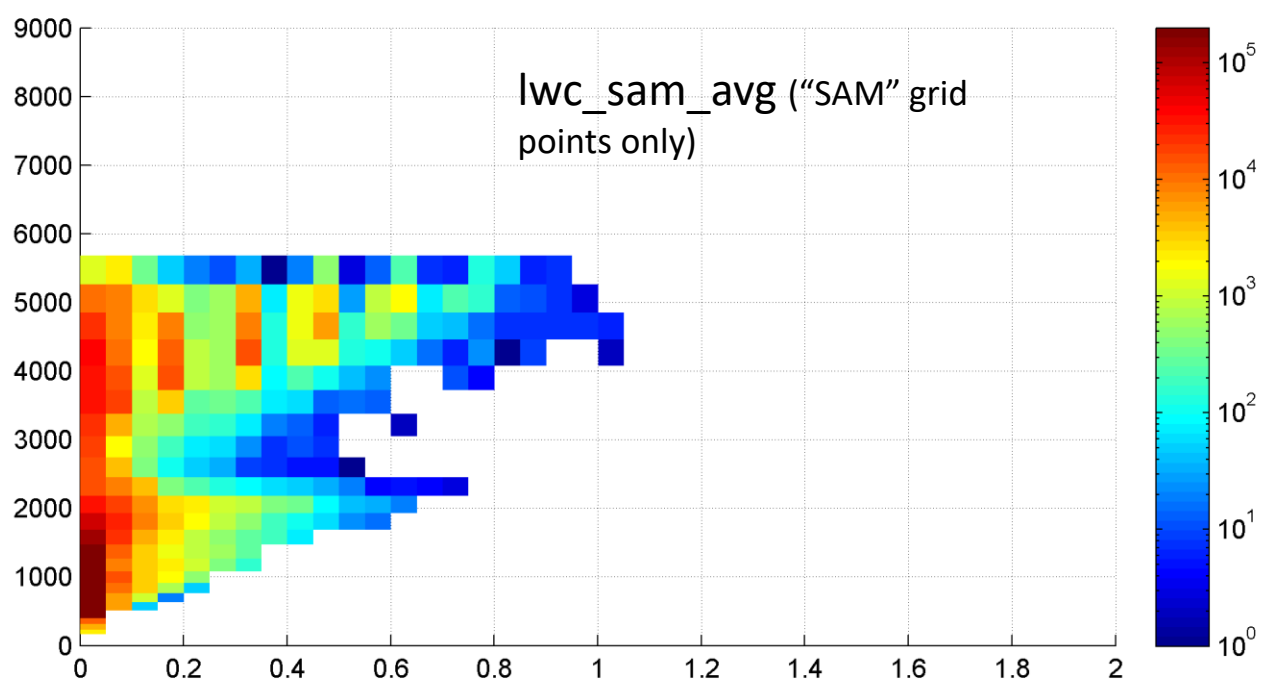


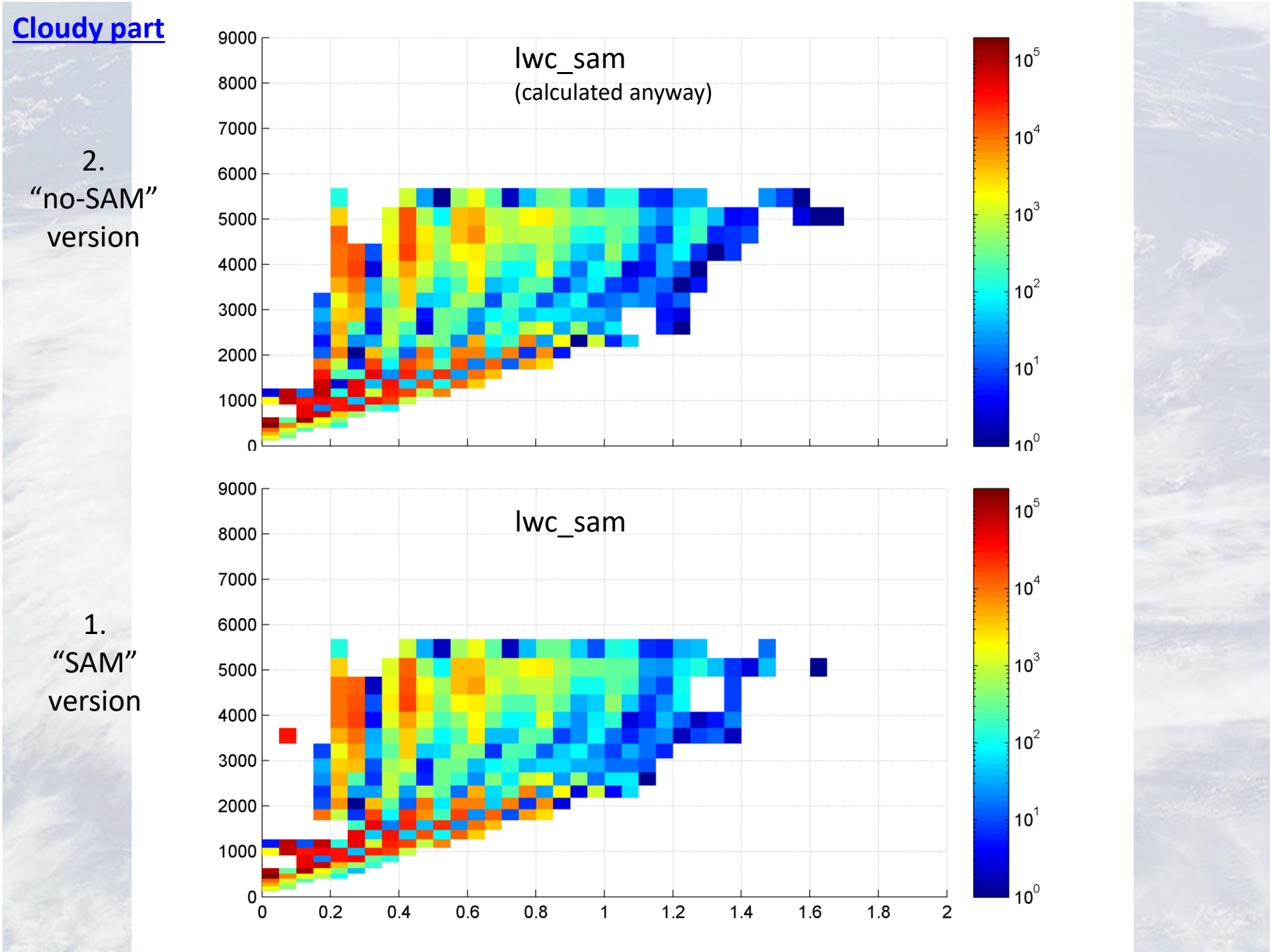
1.
"SAM"
version



Grid-averaged

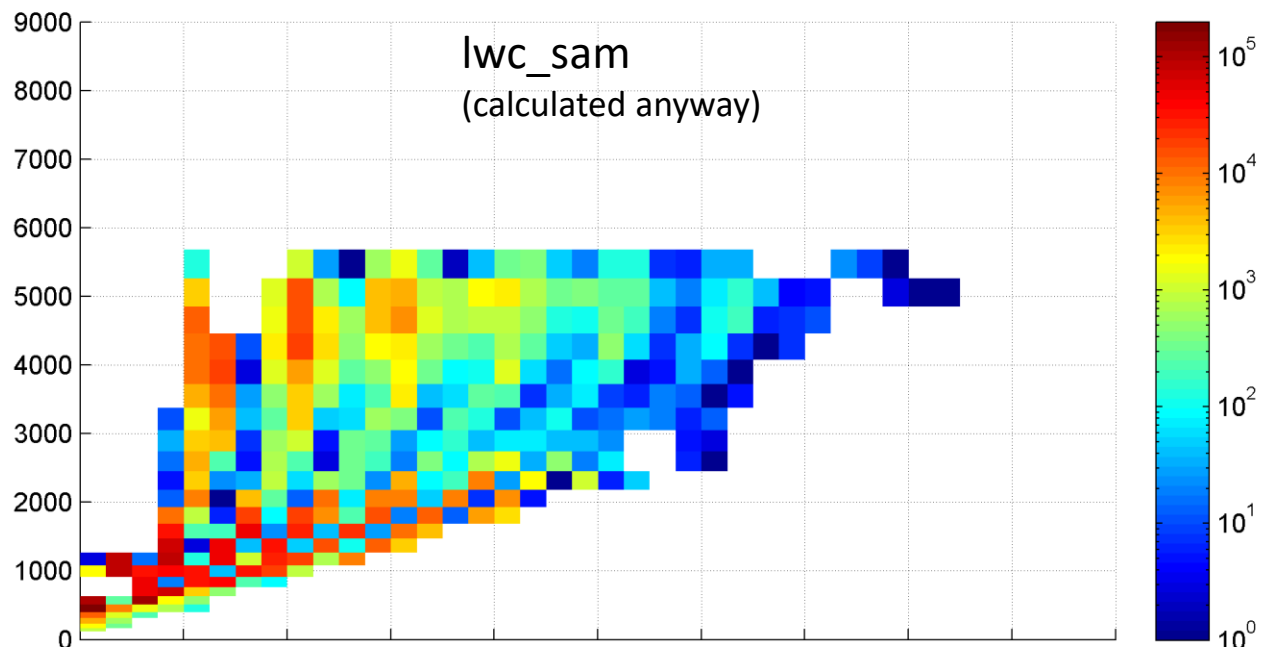
1.
"SAM"
version



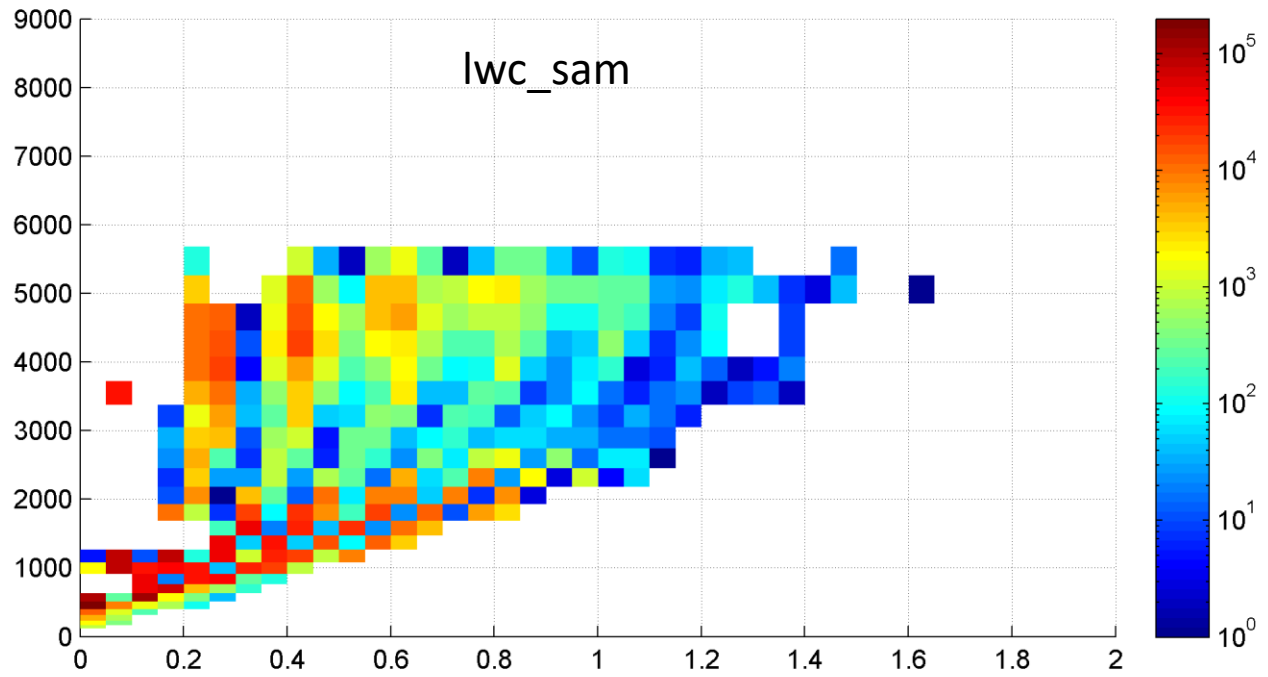


Cloudy part

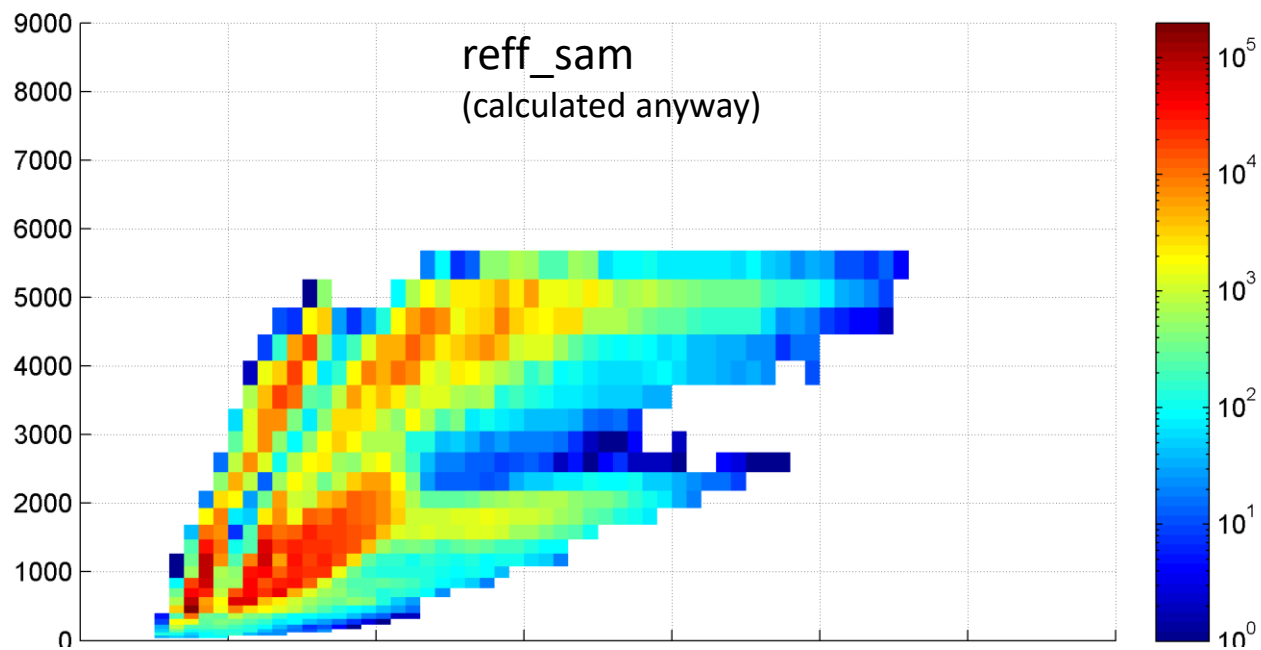
2.
"no-SAM"
version



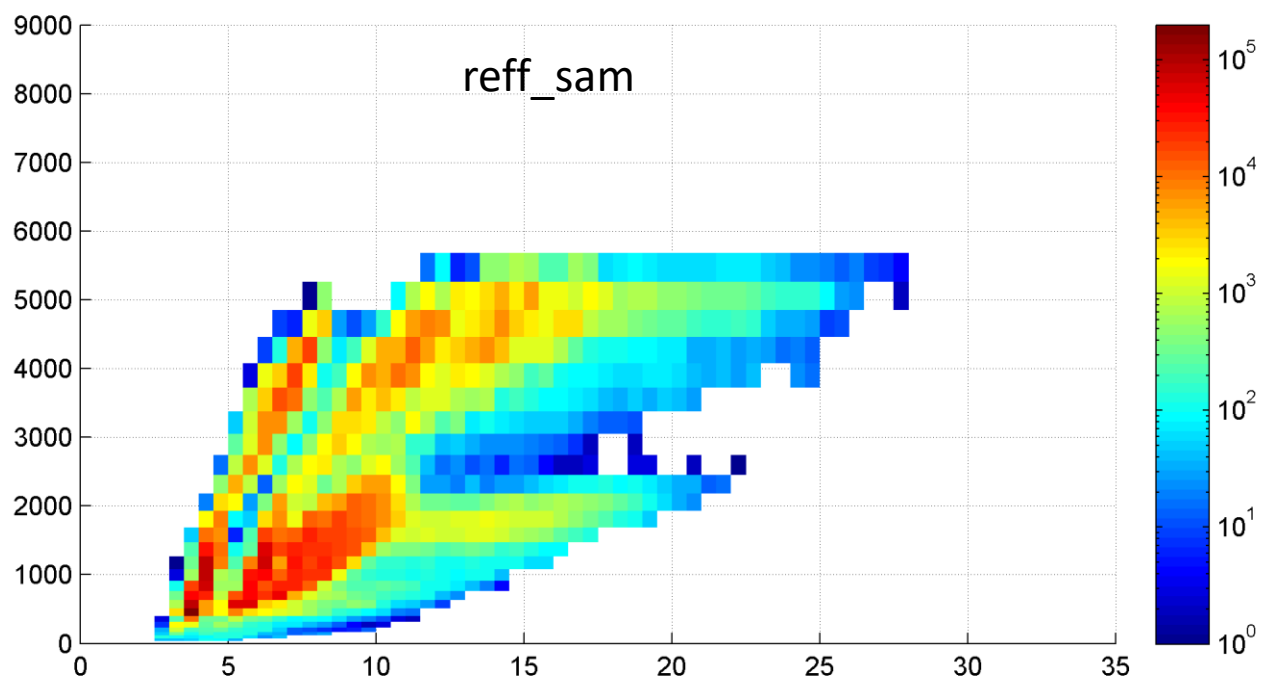
1.
"SAM"
version



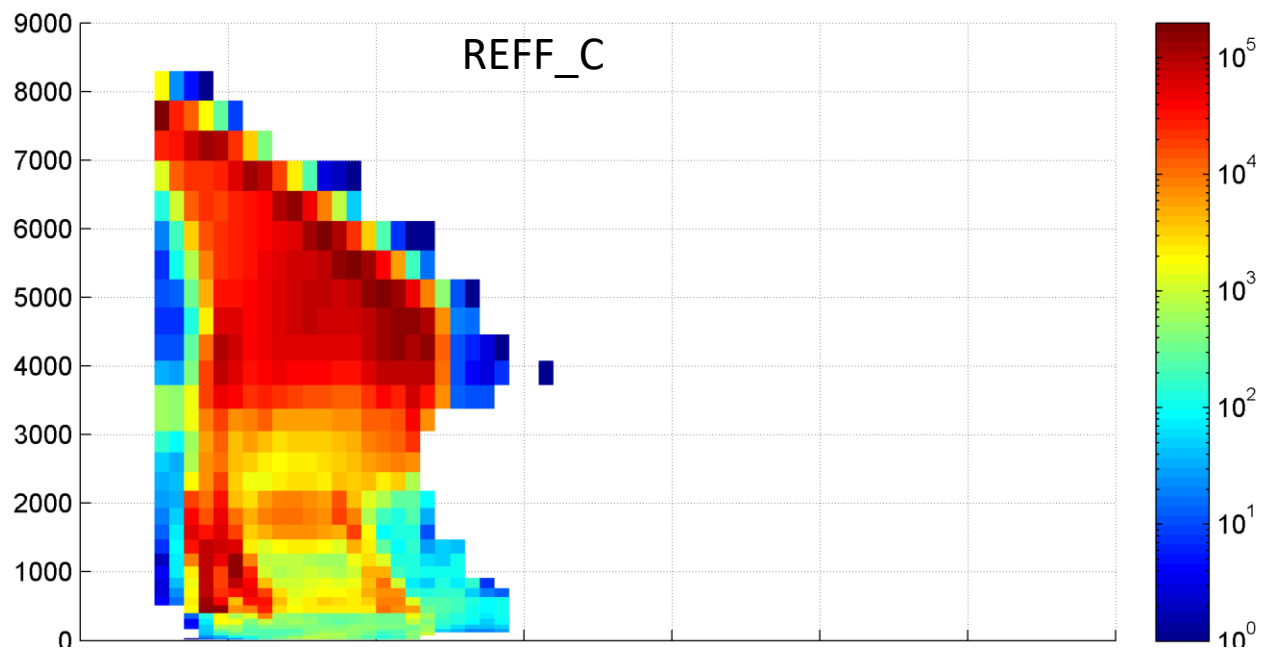
2.
“no-SAM”
version



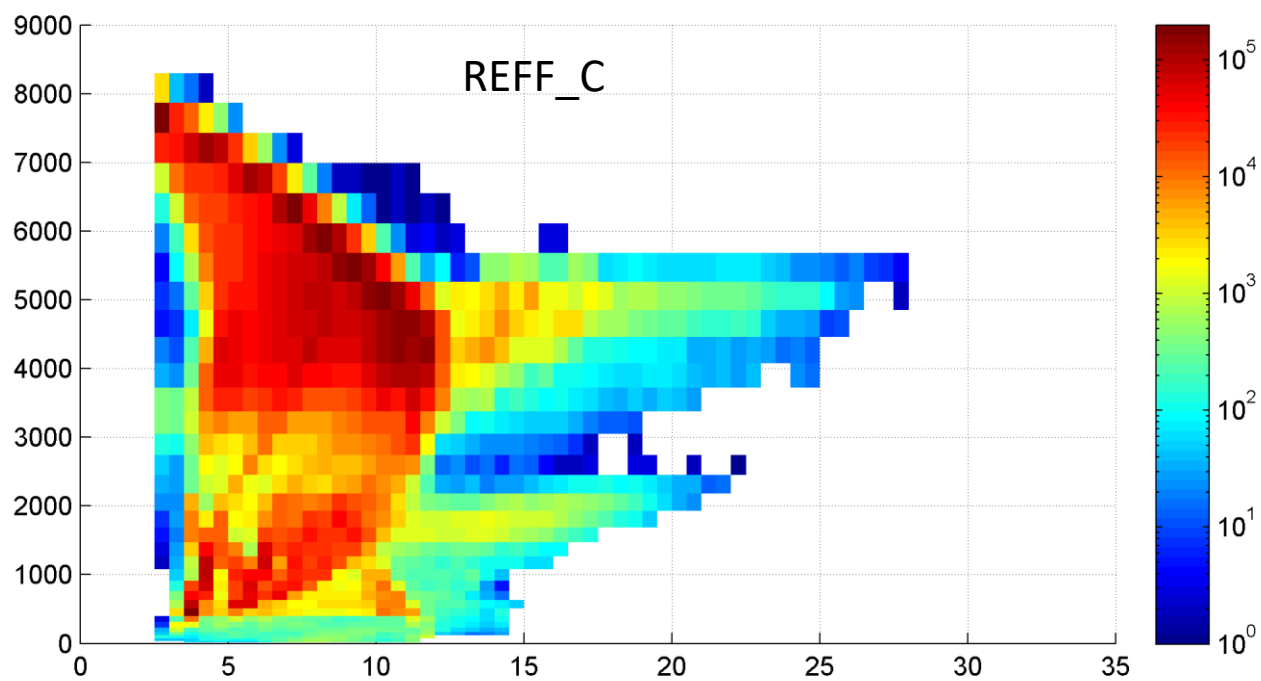
1.
“SAM”
version

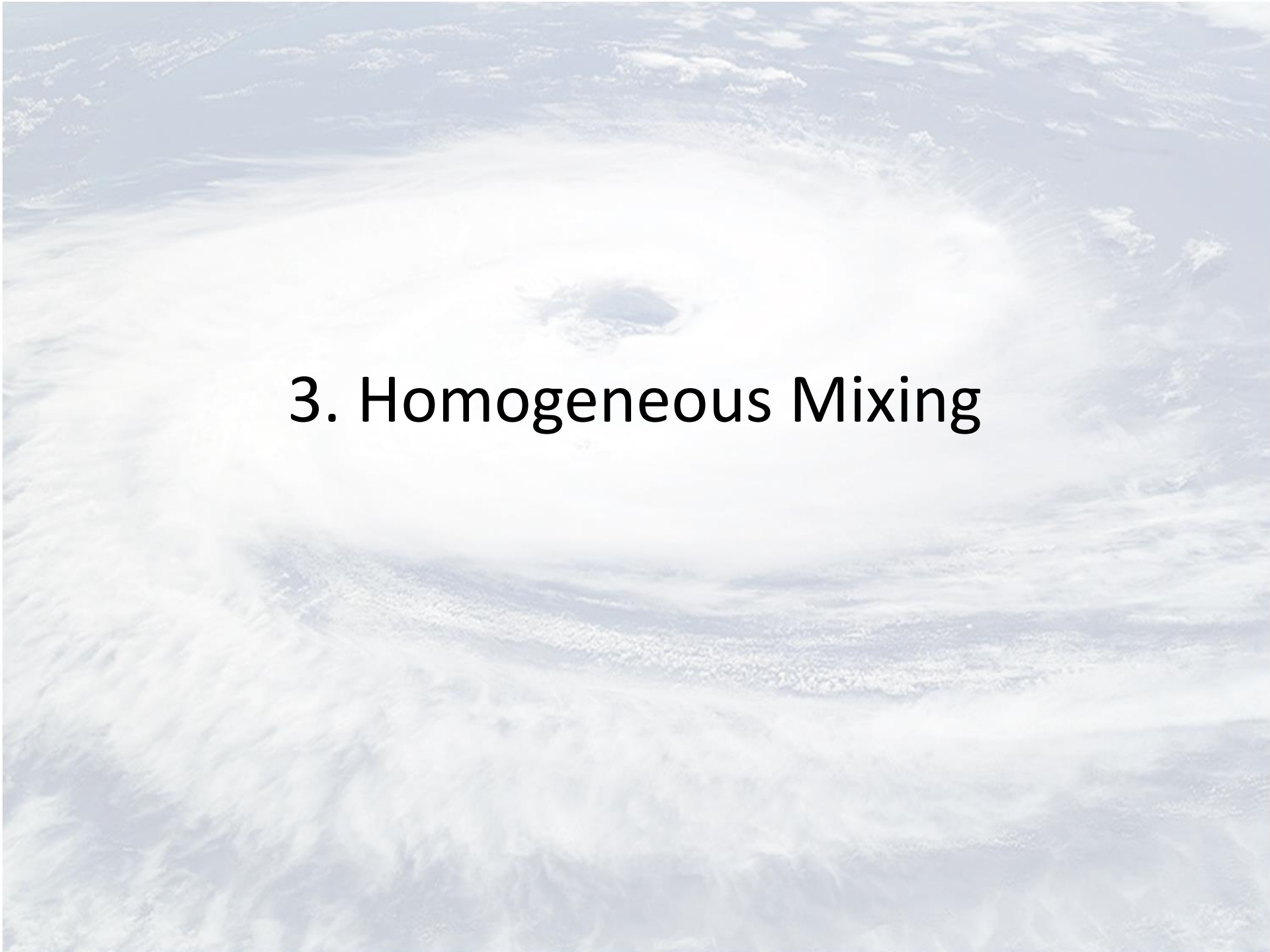


2.
"no-SAM"
version



1.
"SAM"
version



An aerial photograph showing a large, circular, light-colored area in a field, possibly a crater or a large crater, with a smaller, darker crater in the center. The surrounding area is a mix of light and dark patches, suggesting a complex terrain or a large-scale geological feature.

3. Homogeneous Mixing

Pinsky, M., Khain, A., Korolev, A., and Magaritz-Ronen, L.: Theoretical investigation of mixing in warm clouds – Part 2: Homogeneous mixing, Atmos. Chem. Phys., 16, 9255-9272, <https://doi.org/10.5194/acp-16-9255-2016>, 2016.

of turbulent diffusion and droplet evaporation. The first process is mechanical mixing (diffusion), which is governed by turbulence. The turbulent mixing leads to the homogenization of temperature, humidity (and, thus, of supersaturation) and droplet concentration fields within the volume $V = V_1 + V_2$. The second process is the droplet evaporation, which leads to thermodynamical equilibrium of the environment.

Each of the two processes has its own characteristic time scale. The homogenization time τ_{mix} of an entrained volume with linear scale L_{mix} can be evaluated from the relationship (Monin and Yaglom, 1975)

$$\tau_{\text{mix}} = \varepsilon^{-1/3} L_{\text{mix}}^{2/3} \quad (1)$$

where ε is the turbulent kinetic energy dissipation rate. The characteristic time of molecular mixing at the Kolmogorov microscale is short enough to be neglected, unlike the turbulent mixing time determined by Eq. (1). The estimation Eq. (1) suggests that the size of the volume falls within an inertial interval of turbulence. Therefore, after the time of τ_{mix} , volume with a linear scale of about L_{mix} will be mechanically homogenized and all droplets in the volume will experience the same supersaturation.

The characteristic time of the second process, known as the *phase relaxation time*, τ_{pr} (Mazin, 1968; Korolev and Mazin, 2003), determines the rate of change of the supersaturation field

$$\tau_{\text{pr}} = (4\pi D \bar{r} N)^{-1}, \quad (2)$$

where $N = N_0$ is the concentration of droplets in the resulting volume, \bar{r} is the mean radius of droplets and D is the diffusivity of water vapor molecules. The spatial scale at which the mixing time is equal to the phase relaxation time is called a phase relaxation scale L_{pr} (Mazin, 1968). This scale can be calculated from Eqs. (1) and (2) as

$$L_{\text{pr}} = \varepsilon^{1/2} \tau_{\text{pr}}^{3/2} \approx \varepsilon^{1/2} (4\pi D \bar{r} N)^{-3/2} \quad (3)$$

Therefore, after time τ_{pr} volume with a linear scale of about L_{pr} will be saturated because of droplet evaporation.

The value of the Damköhler number is used to determine the type of mixing (Lehmann et al., 2009)

$$Da = \frac{\tau_{\text{mix}}}{\tau_{\text{pr}}} = \frac{4\pi D\bar{r}NL_{\text{mix}}^{2/3}}{\varepsilon^{1/3}} \quad (4)$$

The case with $\tau_{\text{mix}} \ll \tau_{\text{pr}}$ or $Da \ll 1$ corresponds to extreme homogeneous mixing, i.e. mechanical homogenization due to turbulent mixing occurs much faster than does droplet evaporation. The case $Da \gg 1$ corresponds to extreme inhomogeneous mixing. It is reasonable to consider the value $Da = 1$ as a boundary separating two types of mixing. This condition is equivalent to the condition

$$L_{\text{mix}} = L_{\text{pr}} \approx \varepsilon^{1/2} (4\pi D\bar{r}N)^{-3/2} \quad (5)$$

Expression (5) determines the maximum spatial scale when mixing can be considered as homogeneous. The evaluations of the spatial scales under conditions typical of different cloud types are presented in Table 1. One can see that the characteristic volume size in which mixing can be considered as homogeneous ranges from 0.2 to 0.6 m. At larger scales, supersaturation within the total air volume is non-uniform and droplets experience different supersaturations, so the rates of evaporation within the volume may vary. In this case, the mixing should be considered as inhomogeneous. In the majority of cloud-resolving model applications, mixing is considered as homogeneous at substantially larger sub-grid scales. The problem of turbulent mixing representation in numerical cloud models is discussed in Sect. 5.

5 Application of the concept of homogeneous mixing in numerical modeling

The first question that arises with regard to the application of mixing algorithms to cloud models is: “What type of mixing do the models describe”? This question pertains to both the Eulerian models, which calculate microphysical variables on finite different grids (e.g., Benmoshe et al., 2012) and the Lagrangian–Eulerian models, where microphysical values are calculated within movable air parcels (e.g., Pinsky et al., 2008; Magaritz et al., 2009; Magaritz-Ronen et al., 2014). Mixing involves two steps at each model time-step. First, a calculation of turbulent flux divergence of thermodynamic and microphysical quantities between neighbouring parcels or grid points is performed by solving the equation of turbulent diffusion; second, the changes in microphysical values in the parcels or grid points are calculated using these flux divergences.

For time-steps and grid spacing typically used in these models, the changes caused by mixing during a single time-step are small and they do not entirely eliminate spatial gradients of microphysical variables between the mixing parcels (or neighbouring grid points). This stage represents inhomogeneous mixing at resolving scales. In contrast, the changes in the microphysical and thermodynamical variables inside each parcel (or grid points) are considered to be uniform at each time step, and therefore, the modelled mixing can be considered as homogeneous. So, in the numerical simulations, at model domain mixing is inhomogeneous, whereas inside each grid point at every time-step the mixing is homogeneous. Note that the mixing algorithms in models do not operate

with “final” equilibrium values (as assumed in the classical mixing concepts), but with current time-dependent values.

The estimations in Table 1 indicate that mixing should be considered as homogeneous at scales lower than ~ 0.5 m. This means that to simulate homogeneous mixing explicitly the grid spacing (or parcel size) should be less than 0.5 m. In case such grid spacing is used, the separation between mixing types would be described explicitly. However, grid spacing (and parcel size) in most models is substantially larger than this value. The modern models separate mixing types at a substantially larger scale than that in Table 1. This brings up a question: “What error is introduced when the spatial scale that separates mixing types in models is much larger than 0.5 m, and “Why are spectral microphysics models with a resolution of 40–50 m able to reproduce observed DSDs and their moments with high accuracy (Benmoshe et al., 2012; Khain et al., 2013, 2015; Magaritz-Ronen et al., 2014)?”

There are several factors that compensate errors in segregating type of mixing in cloud models and allow using grid scale $L > L_{pr}$ with little effect on DSD. The first factor is that mixing leads to the formation of homogeneous zones in clouds characterized by a spatial correlation radius of temperature, humidity and droplet concentration of about 150–250 m (Magaritz-Ronen et al., 2014). Numerical experiments (Magaritz-Ronen et al., 2014) with parcels of linear sizes of 20 and 40 m have shown that the results are not sensitive to the choice of parcel size if the parcel size is substantially smaller than the spatial radius of correlation. Therefore, type of mixing has a minor effect on the results of mixing at scales lower than the radius of correlation.

The second factor is that in many cases in-cloud mixing takes place at conditions close to saturation. At such a high humidity, results of homogeneous and inhomogeneous mixings become indistinguishable from one another. Indeed, the mixing diagrams in the case of a low saturation deficit do not allow for a separate type of mixing, since in this case the effective (or mean volume) radius does not change as a result of mixing (Burnet and Brenguier, 2006). The similarity of results for the two mixing types

is attributable to the fact that mixing in clouds is not accompanied by an appreciable phase transition.

Hill et al. (2009) explained the insensitivity of the evolution of stratocumulus clouds to the sub-grid mixing assumption by the fact that the rates of condensation/evaporation caused by resolved dynamics are two orders of magnitude greater than the condensation/evaporation rate caused by sub-grid processes. Changes in DSDs during turbulent mixing are caused by low intensity turbulent fluctuations of supersaturation, which are several orders of magnitude weaker than the corresponding processes at resolved scales.

The third factor that permits us to treat sub-grid mixing as homogeneous near cloud interfaces is that DSDs are polydisperse, which is opposite what is assumed in the conventional mixing considerations. In the present study it was shown that for a broad DSD, the changes of r_{eff} remain small during mixing. So, a relatively small partial evaporation of droplets provide sufficient amount of water vapor for saturation of the volume. In this case homogeneous mixing will become indistinguishable from inhomogeneous. The saturation of the volume may be facilitated by entrainment of water vapor from neighboring cloud volumes. The existence of high RH in the air volumes in the vicinity of cloud edges is reported and discussed by Gerber et al. (2008).

We believe that the obtained results justify the use of parcel models for the analysis of microphysical processes in cloud volumes ascending several hundred and even thousands of meters (Pruppacher and Klett, 1997; Korolev, 1995; Pinsky and Khain, 2002; Korolev and Isaac, 2003; Ghan et al., 2011; Pinsky et al., 2013). The linear scale of these parcels is certainly assumed to be on the order of several hundred meters (e.g., Ferrier et al., 1989; Anthes, 1982). The air in such volumes is assumed to be well mixed, i.e. all droplets experience the same supersaturation, thus fulfilling the definition of homogeneous mixing.

Table 1. Linear scales of volumes experiencing homogeneous mixing under conditions typical of different cloud types.

Cloud type	N, cm^{-3}	q_w, gm^{-3}	$r, \mu\text{m}$	Dissipation rate, $\text{cm}^2 \text{s}^{-3}$	Phase relaxation time, s	Phase scale, m
Maritime convective	100	2.0	16.8	300	2.01	0.49
Maritime Stratocumulus	100	0.5	10.6	10	3.19	0.18
Weak Stratocumulus	100	0.2	7.8	5	4.33	0.2
Continental convective	500	2	8.0	500	0.75	0.6